T. van den Boom

Diatomic FPUT lattices and the behavior of their limits

Bachelor thesis

July 6, 2020

Thesis supervisors: dr. T.E. Faver
dr. H.J. Hupkes

Leiden University
Mathematical Institute

Contents

Chapter 1

Introduction

The subject of this paper is the Fermi-Pasta-Ulam-Tsingou (FPUT) lattice. An FPUT lattice is a one-dimensional line of masses which are interconnected by springs. Each mass is connected to its right and left neighbour. An FPUT lattice is shown in Figure 1.1.

Figure 1.1: A monatomic FPUT lattice where all masses have value m.

The FPUT lattice is a way of modelling certain molecular structures and is applied in fields of study such as nonlinear optics, atomic physics, granular crystals and metamaterials, but also in biology, where DNA strand dynamics are studied. See [1] for more applications. An FPUT model can be seen as the structure of interconnected atoms, which is why it has most of its applications in physics, since for example energy transportation through certain materials is of utmost interest to physicists and related fields of study.

The behavior of energy transported across the lattice is influenced by various parameters, such as the weight of the masses and the force the springs exert on the masses. Since we will be looking closely at the situation described in [2], our main interest is in the diatomic lattice, or mass dimer, which has two different masses varying periodically in an alternating fashion, as seen in Figure 1.2 below. Since monatomic lattices, where all the masses are the same, have been studied for many years now because of its relevance in physics, its solutions are well understood. We want to gain a better understanding of solutions to more complicated problems, such as the diatomic lattice, because studies of nonlinear wave theory for the diatomic problem are relatively recent compared to studies of the monatomic problem, which means there is still much to be understood about the diatomic problem and the diatomic case is just as relevant to physics.

Figure 1.2: A diatomic FPUT lattice where masses alternate between values 1 and m.

We will describe here the situation that was set out by Giardetti, Shapiro, Windle and Wright in [2]. Let $x_n(t)$ be the position of the nth particle on the lattice at time t and let m_n be the mass of the nth particle ($n \in \mathbb{Z}$). Each particle is connected to two massless springs, which pull from either the left or the right side of the particle. The nth spring connects the nth and $(n+1)$st particle on the lattice. The force needed to stretch the nth spring a distance r from its equilibrium position is given by $F_n(r)$. The movement of the particles is one-dimensional, in line with the lattice itself. Aside from the spring forces, there are no other forces, like gravity or friction, working on the lattice. To describe the motion of the particles on the lattice, we use Newton's second law:

$$m_n \ddot{x}_n = F_n(x_{n+1} - x_n) - F_{n-1}(x_n - x_{n-1}). \tag{1.1}$$

By varying m_n and F_n, we can describe different kinds of lattices. If we take $m_n = m$ and $F_n = F$, we get a monatomic lattice. For a diatomic lattice, we take $m_n = m_{n+2}$ and $F_n = F$. To describe a lattice which is called a "spring dimer" we take $m_n = m$ and let the forces of the springs vary periodically: $F_n = F_{n+2}$. For a "general dimer" we also let the masses vary, so we take $m_n = m_{n+2}$ and $F_n = F_{n+2}$. There are many natural ways to define the spring force, see [3, 4, 5, 6, 7] for examples. We choose to focus on $F_n(r) := \kappa_n r + \beta_n r^2$, which has both a linear and a nonlinear term. Here, κ_n and β_n are the spring constants. For the most part we will take $\kappa = \beta = 1$. Later, as we will be doing simulations, we will vary κ_n and β_n.

If we let $p_n := \dot{x}_n$ and $r_n := x_{n+1} - x_n$, the equation of motion can be written as a system of first-order differential equations:

$$\dot{r}_n = p_{n+1} - p_n \tag{1.2}$$

$$\dot{p}_n = \frac{1}{m_n}(F_n(r_n) - F_{n-1}(r_{n-1})) \tag{1.3}$$

Here, the velocity of the nth particle is given by p_n and the relative displacement is given by r_n, which is the same as the distance between successive particles.

There exist certain families of special solutions to these equations. We are interested in the stability of such families of solutions, meaning we are interested in what happens, over very long times, to solutions that start close to these families. For rigorous definitions of stability, see [8]. The goal of the thesis is to generate data for the study of stability of said families of solutions to the lattice equations of motion. In Chapter 3, we will describe these families of solutions and after presenting lots of data in Chapter 4, we will make some conjectures in Chapter 5.

To give the reader a better idea where the solutions to this system of equations come from, we will first dive into the work that other scientists have done regarding this subject.

Chapter 2

Background

In the 1950s, the physicist Enrico Fermi had begun showing interest in a certain field of physics where nonlinear differential equations played a role. To get a better understanding for nonlinear problems, Fermi, together with John Pasta and Stanislaw Ulam, created the FPUT lattice problem: a finite chain of masses connected by springs. To make it into a nonlinear problem, the restoring force of the springs was made to be nonlinear. Because of the nonlinear nature of the problem, they needed to implement it into the computer to study the behavior of the lattice, for it would be too hard to solve analytically by hand. Mary Tsingou created an implementation [9] for the MANIAC, one of the earliest digital computers. They expected that, in the long run, the starting energy of the springs would become equally divided among the lattice. The actual results were far from the equipartitioning which was expected. The lattice almost came back to its starting position. The energy was not being divided among the lattice, but rather travelled along the lattice. See [10, 11] for more details.

Ten years later, Zabusky and Kruskal began studying a modified version of the FPUT lattice. They used infinitesimally small masses and springs to represent a continuous line of deformable material, like a string. After some changes of variables and formal Taylor series expansions, Zabusky and Kruskal discovered that solutions to the monatomic FPUT equations of motion approximated solutions to the Korteweg-de Vries (KdV) equation. These results were somewhat surprising, not only because of the fact that FPUT is a discrete problem, whereas the KdV problem is a continuous one, but also because FPUT only models a single chain, whereas the KdV equation models the motion of waves in shallow water where the wavelength is long compared to the depth of the water [12]. The KdV equation consist of the sum of a linear and a nonlinear term, like the equations for the FPUT lattice. Up to rescalings of time and space, the KdV equation can be written as

$$u_t + 6uu_x + u_{xxx} = 0,$$

which is only one of the ways to write the KdV equation. This equation has a solution of the following form:

$$u(x,t) = \frac{c}{2}\operatorname{sech}^2\left(\frac{\sqrt{c}}{2}(x-ct)\right) \tag{2.1}$$

where $\operatorname{sech}(y) := 2/(e^y + e^{-y})$. This solution to the KdV equation was discovered in 1895 by Dutch physicists Korteweg and de Vries. It is called a "solitary wave" solution, as the graph of the solution looks like a single wave which goes to zero at spatial infinity. This is shown in Figure 2.1.

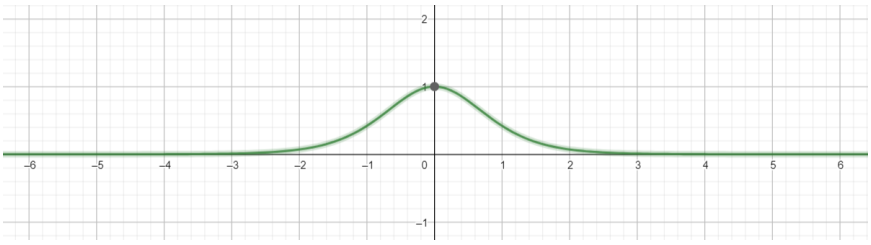

Figure 2.1: Graph of $y = \operatorname{sech}^2(x)$.

In the solution, observe the $x - ct$ part inside sech^2. This is the part of the solution that makes it a "traveling wave". As time goes on, the peak of the graph will move to the right because ct is subtracted from x. See Friesecke and Wattis [4] for the first proof of the existence of solitary wave solutions in monatomic FPUT lattices.

We are interested in the FPUT problem which has solitary wave solutions, or solitons, of long wavelength and small amplitude. This situation is called the "long wave limit" or "KdV limit" [3], since the solutions to this problem can be closely approximated by suitably scaled solutions of the KdV equations, which are sech^2-type solutions like in (2.1), for long periods of time and, in the monatomic case, remain close to the scaled solutions of the KdV equations for all time, as established by Schneider and Wayne in [13].

Chapter 3

FPUT lattice solutions

3.1 Solitary and nanopteron traveling waves

Recall the given system of differential equations:

$$\begin{cases} \dot{r}_n = p_{n+1} - p_n \\ \dot{p}_n = \dfrac{1}{m_n}(F_n(r_n) - F_{n-1}(r_{n-1})) \end{cases}$$

In this section we will be talking about either the monatomic or the diatomic lattice, which means all the spring will be the same, so we take $F_n(r) = F(r) = r + r^2$. After suitable rescaling and nondimensionalization of the problem, as described in [3, 14], we can assume that the coefficients κ and β in the spring force are equal to 1.

For $0 < \epsilon \ll 1$, according to Gaison, Moskow, Wright and Zhang [15], a solution is given by a leading order sech^2 term, like in the solution to the KdV equation, which creates the solitary wave shape of the solution, and a certain error term:

$$\mathbf{r}_n(t) = \mathbf{\Psi}_n^{m_1,m_2,\epsilon}(t) := 3\epsilon^2 \operatorname{sech}^2(\beta\epsilon(n - c_\epsilon t))\mathbf{v} + \mathbf{z}_n(t), \tag{3.1}$$

where

$$\beta = \sqrt{\frac{3(m_1^2 + 2m_1m_2 + m_2^2)}{2(m_1^2 - m_1m_2 + m_2^2)}}, \quad c_\epsilon = (1 + \epsilon^2)\sqrt{\frac{2}{m_1 + m_2}} \quad \text{and} \quad \mathbf{v} := (1, -c_0). \tag{3.2}$$

Here, c_ϵ is what we call the wave speed and, when $\epsilon = 0$, the number c_0 is called the speed of sound. It is called the speed of sound, because of the fact that, in the monatomic lattice with linear spring forces, where $m_1 = m_2 = 1$ and $F(r) = r$, it turns out to be the maximum wave speed of a plane wave ansatz to its corresponding FPUT equations. This maximum wave speed is equal to 1. On the other hand, the speed of sound is the infimum of the allowed wave speeds for the long wave diatomic FPUT solutions. See [16, 4]. The long wave limit is sometimes called the "near-sonic" limit, since the wavespeeds c_ϵ will be close to the speed of sound c_0.

Since the solution to the KdV equations only approximate the solutions to the FPUT equations, there is a certain error, which is given by the function $\mathbf{z}(t)$. The mapping $t \mapsto \mathbf{z}(t)$ is the mapping $\mathbb{R} \to \ell^2 \times \ell^2$ whose nth component is $\mathbf{z}_n(t) = (z_{n,1}(t), z_{n,2}(t))$. See Appendix A for a discussion about ℓ^2. The solution given in (3.1) is a very good approximation for a large amount of time:

$$\sup_{|t| \leqslant T_0\epsilon^{-3}} ||\mathbf{z}(t)||_{\ell^2 \times \ell^2} \leqslant C\epsilon^{5/2} \tag{3.3}$$

for some constants C and T_0. In the monatomic case, where $m_1 = m_2 > 0$, $\mathbf{z}(t)$ is less than $\mathcal{O}_{\ell^2 \times \ell^2}(\epsilon^{7/2})$ according to Schneider and Wayne [13]. As done in [2], the computational part of this paper will examine the behavior of this approximated solution for times which greatly exceed T_0/ϵ^3.

For the monatomic case, in which $m_1 = m_2 > 0$, according to Friesecke and Pego [3], under the ansatz $r_n(t) = p(n - ct)$, where $p = p(y)$ is a function of the real variable y, a traveling wave solution to the FPUT problem is a solitary wave given by

$$\mathbf{r}_n(t) = \mathbf{\Sigma}_n^{m,\epsilon}(t) := 3\epsilon^2 \operatorname{sech}^2(\beta\epsilon(n - c_\epsilon t))\mathbf{v} + \boldsymbol{\eta}_\epsilon(n - c_\epsilon t) \tag{3.4}$$

with β, c_ϵ and $\mathbf{v}$ as in (3.2). The traveling wave profile for r_n is given by $3\epsilon^2 \operatorname{sech}^2(\beta\epsilon y)\mathbf{v} + \boldsymbol{\eta}_\epsilon(y)$. In this solution the solitary core consists not only of the sech^2 function as in (3.1), but a certain unknown function $\boldsymbol{\eta}_\epsilon(y)$ is added. The function $\boldsymbol{\eta}_\epsilon(y)$ is particularly small, such that, for a certain $\widetilde{\beta} > 0$, $\cosh(\widetilde{\beta}y)\boldsymbol{\eta}_\epsilon(y/\epsilon) = \mathcal{O}_{H^s \times H^s}(\epsilon^4)$. This estimate holds for each $s \in \mathbb{N}$. If $f = f(y)$ is a function such that $\cosh(\widetilde{\beta})f \in H^s$ for some $s \geqslant 1$, then f must vanish exponentially fast. We call such a function "exponentially localized". For details on H^s see Appendix A. The scaling by $1/\epsilon$ inside $\boldsymbol{\eta}_\epsilon$ is a technical artifact of the long wave scaling Friesecke and Pego use.

For the diatomic case, according to Faver and Wright [17], a traveling wave solution is given by the superposition of a solitary wave solution and a small ripple, which was called a nanopteron by Boyd [18]:

$$\mathbf{r}_n(t) = \mathbf{\Gamma}_n^{m_1,m_2,\epsilon}(t) := 3\epsilon^2 \operatorname{sech}^2(\beta\epsilon(n - c_\epsilon t))\mathbf{v} + \boldsymbol{\eta}_{n,\epsilon}(n - c_\epsilon t) + \boldsymbol{\phi}_{n,\epsilon}(n - c_\epsilon t). \tag{3.5}$$

The nanopteron profile in (3.5) is $3\epsilon^2 \operatorname{sech}^2(\beta\epsilon y)\mathbf{v} + \boldsymbol{\eta}_{n,\epsilon}(y) + \boldsymbol{\phi}_{n,\epsilon}(y)$, which is the sum of an exponentially localized term and a periodic term. Here, $\boldsymbol{\phi}_{n,\epsilon}(y)$ is the small ripple added to the solitary wave core and β, c_ϵ and $\mathbf{v}$ are again the same as in (3.2). The functions $\boldsymbol{\eta}_{n,\epsilon}(y)$ and $\boldsymbol{\phi}_{n,\epsilon}(y)$ have the same periodicity as the lattice, for all $n \in \mathbb{Z}$ and $y \in \mathbb{R}$ we have the following: $\boldsymbol{\eta}_{n,\epsilon}(y) = \boldsymbol{\eta}_{n+2,\epsilon}(y)$ and $\boldsymbol{\phi}_{n,\epsilon}(y) = \boldsymbol{\phi}_{n+2,\epsilon}(y)$. Again, $\boldsymbol{\eta}_{n,\epsilon}(y)$ is small, such that, for a certain $\widetilde{\beta} > 0$, $\cosh(\widetilde{\beta}y)\boldsymbol{\eta}_{n,\epsilon}(y/\epsilon) = \mathcal{O}_{H^s \times H^s}(\epsilon^3)$. The amplitude of the ripple is extremely small. For all $n, s \in \mathbb{N}$ we have the following:

$$\lim_{\epsilon \to 0^+} \epsilon^{-n} ||\boldsymbol{\phi}_{n,\epsilon}||_{W^{s,\infty} \times W^{s,\infty}} = 0.$$

This limit is a small beyond all orders of ϵ estimate. For each $n, s \in \mathbb{N}$, it is equivalent to the existence of a constant $C(n, s)$, such that $||\boldsymbol{\phi}_{n,\epsilon}||_{W^{s,\infty}} \leqslant C(n, s)\epsilon^n$. See Appendix A for the definition of $W^{s,\infty}$.

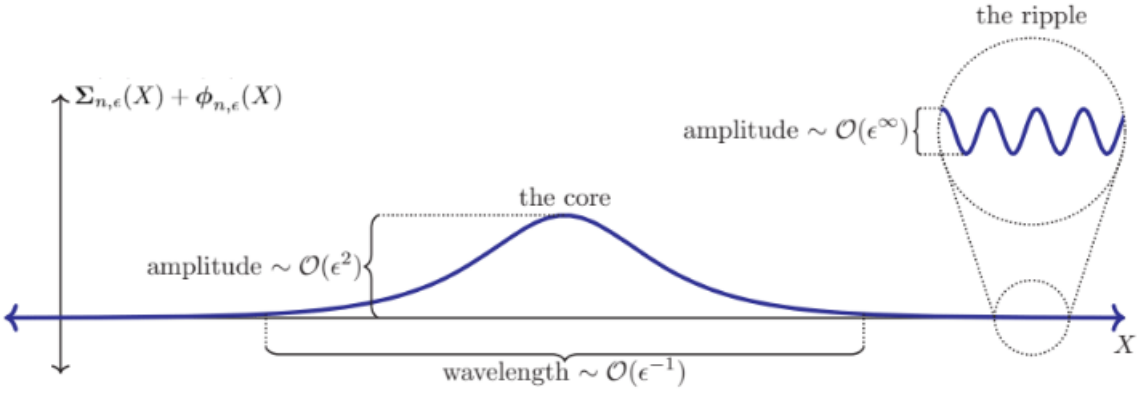

Figure 3.1: Sketch of a nanopteron, where $\boldsymbol{\Sigma}_{n,\epsilon}(X) := 3\epsilon^2 \operatorname{sech}^2(\beta\epsilon X)\mathbf{v} + \boldsymbol{\eta}_{n,\epsilon}(X)$, taken from [19].

A nanopteron is also sometimes called a "generalized solitary wave" or a "weakly nonlocal solitary wave". Like the solitary wave, it has an intimate connection to water wave problems. The first proof of this was given by Beale [20] and later different proofs were given by Sun [21] and Lombardi [22].

The main difference between solitary wave solutions in the monatomic case and nanopteron solutions in the diatomic case is the ripple. By [15], both monatomic and diatomic cases have solutions of the form (3.1), where the remainder term $\mathbf{z}_n$ satisfies (3.3). We know from the work of Mizumachi [23] that, for the monatomic solution, for some $t' \sim 0$, $\epsilon' \sim \epsilon$ and as $t \to \infty$, in a certain space the monatomic solution (3.1) converges to the solitary wave solution (3.4):

$$\mathbf{\Psi}_n^{m,m,\epsilon}(t) \longrightarrow \mathbf{\Sigma}_n^{m,\epsilon'}(t - t').$$

A reasonable question is whether, if at all, the nanopteron (3.5) might converge to a relative of the diatomic solution (3.1). While we will not purse the details in this thesis, Mizumachi's proof for the monatomic solitary wave rests on the following. There is a physically natural way to define the 'mechanical energy' of a lattice as a numerical quantity in such a way that the solitary wave inherently has

'finite' mechanical energy, but the nanopteron's ripples causes it to have 'infinite' mechanical energy. Mizumachi's proof relies on having finite mechanical energy. This makes it unclear whether the solution given by (3.1) could stay close to the nanopteron solution (3.5) for infinite amounts of time.

Because $\boldsymbol{\eta}(y)$ is unknown in both cases, and $\boldsymbol{\phi}(y)$ is unknown in the diatomic case, we must use (3.1) to numerically calculate the solutions to the differential equations.

3.2 Numerical methods

In [2], MATLAB was used to analyse the behavior of (3.1) as time goes to infinity for $m_1 \neq m_2$. They used the RK4 method with a fixed time step of $h = 1/10$ to approximate the solutions. The size of the domain was chosen to be $N = 2^{10}$, such that $n \in [-N/2+1, N/2] \cap \mathbb{Z}$. For the initial condition they left out the ripple and also took $\mathbf{z}_n(0) = 0$:

$$\mathbf{r}_n(0) = 3\epsilon^2 \operatorname{sech}^2(\beta\epsilon n)\mathbf{v}, \tag{3.6}$$

where ϵ, m_1 and m_2 had been chosen beforehand and where β and $\mathbf{v}$ are as in (3.1). The solution in this case will be a traveling solitary wave which will start very close to the nanopteron, because of the fact that $\boldsymbol{\eta}(y)$ and $\boldsymbol{\phi}(y)$ in the nanopteron are so small. They took $\mathbf{r}_{N/2}(t) = \mathbf{r}_{-N/2+1}(t)$ to make the wave move along an "infinite lattice". Once the solution gets to the edge, it comes back around on the other side of the domain to continue as it would on the infinite lattice. To make sure that the solitary wave will not be disturbed by anything that succeeds the wave, as the wave comes around on the other side of the domain, they coded in a "window". Everything outside of the window will vanish, so anything that reaches the edge of the window will vanish and will not interfere with the solitary wave once it loops back around the domain.

The solution leaves behind a small amplitude ripple with relatively high frequency for all time. In the monatomic case, the ripple will eventually disconnect from the solitary part and the solitary wave will continue on its own. Initially, for small times, the ripple will look very chaotic, while as time goes on, the ripple will eventually oscillate at a regular frequency. The numerical ripple is not to be mistaken with the nanopteron's ripple from (3.5), they are two very different things. Where the ripple in (3.5) is an extremely small ripple, probably invisible to the naked eye, which covers the entire lattice, the ripple in the numerical solutions seems to be far bigger and only follows the solitary wave. It also takes away energy from the solitary wave to feed itself, so as time goes on, the solitary wave becomes smaller, while the "oscillatory wake" takes up more space among the lattice.

In [2], they also kept track of the amplitudes of the solitary wave and the ripples. For the amplitude of the leading solitary part, we just have to look at the maximum value of the solution on the interval we specified and keep track of these values for each timestep. For the amplitude of the ripples, [2] used a so-called "peak to trough" measure of the amplitude, which results in the following formula:

$$amp_{wake}(t) := \frac{1}{2}\left(\max_{n-n_{max}\in[-7N/8,-3N/4]} r_n(t) - \min_{n-n_{max}\in[-7N/8,-3N/4]} r_n(t)\right).$$

This formula gives the amplitude of the biggest ripple in an interval a fixed distance away from the leading solitary wave. The interval in which they used is quite big. However, this is done to ensure that they are searching for the amplitude in an area not too close to the leading solitary wave, since this part of the ripples may be distorted. Also, the period of the ripples can get quite large, but as a large interval was taken, this is no problem, because this will capture an entire period of the ripples regardless.

After observing the behavior of the implementation of (3.1) with various different masses and values of ϵ, [2] conjectures that (3.5) is a so called "metastable" solution, whereas (3.4) was a stable solution. A solution that starts close to a stable solution will remain close to it for all time. Solutions that start close to a metastable solution, in our case (3.5), need not stay close for all time, but could move away from it and come back to it again, possibly even repeating this process of moving away and coming back again. Metastable could also mean that a solution that starts close to the metastable solution, remains close for a very long time, but eventually as time goes to infinity, will vanish. We see in [2] that as time goes to infinity, some cases show a clear decay in the amplitude of the leading solitary waves, while other cases imply that the amplitude stays constant. However, [2] says that the amplitude is actually not constant, but decays at such a slow rate, that we are unable to see it. Once the leading solitary part has decayed to zero, the simulation which started close to the nanopteron, is clearly not close to the nanopteron anymore, since the nanopteron will preserve its shape, which implies the metastability of the nanopteron.

3.2.1 Simulation goals

What we are interested in is doing some experimental mathematics on the code used in [2]. We want to look at the following limits:

- The small mass limit;
- The equal mass limit;
- The stiff spring limit.

As discussed by Hoffman and Wright in [24] and by Faver and Hupkes in [25], the small mass limit is the situation in which we take $m_1 = 1$ and $m_2 = \mu$ with μ small. We will be looking at what happens as $\mu \to 0$. When μ is close to 0, there are traveling wave solutions that are nanopterons similar to (3.5), with several differences. Firstly, the wave speed does not depend on the small parameter μ, but is instead fixed at a value slightly greater than 1. Secondly, the leading order term is not an exact sech^2 term, but is rather a genuine monatomic solitary wave profile like (3.4), with ϵ fixed at some small value. The periodic ripples of the small mass solution are still small beyond all orders of μ. As seen in Figure 3.2 below, the lattice will approach a monatomic lattice with double the spring length.

Figure 3.2: Under the small mass limit, the mass dimer from Figure 1.2 turns into this monatomic lattice.

As discussed by Hoffman and Wright in [24], who proved the existence of micropteron [18] solutions, and by Faver and Hupkes in [25], for the equal mass limit we take $m_1 = 1$ and $m_2 = 1 + \mu$ with μ small. Again, we let $\mu \to 0$. The micropteron traveling wave solution has a similar structure to the nanopteron, in the sense that it is the superposition of an exponentially localized term and a periodic term, except now the periodic amplitude is only $\mathcal{O}(\mu)$ and not small beyond all orders of μ. The micropteron ripple is "algebraically small". The difference in size of the periodic term is due to a singular perturbation that appears in the structure of the traveling wave problem for the small mass limit and the diatomic KdV limit, but not in the equal mass traveling wave problem. The situation of the equal mass limit will again approach a monatomic lattice, but this time with the regular spring length as seen in Figure 3.3.

Figure 3.3: Under the equal mass limit, the mass dimer from Figure 1.2 turns into this monatomic lattice.

For the stiff spring limit, we will be looking at two situations. For the first situation, we take $m_1 = m_2 = 1$ and let the spring force function alternate between $F(r) = r + r^2$ and $F(r) = \kappa r + \beta r^2$. We will fix β and take κ to be increasingly large, for example first $\kappa = 10$, then $\kappa = 100$, and finally $\kappa = 1000$. We call this a "spring dimer lattice" as seen in Figure 3.4 below. See [19, 26] for more about the spring dimer.

Figure 3.4: A spring dimer where all masses have mass m.

In the second situation, we will make the springs alternate in the same way, but now we will also alternate the masses, such that $m_1 \neq m_2$. For the purpose of our numerics, we will take $m_1 = 1$ and $m_2 = 1/2$, but any two different values of m_1 and m_2 are permissible. This is called a "general dimer lattice", as seen below in Figure 3.5. Increasing κ as done above will result in the stiff spring limit,

which is also seen below. Both situations will approach a certain monatomic lattice, where a single mass consists of m_1, m_2 and the stiff spring, which means this mass now has the value $m_1 + m_2$, given that the springs are massless.

Figure 3.5: A general dimer where the masses alternate between 1 and m.

Figure 3.6: The resulting monatomic lattice in the stiff spring limit for a general dimer where all masses have the value $1 + m$.

Nanopteron solutions to the stiff spring limit in spring dimers and general dimers have not yet been proven to exist, but we expect them to, at least in the spring dimer case. A stiff spring program has been succesful in a breed of lattices related to the diatomic lattice called mass-in-mass lattices. See [27] for more on this. We do know, from [19, 26], that it is proven that the spring dimer has long wave nanopterons like (3.5), except the leading order sech^2 term has an additional coefficient that depends on n but is independent of ϵ.

We will also be looking at large wave speed situations in which ϵ is taken to be large. We know of the existence of such waves for monatomic FPUT lattices with "Lennard-Jones-type spring forces", as it was proved in [5, 6, 7]. In [4], it is not implied that there is an upper bound for the wave speed of solitary waves for monatomic FPUT, which gives some room to hope for large amplitude solitary waves. If such waves exist, uniqueness results from Friesecke and Pego [3] prevent such solitary waves from existing in the long wave regime and being close to sech^2-type profiles. Also, in [25], it is proved that in the equal mass limit, there exist micropteron traveling waves for arbitrary wave speeds, given suitable hypotheses which mainly concern the existence and properties of a solitary wave solution to monatomic FPUT. It would be interesting to see how (3.1) would behave, because for large ϵ, (3.1) has turned into a small wavelength, large amplitude solitary wave, which is basically the opposite of the KdV limit.

Chapter 4

Numerical results

4.0.1 Overview of the results

For all simulations, $\epsilon = 1/4$, so the wave speed is fixed. We take the same initial condition 3.6 as in [2] and also take the same time steps and the same size and "windowing" for the domain. All plots are of the r-component of the solutions against $n - n_{\max}$, where n_{max} is the position of the leading solitary wave. All figures are after 10^5 time steps unless otherwise stated. We will show figures of the simulations done and examine the way these limits approach the monatomic FPUT solution. In general we will see an initial disorder in the amplitude of the leading solitary wave, and an eventual oscillation of the amplitude around a certain value which decays very slowly. For the most part the ripples will tend towards the localized monatomic situation in various ways.

In [17], to prove the existence of nanopterons, traveling wave ansatzes are made for even and odd indices seperately, which look something like this:

$$r_n(t) = \begin{cases} p_1(n - ct), & n \text{ odd} \\ p_2(n - ct), & n \text{ even} \end{cases}$$

This makes it interesting to look at the graphs of the relative displacement for even and odd indices seperately, which is why we will dedicate a section of this chapter to it. We expect slightly different behavior for even indexed relative displacement from odd indexed ones.

In Section 4.8 there will be some results for different values of ϵ.

4.1 Monatomic behavior

We will first look at the behavior of (3.1) in the monatomic case. We take $m_1 = m_2 = 1$. We get the following results.

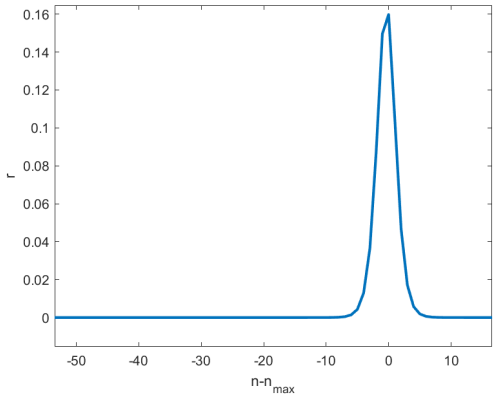

Figure 4.1: The resulting monatomic wave.

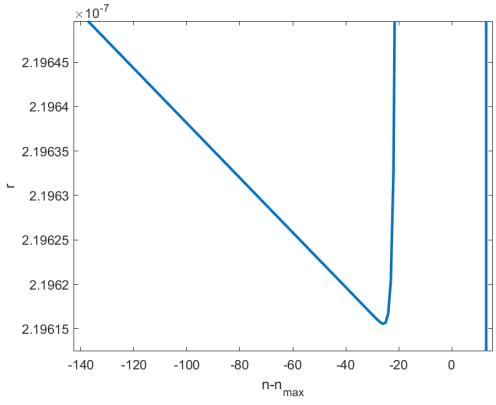

Figure 4.2: The monatomic wave, zoomed in on the tail.

The results show us that in fact the amplitude of the solitary wave does decay, as seen in Figure 4.3. If we look at Figure 4.2, we see that the tail of the solitary wave is going upward at an angle, which could

be the result of the fact that the solution has not fully disconnected from the initial oscillatory wake. Because of this, the solution may still be leaking energy into the tail. This leak is very slow however, the upward slope of the tail is not to be seen in Figure 4.1.

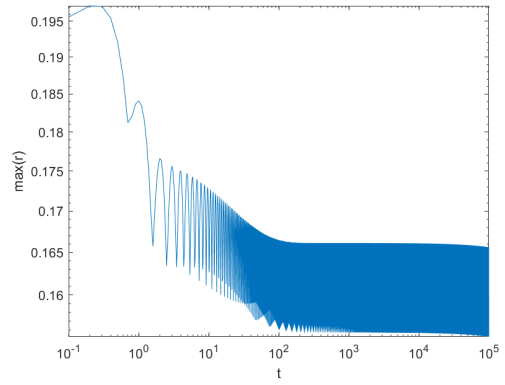

Figure 4.3: Loglog plot of the amplitude of the monatomic wave for all t up to 10^5.

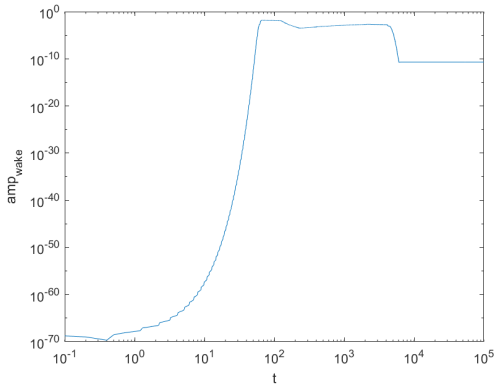

Figure 4.4: Loglog plot of the monatomic ripple amplitude for all t up to 10^5.

4.2 Small mass limit

For the small mass limit we take $m_1 = 1$ and $m_2 = \mu$ with $\mu = 2^{-n}$ for $n \in \{2, 3, 4, 5, 6\}$. The results are seen below.

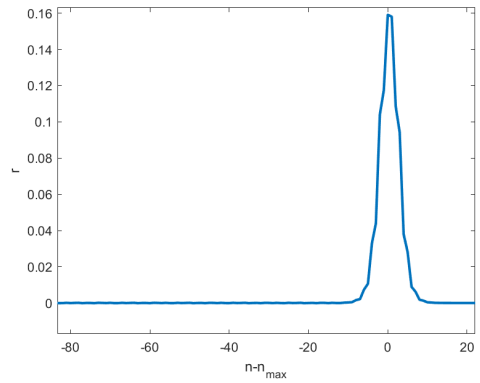

Figure 4.5: Small mass limit with $\mu = 1/4$.

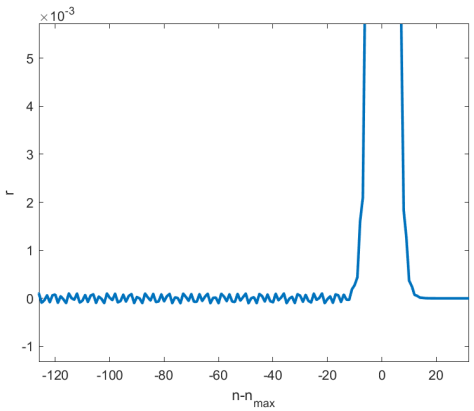

Figure 4.6: Small mass limit with $\mu = 1/4$, zoomed in on ripples.

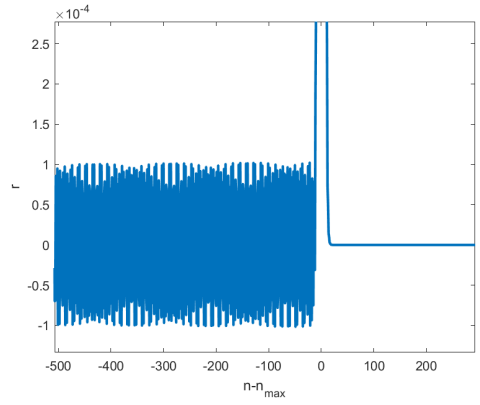

Figure 4.7: Small mass limit with $\mu = 1/4$, showing the ripple envelopes.

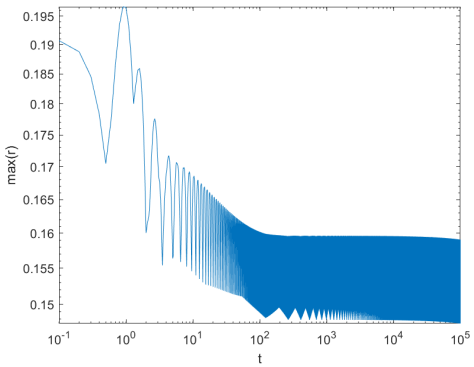

Figure 4.8: Loglog plot of small mass limit leading solitary wave amplitude with $\mu = 1/4$ for all t up to 10^5.

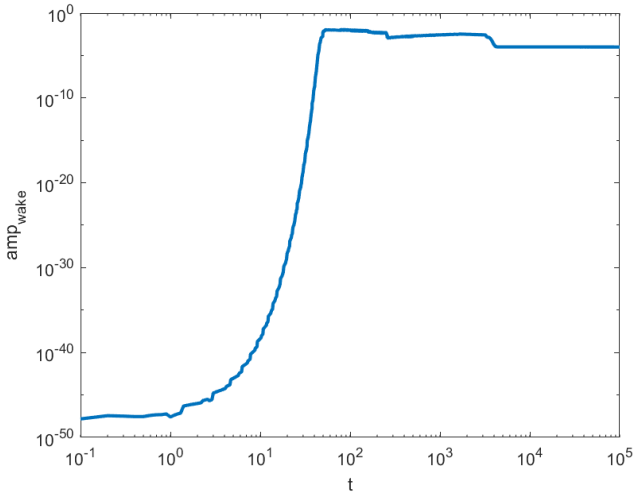

Figure 4.9: Loglog plot of the small mass limit ripple amplitude with $\mu = 1/4$ for all t up to 10^5.

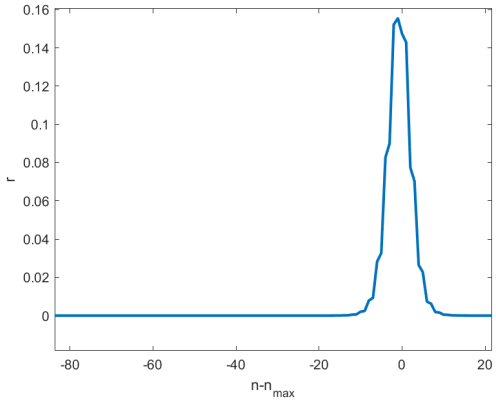

Figure 4.10: Small mass limit with $\mu = 1/8$.

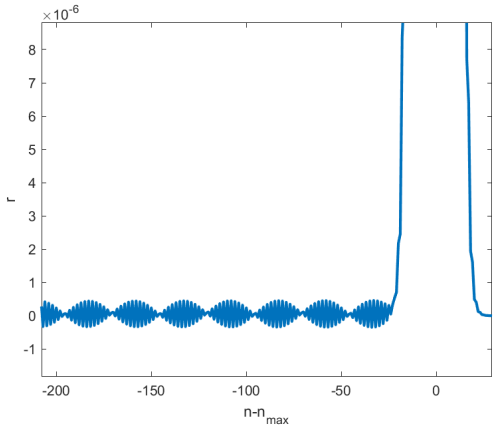

Figure 4.11: Small mass limit with $\mu = 1/8$, zoomed in on ripples.

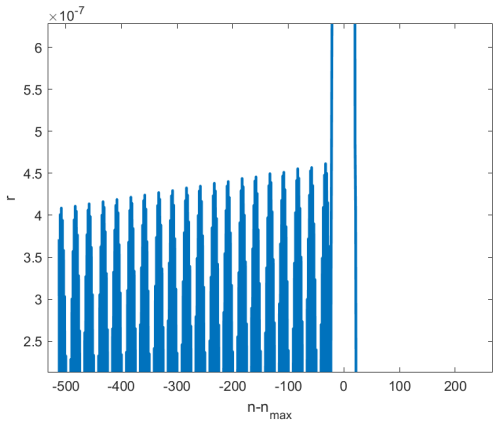

Figure 4.12: Small mass limit with $\mu = 1/8$, showing the ripple amplitudes.

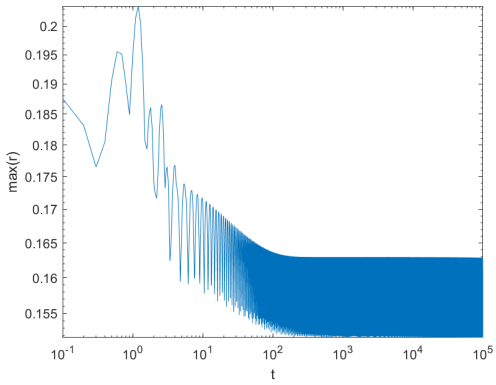

Figure 4.13: Loglog plot of small mass limit leading solitary wave amplitude with $\mu = 1/8$ for all t up to 10^5.

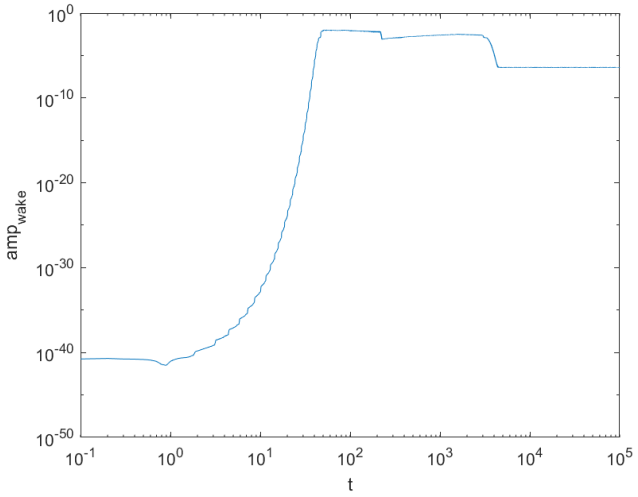

Figure 4.14: Loglog plot of the small mass limit ripple amplitude with $\mu = 1/8$ for all t up to 10^5.

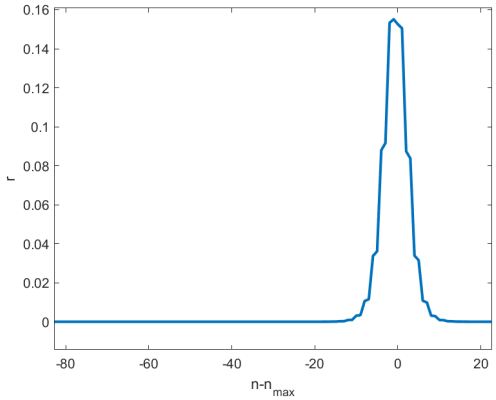

Figure 4.15: Small mass limit with $\mu = 1/16$.

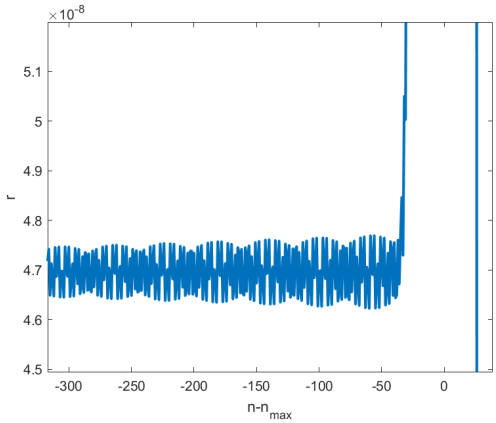

Figure 4.16: Small mass limit with $\mu = 1/16$, zoomed in on ripples.

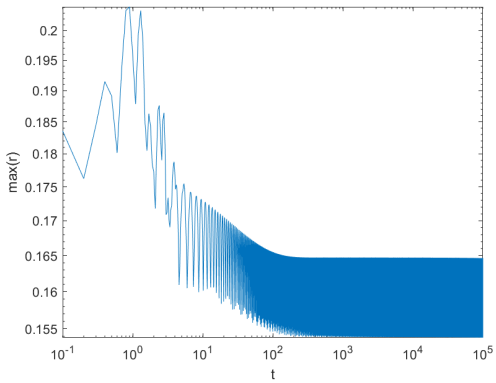

Figure 4.17: Loglog plot of small mass limit leading solitary wave amplitude with $\mu = 1/16$ for all t up to 10^5.

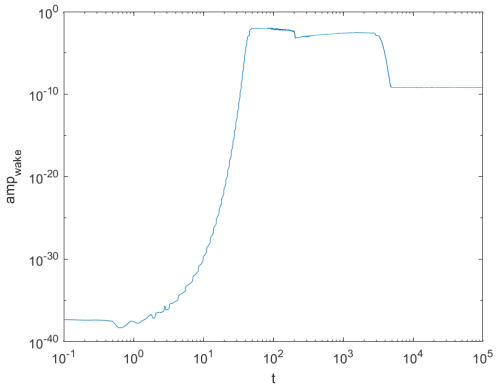

Figure 4.18: Loglog plot of small mass limit ripple amplitude with $\mu = 1/16$ for all t up to 10^5.

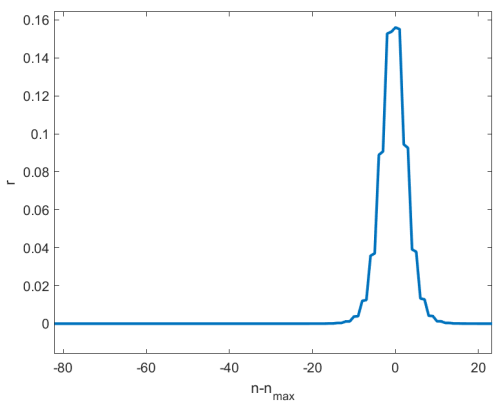

Figure 4.19: Small mass limit with $\mu = 1/32$.

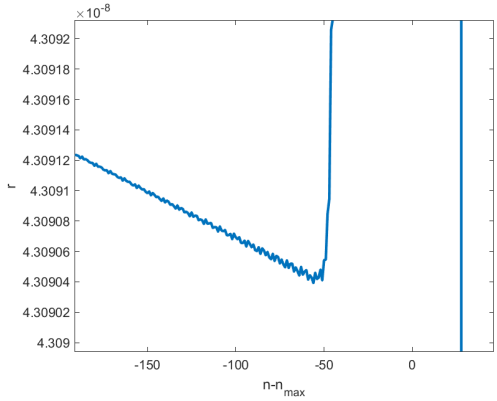

Figure 4.20: Small mass limit with $\mu = 1/32$, zoomed in on ripples.

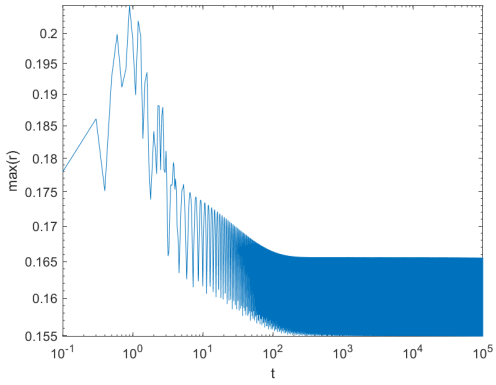

Figure 4.21: Loglog plot of small mass limit leading solitary wave amplitude with $\mu = 1/32$ for all t up to 10^5.

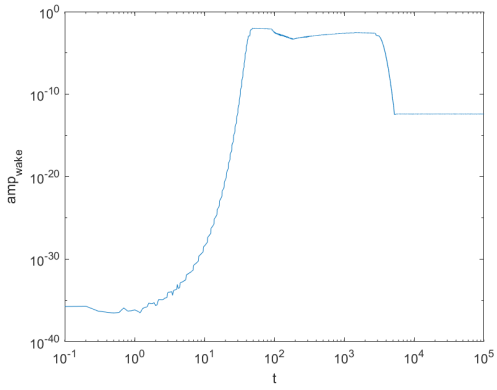

Figure 4.22: Loglog plot of small mass limit ripple amplitude with $\mu = 1/32$ for all t up to 10^5.

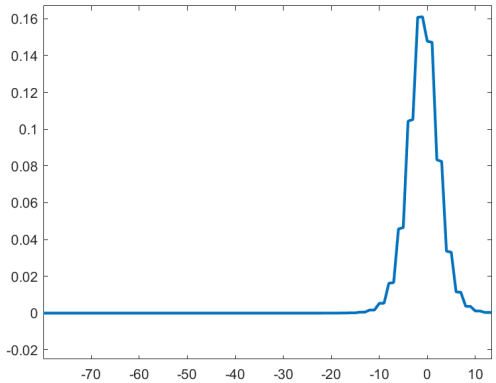

Figure 4.23: Small mass limit with $\mu = 1/64$.

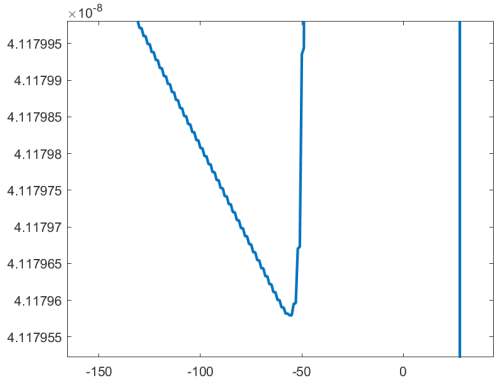

Figure 4.24: Small mass limit with $\mu = 1/64$, zoomed in on ripples.

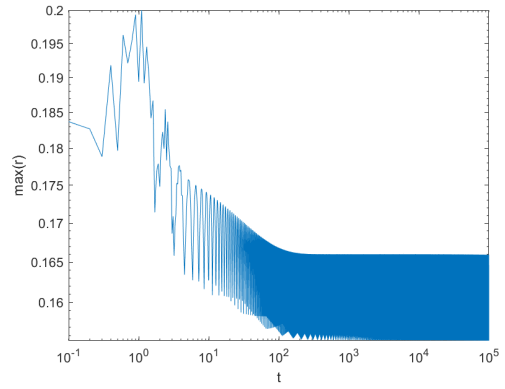

Figure 4.25: Loglog plot of small mass limit leading solitary wave amplitude with $\mu = 1/64$ for all t up to 10^5.

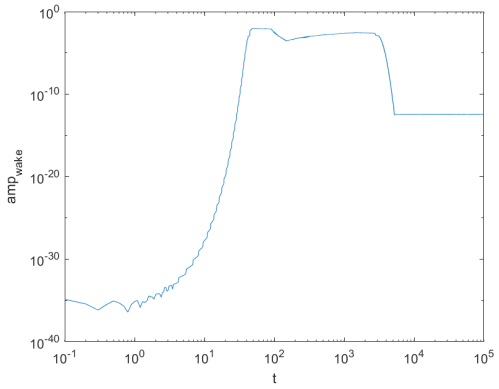

Figure 4.26: Loglog plot of small mass limit ripple amplitude with $\mu = 1/64$ for all t up to 10^5.

These results show us that as $\mu \to 0$, the wave looks more and more like the monatomic wave. We see in the amplitude plots that, at around $t = 10^2$, the amplitudes start to swing around a certain average value. This average value gets closer to the average value of the amplitude of the monatomic wave as μ gets smaller. The ripple also gets smaller as μ gets smaller and displays similar behavior to the tail of the monatomic wave. Figures 4.20 and 4.24 show a similar upward trend in the tail. Figures 4.12, 4.16 and 4.20 show how the amplitudes of the ripples seem to get smaller as the ripple gets further away from the leading solitary wave. These amplitudes may eventually even approach zero as $t \to \infty$, which approaches the monatomic, since there are no ripples.

4.3 Equal mass limit

For the equal mass limit we take $m_1 = 1$ and $m_2 = 1 + \mu$ with $\mu = 2^{-n}$ for $n \in \{2, 3, 4, 5, 6\}$. The results are seen below.

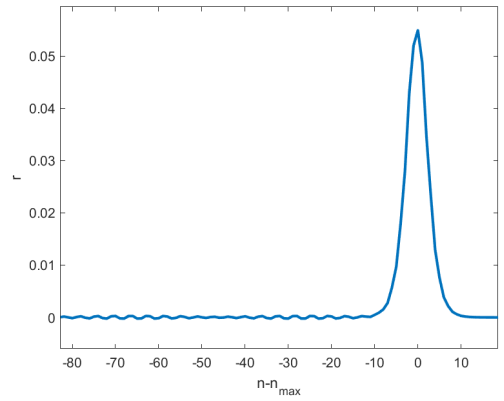

Figure 4.27: Equal mass limit with $\mu = 1/4$.

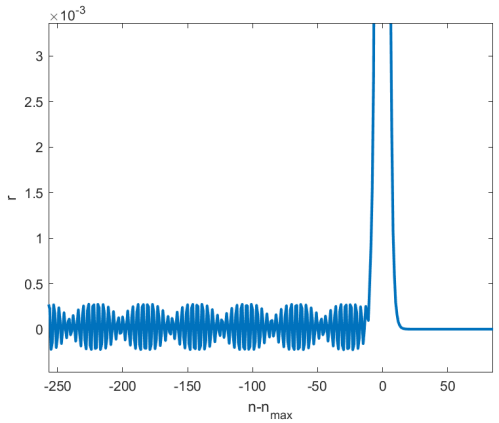

Figure 4.28: Equal mass limit with $\mu = 1/4$, zoomed in on ripples.

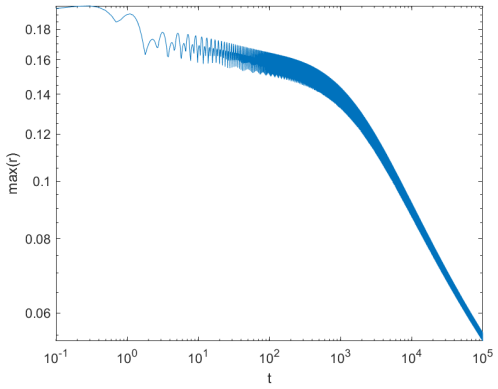

Figure 4.29: Loglog plot of equal mass limit leading solitary wave amplitude with $\mu = 1/4$ for all t up to 10^5.

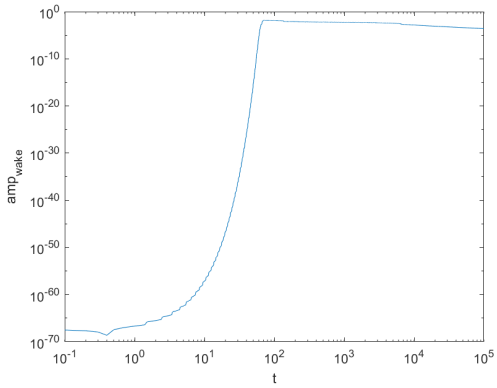

Figure 4.30: Loglog plot of small mass limit ripple amplitude with $\mu = 1/4$ for all t up to 10^5.

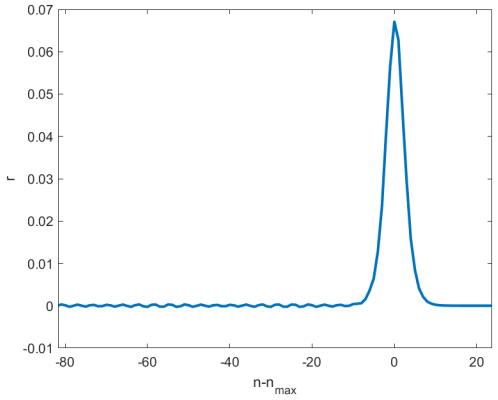

Figure 4.31: Equal mass limit with $\mu = 1/8$.

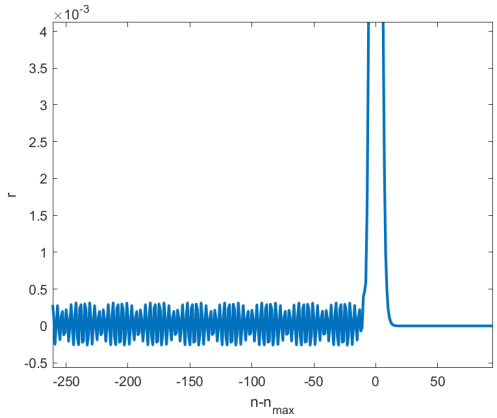

Figure 4.32: Equal mass limit with $\mu = 1/8$, zoomed in on ripples.

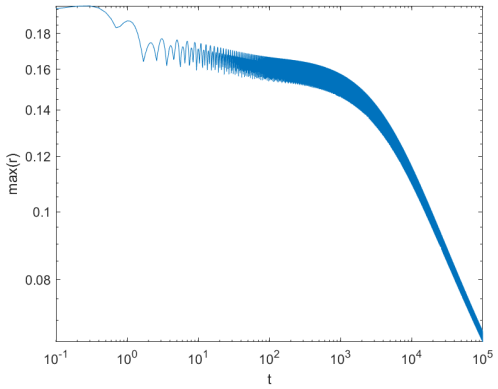

Figure 4.33: Loglog plot of equal mass limit leading solitary wave amplitude with $\mu = 1/8$ for all t up to 10^5.

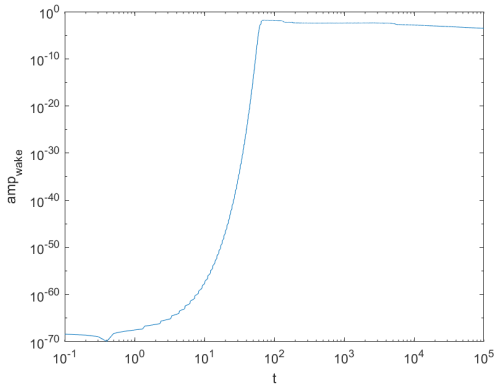

Figure 4.34: Loglog plot of small mass limit ripple amplitude with $\mu = 1/8$ for all t up to 10^5.

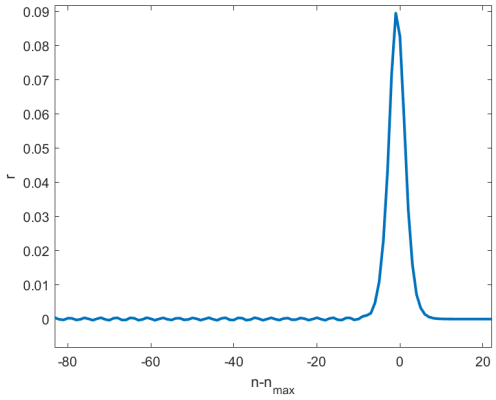

Figure 4.35: Equal mass limit with $\mu = 1/16$.

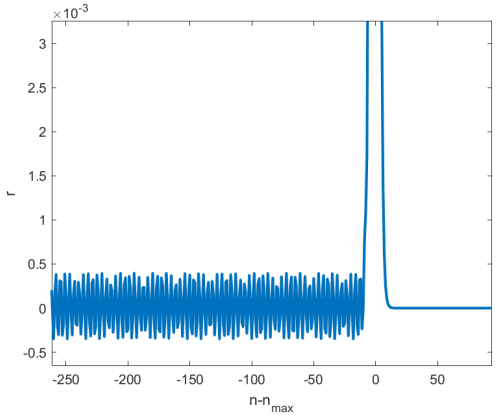

Figure 4.36: Equal mass limit with $\mu = 1/16$, zoomed in on ripples.

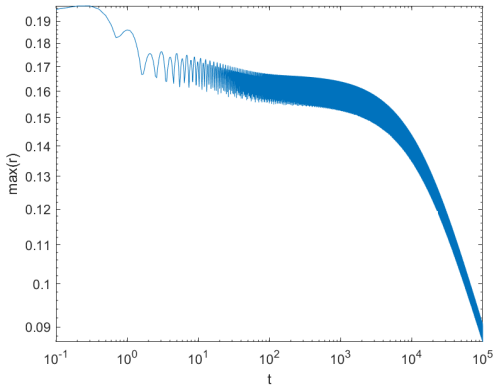

Figure 4.37: Loglog plot of equal mass limit leading solitary wave amplitude with $\mu = 1/16$ for all t up to 10^5.

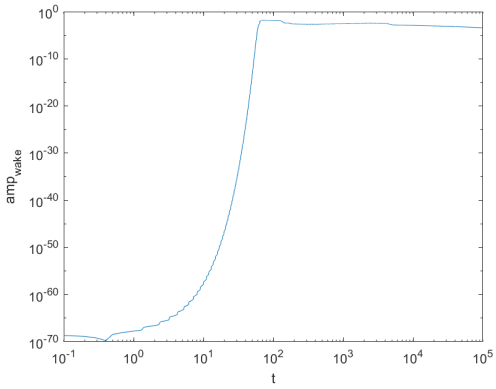

Figure 4.38: Loglog plot of small mass limit ripple amplitude with $\mu = 1/16$ for all t up to 10^5.

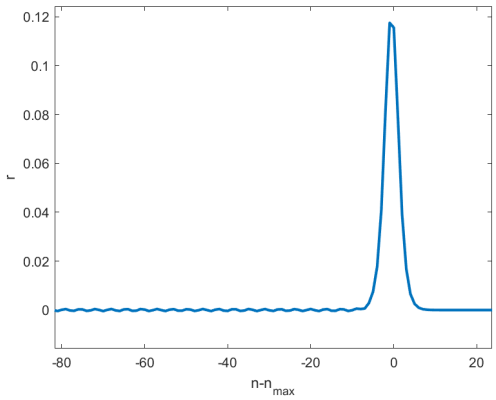

Figure 4.39: Equal mass limit with $\mu = 1/32$.

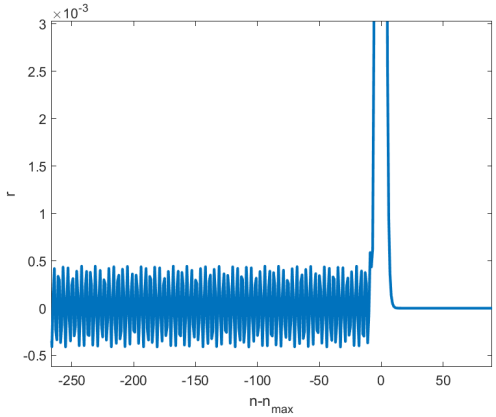

Figure 4.40: Equal mass limit with $\mu = 1/32$, zoomed in on ripples.

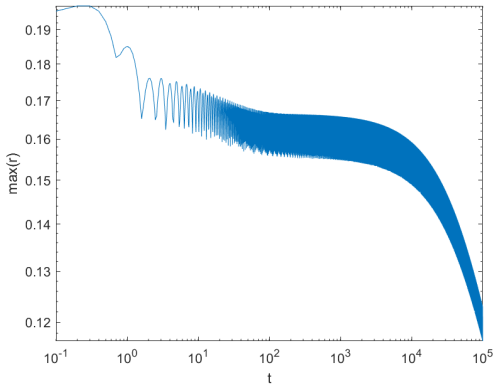

Figure 4.41: Loglog plot of equal mass limit leading solitary wave amplitude with $\mu = 1/32$ for all t up to 10^5.

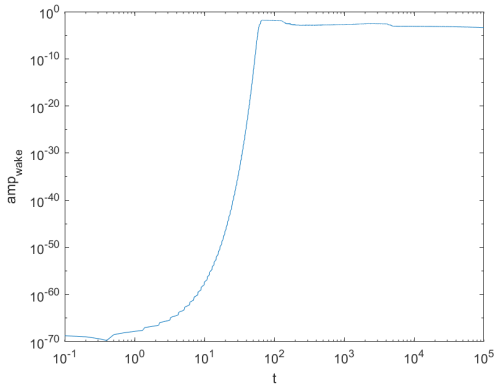

Figure 4.42: Loglog plot of small mass limit ripple amplitude with $\mu = 1/32$ for all t up to 10^5.

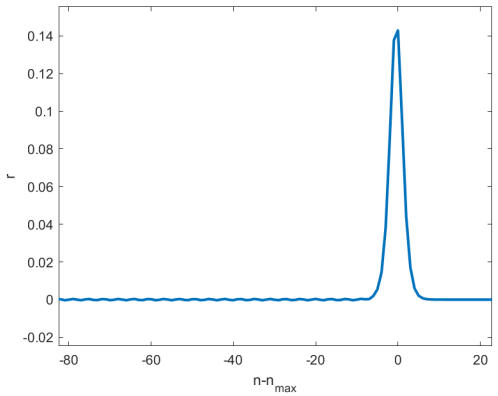

Figure 4.43: Equal mass limit with $\mu = 1/64$.

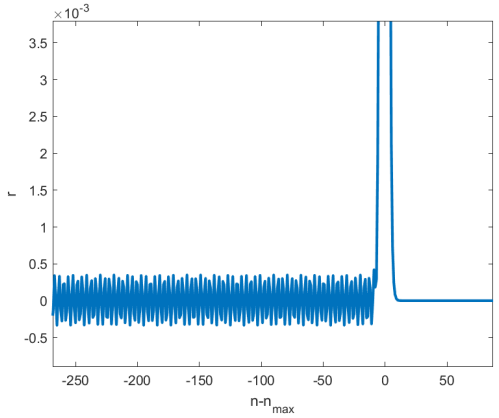

Figure 4.44: Equal mass limit with $\mu = 1/64$, zoomed in on ripples.

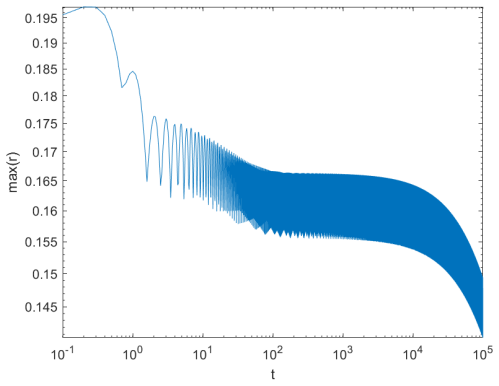

Figure 4.45: Loglog plot of equal mass limit leading solitary wave amplitude with $\mu = 1/64$ for all t up to 10^5.

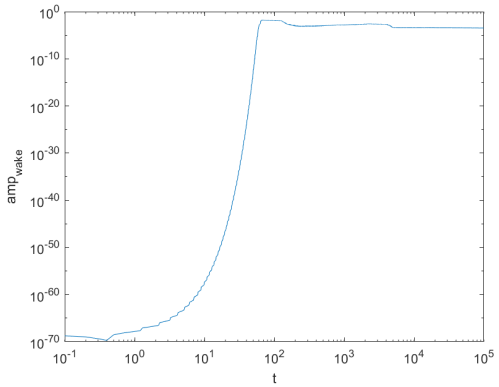

Figure 4.46: Loglog plot of small mass limit ripple amplitude with $\mu = 1/64$ for all t up to 10^5.

The results show us that the equal mass limit shows somewhat similar behavior to the monatomic case as $\mu \to 0$. The ripple envelopes seem to get squished together, which is a certain way of approaching the non-ripple tail of the monatomic wave. The ripple seems to oscillate around 0 more quickly as μ gets closer to 0. The decay of amplitude of the leading solitary wave happens more quickly in the equal mass limit as seen in the figures. The amplitude seems to rapidly decay for times beyond $t = 10^3$ in Figures 4.29, 4.33 and 4.37, however, since these plots are loglog plots, this actually translates into algebraic

decay in real time against real amplitude. Moreover, as we take μ smaller, this rapid decay in the loglog plots seems to get postponed more and more. In Figures 4.41 and 4.45 the rapid decay starts around $t = 10^4$. Before this decay happens, the values of the amplitude actually oscillate around the same average value as the monatomic wave amplitude. In Figure 4.47 below, a plot of the time it takes before the amplitude has reached half its size for various values of μ is given. This plot is an interpolation of 16 data points. The plot clearly shows, as μ approaches zero, the time it takes to decay to half its size increases drastically.

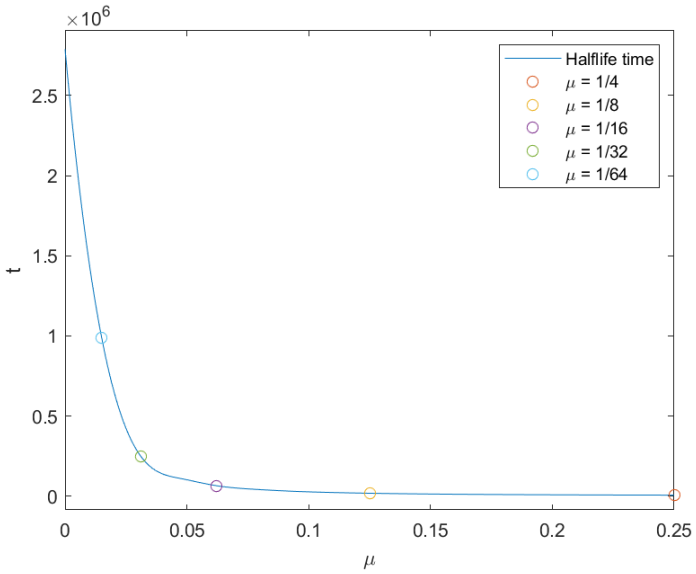

Figure 4.47: Equal mass half life time interpolation of 16 data points, for $\mu = i/64$ for $i = 1, \ldots, 16$.

4.4 Stiff spring limit

For the stiff spring limit we have two cases. In the first case, all masses are the same and we periodically vary the spring force function such that $F_n(r) = F_{n+2}(r)$ for all $n \in \mathbb{Z}$, which results in a spring dimer. In the second case, we periodically vary the masses, such that $m_n = m_{n+2}$, while varying the spring force function in a similar fashion, which results in a general dimer.

4.4.1 Spring dimer

We take $F_1(r) = \kappa r + r^2$ and $F_2(r) = r + r^2$ where $\kappa = 5, 10, 15, 20, 25, 100, 300$. The results are seen below.

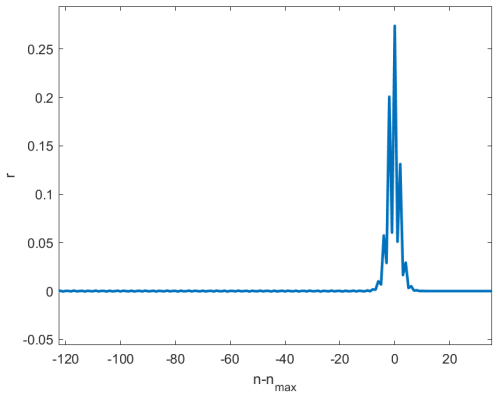

Figure 4.48: Spring dimer with $\kappa = 5$.

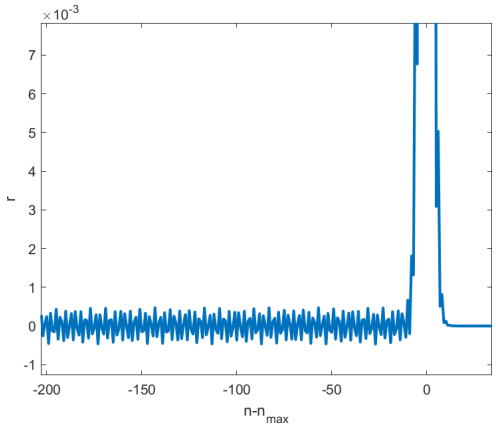

Figure 4.49: Spring dimer ripples with $\kappa = 5$.

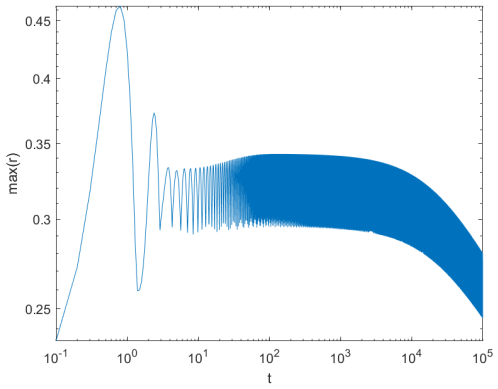

Figure 4.50: Loglog plot of spring dimer leading solitary wave amplitude with $\kappa = 5$ for all t up to 10^5.

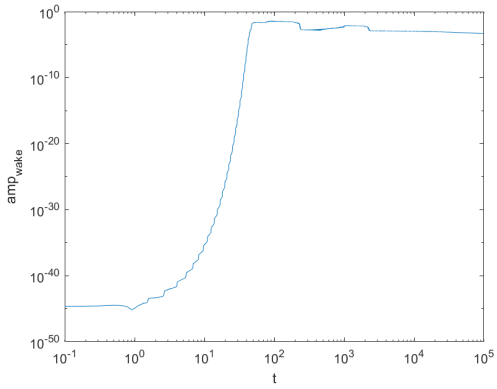

Figure 4.51: Loglog plot of spring dimer ripple amplitude with $\kappa = 5$ for all t up to 10^5.

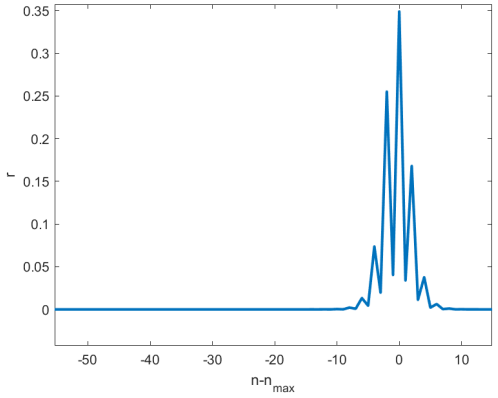

Figure 4.52: Spring dimer with $\kappa = 10$.

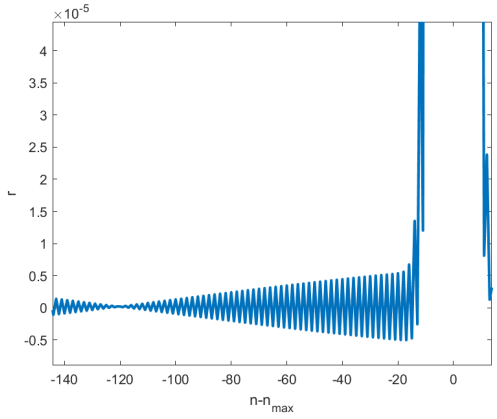

Figure 4.53: Spring dimer ripples with $\kappa = 10$.

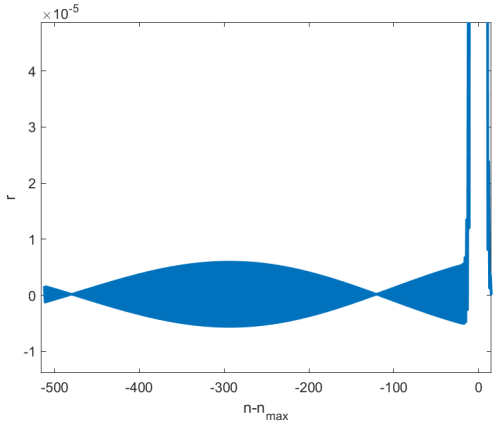

Figure 4.54: Spring dimer ripples with $\kappa = 10$, zoomed out.

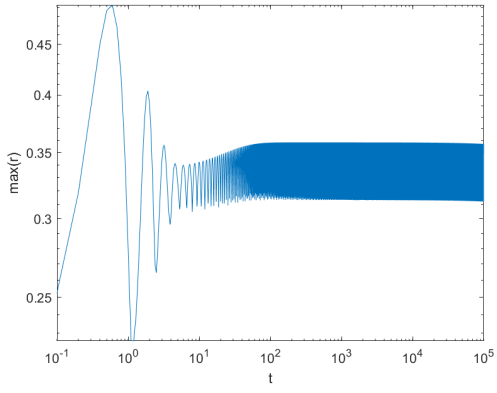

Figure 4.55: Loglog plot of spring dimer leading solitary wave amplitude with $\kappa = 10$ for all t up to 10^5.

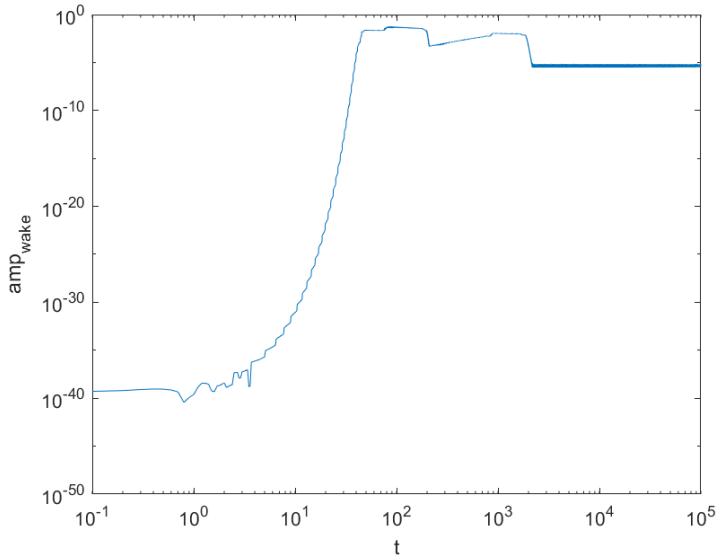

Figure 4.56: Loglog plot of spring dimer ripple amplitude with $\kappa = 10$ for all t up to 10^5.

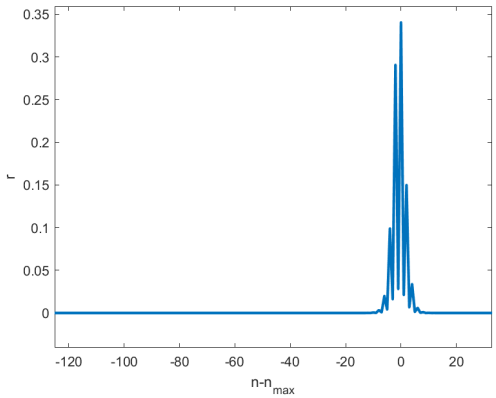

Figure 4.57: Spring dimer with $\kappa = 15$.

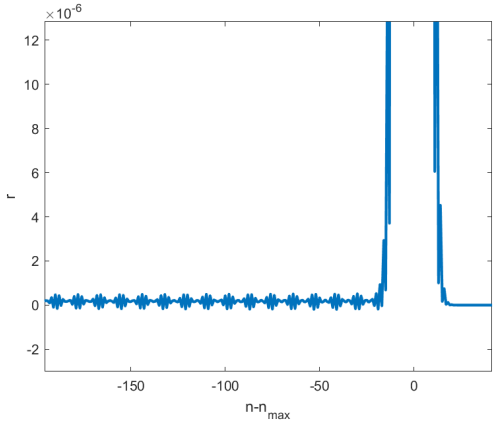

Figure 4.58: Spring dimer ripples with $\kappa = 15$.

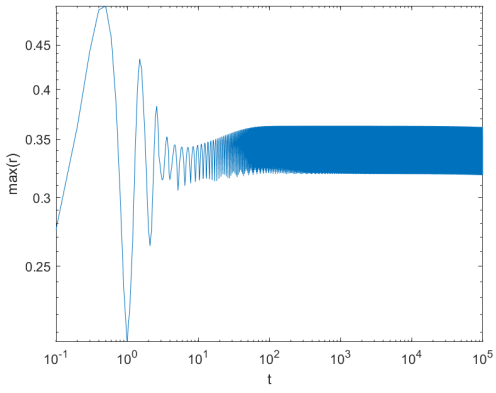

Figure 4.59: Loglog plot of spring dimer leading solitary wave amplitude with $\kappa = 15$ for all t up to 10^5.

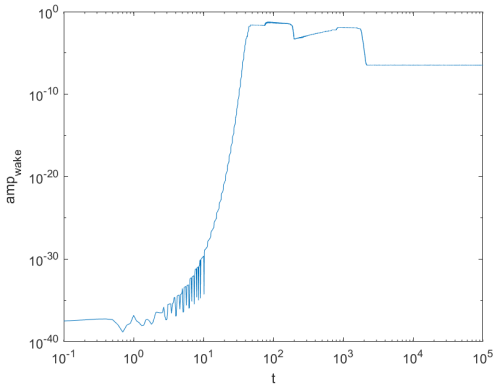

Figure 4.60: Loglog plot of spring dimer ripple amplitude with $\kappa = 15$ for all t up to 10^5.

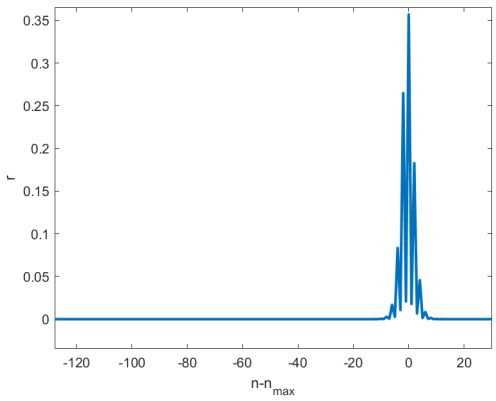

Figure 4.61: Spring dimer with $\kappa = 20$.

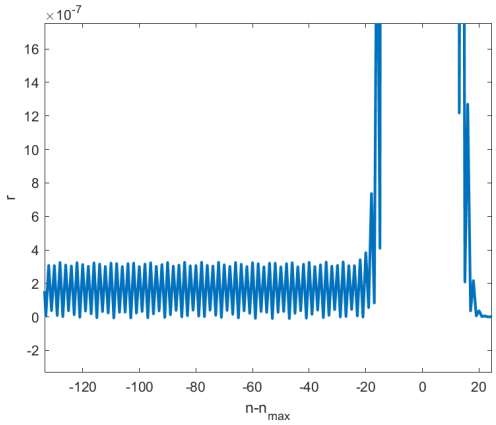

Figure 4.62: Spring dimer ripples with $\kappa = 20$.

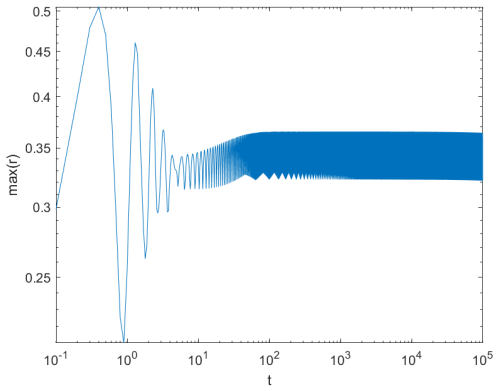

Figure 4.63: Loglog plot of spring dimer leading solitary wave amplitude with $\kappa = 20$ for all t up to 10^5.

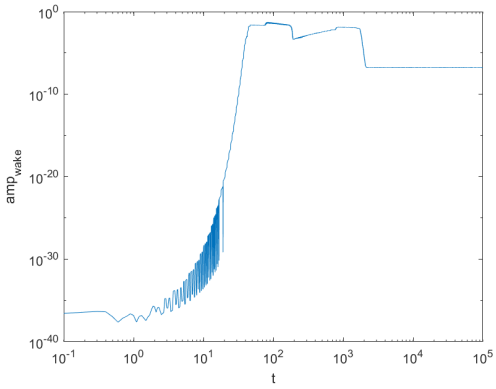

Figure 4.64: Loglog plot of spring dimer ripple amplitude with $\kappa = 20$ for all t up to 10^5.

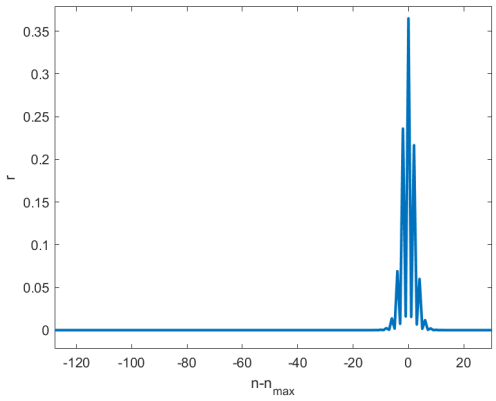

Figure 4.65: Spring dimer with $\kappa = 25$.

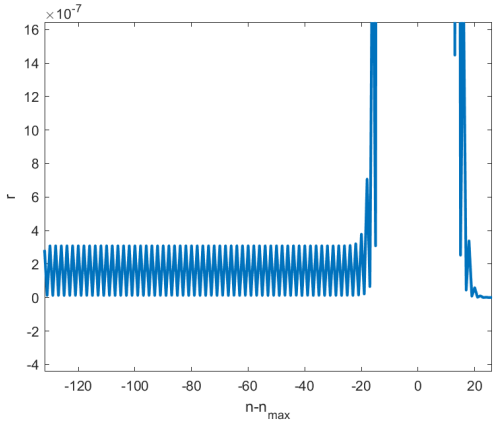

Figure 4.66: Spring dimer ripples with $\kappa = 25$.

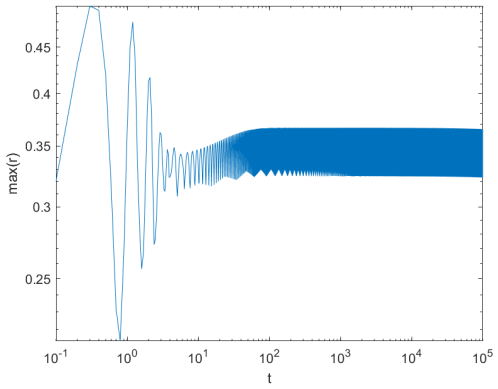

Figure 4.67: Loglog plot of spring dimer leading solitary wave amplitude with $\kappa = 25$ for all t up to 10^5.

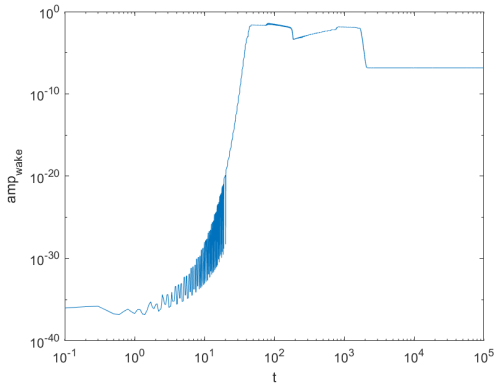

Figure 4.68: Loglog plot of spring dimer ripple amplitude with $\kappa = 25$ for all t up to 10^5.

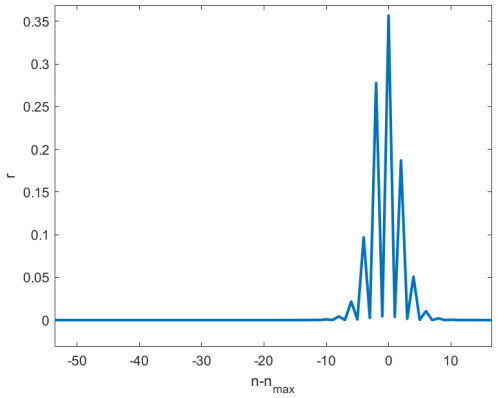

Figure 4.69: Spring dimer with $\kappa = 100$.

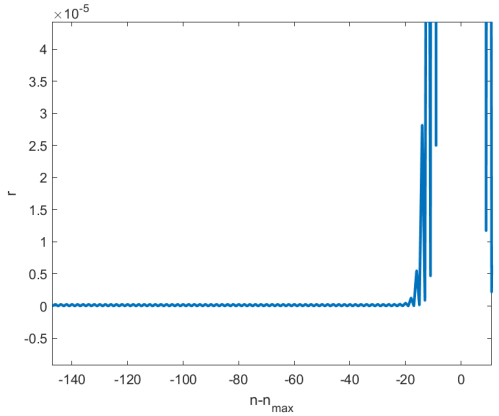

Figure 4.70: Spring dimer ripples with $\kappa = 100$.

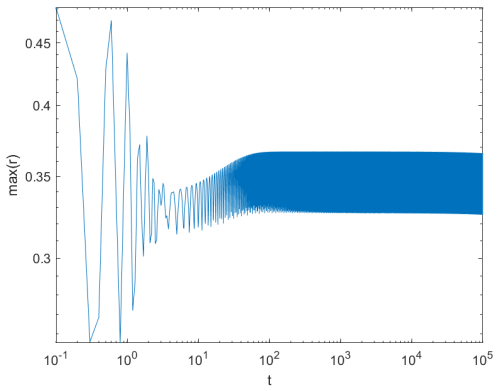

Figure 4.71: Loglog plot of spring dimer leading solitary wave amplitude with $\kappa = 100$ for all t up to 10^5.

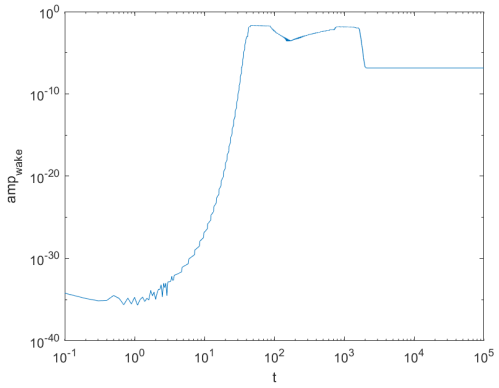

Figure 4.72: Loglog plot of spring dimer ripple amplitude with $\kappa = 100$ for all t up to 10^5.

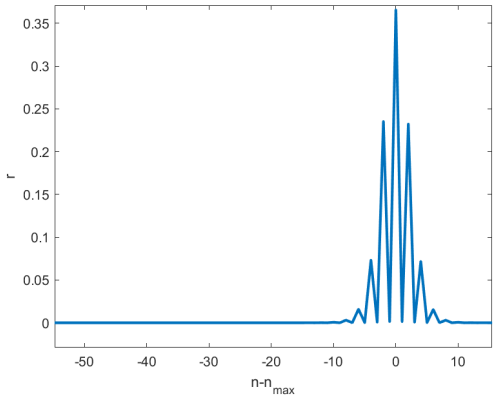

Figure 4.73: Spring dimer with $\kappa = 300$.

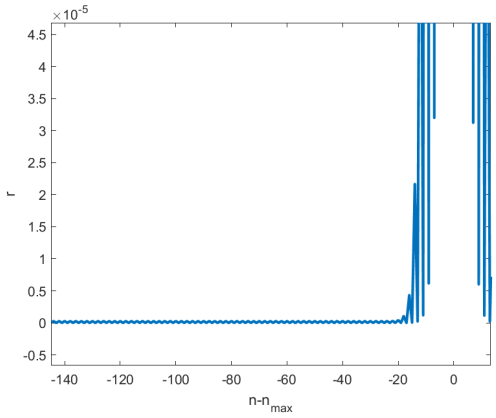

Figure 4.74: Spring dimer ripples with $\kappa = 300$.

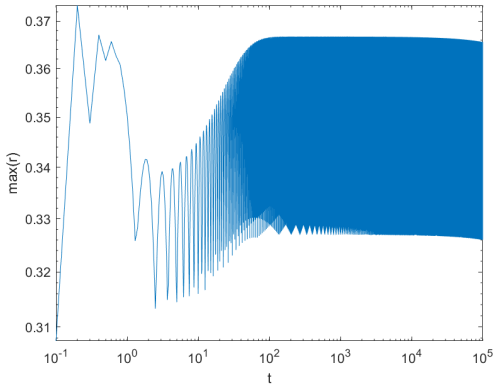

Figure 4.75: Loglog plot of spring dimer leading solitary wave amplitude with $\kappa = 300$ for all t up to 10^5.

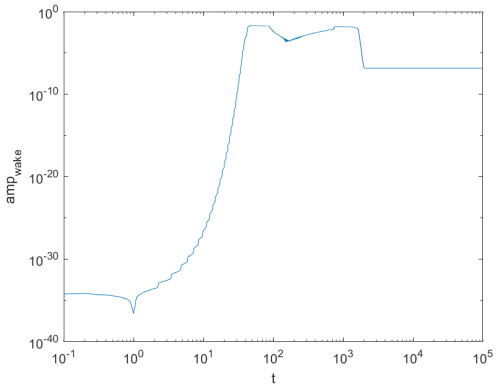

Figure 4.76: Loglog plot of spring dimer ripple amplitude with $\kappa = 300$ for all t up to 10^5.

For the stiff spring limit in the spring dimer case, the amplitudes of the solitary waves start oscillating around a certain value again at around $t = 10^2$, as seen in Figures 4.55, 4.71 and 4.75. The amplitudes behave similarly to the monatomic wave amplitude, but the amplitudes in this case are about double the size of the monatomic wave amplitude. For $\kappa = 5$, the amplitude shows again this kind of rapid decay as we have seen in the equal mass limit, which translates to algebraic decay in a regular plot. As κ gets bigger, we see that this rapid decay gets delayed to the point where we do not see it in our limited time period. The ripples change from one shape to the other, not showing a clear behavioral pattern, but they eventually settle into a small, regular patterned, jagged shaped ripple. In Figures 4.70 and 4.74 there seems to be no difference in size of the ripples. As κ gets bigger, it appears that the ripples do not change much anymore. We observe a certain jaggedness in the relative displacement figures. We call these jagged waves "stegotons", as mentioned in [19].The jagged phenomena resembles the behavior of the long wave solutions to spring dimers from [19], which ultimately arises from a coefficient on the leading order term in the nanopteron that depends on the parity of lattice index n. In the stiff spring limit, since there are dramatic differences between successive springs, we expect such stegoton behavior here. This behavior will "smooth out" when we consider only even/odd-indexed sites, since there the coefficient's behavior will be the same throughout.

4.4.2 General dimer

We take $m_1 = 1$ and $m_2 = 1/2$. $F_1(r) = r + r^2$ and $F_2(r) = \kappa r + r^2$ where $\kappa = 5, 10, 15, 17, 20, 100, 250$. The results are seen below.

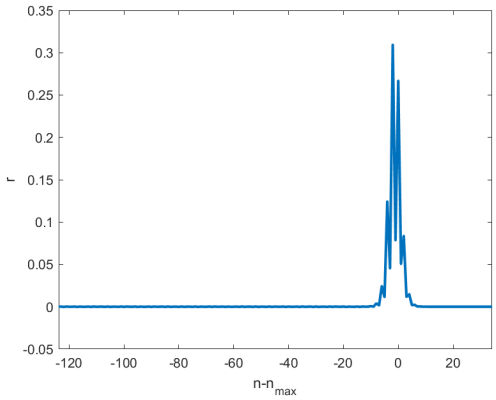

Figure 4.77: General dimer with $\kappa = 5$.

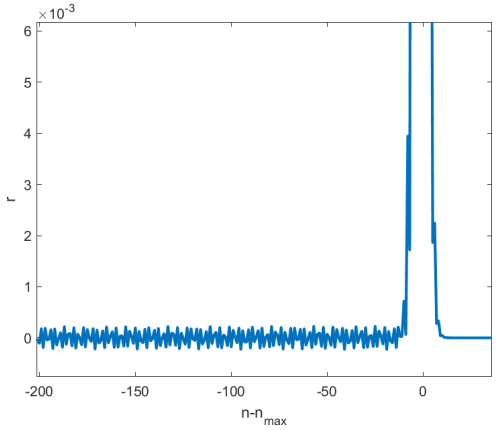

Figure 4.78: General dimer ripples with $\kappa = 5$.

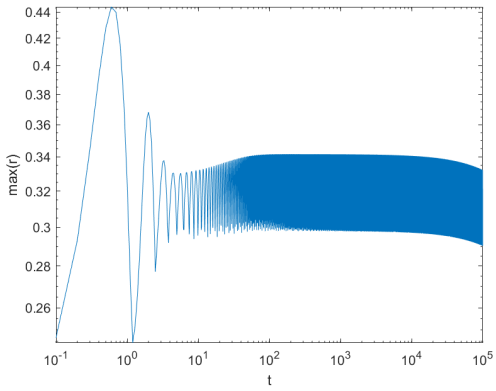

Figure 4.79: Loglog plot of general dimer leading solitary wave amplitude with $\kappa = 5$ for all t up to 10^5.

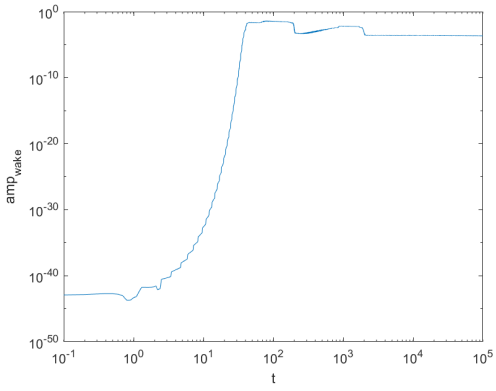

Figure 4.80: Loglog plot of general dimer ripple amplitude with $\kappa = 5$ for all t up to 10^5.

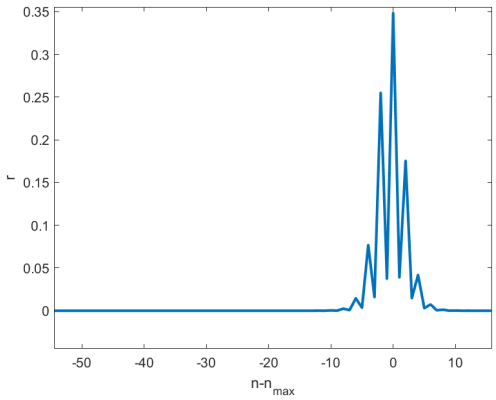

Figure 4.81: General dimer with $\kappa = 10$.

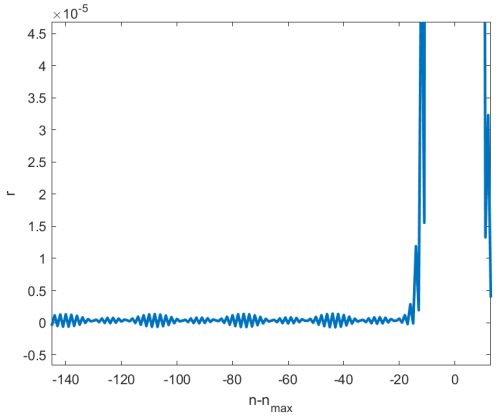

Figure 4.82: General dimer ripples with $\kappa = 10$.

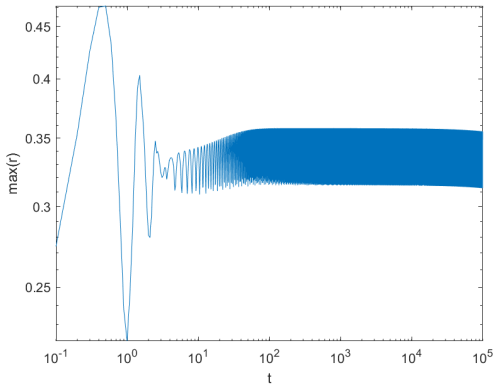

Figure 4.83: Loglog plot of general dimer leading solitary wave amplitude with $\kappa = 10$ for all t up to 10^5.

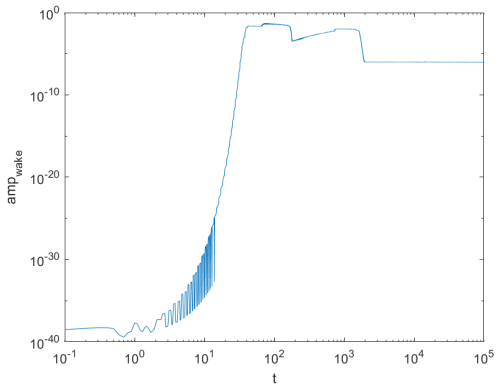

Figure 4.84: Loglog plot of general dimer ripple amplitude with $\kappa = 10$ for all t up to 10^5.

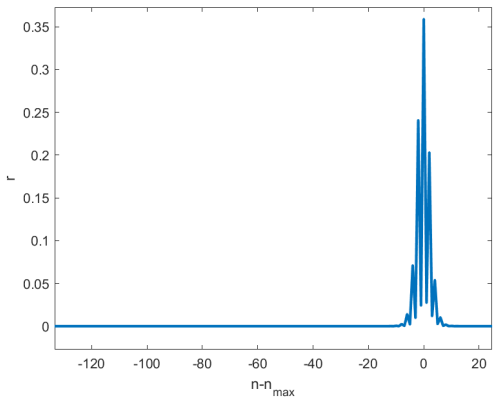

Figure 4.85: General dimer with $\kappa = 15$.

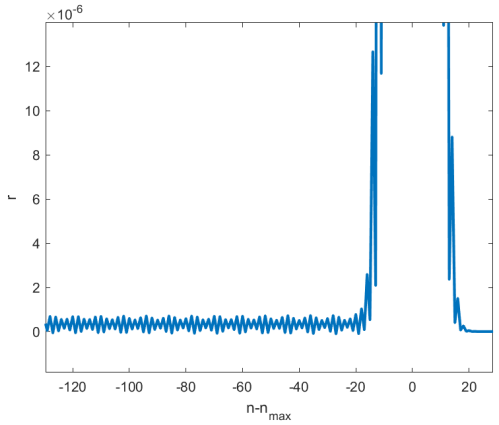

Figure 4.86: General dimer ripples with $\kappa = 15$.

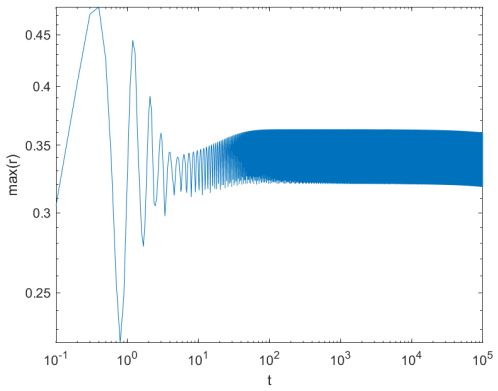

Figure 4.87: Loglog plot of general dimer leading solitary wave amplitude with $\kappa = 15$ for all t up to 10^5.

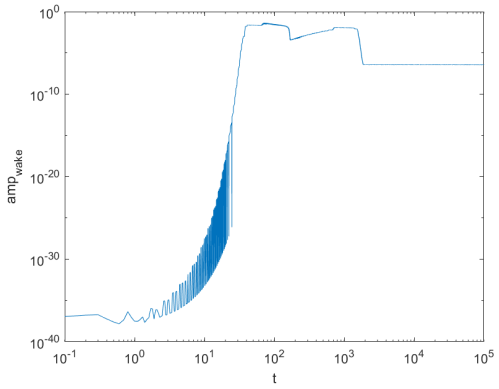

Figure 4.88: Loglog plot of general dimer ripple amplitude with $\kappa = 15$ for all t up to 10^5.

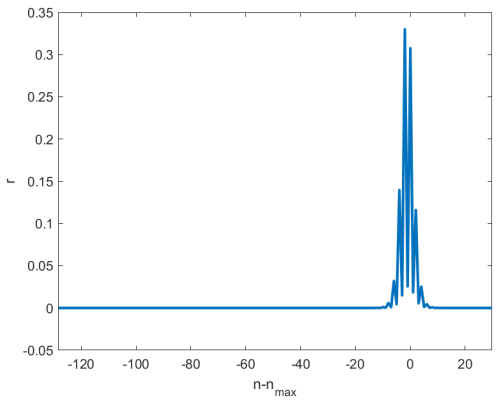

Figure 4.89: General dimer with $\kappa = 17$.

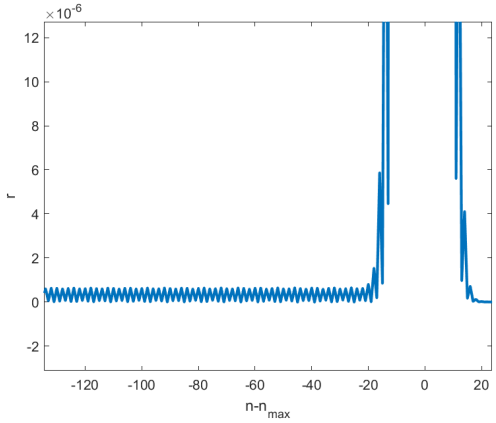

Figure 4.90: General dimer ripples with $\kappa = 17$.

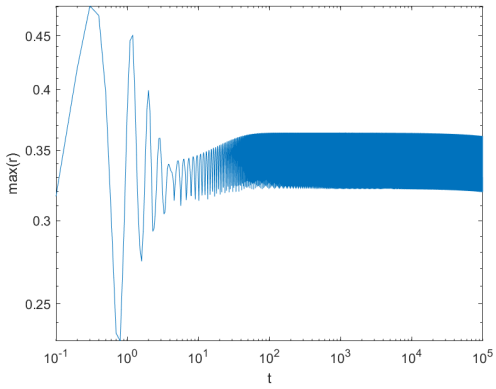

Figure 4.91: Loglog plot of general dimer leading solitary wave amplitude with $\kappa = 17$ for all t up to 10^5.

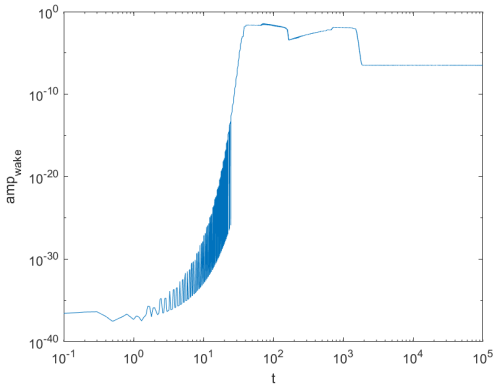

Figure 4.92: Loglog plot of general dimer ripple amplitude with $\kappa = 17$ for all t up to 10^5.

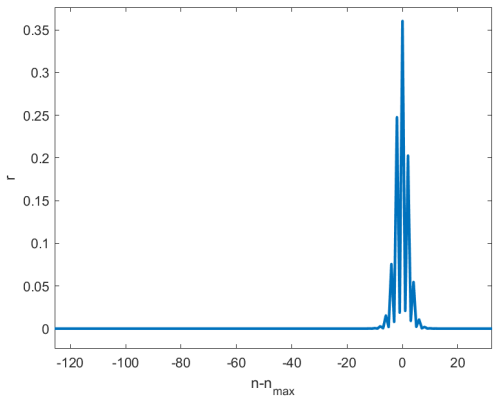

Figure 4.93: General dimer with $\kappa = 20$.

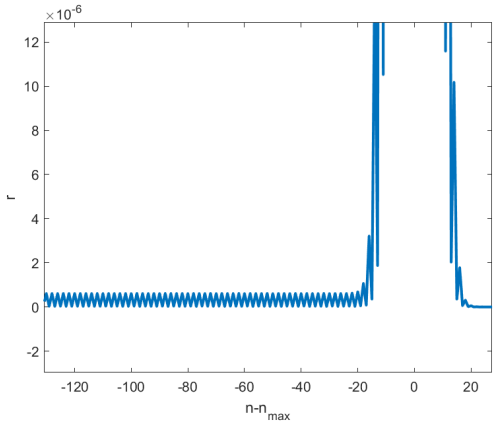

Figure 4.94: General dimer ripples with $\kappa = 20$.

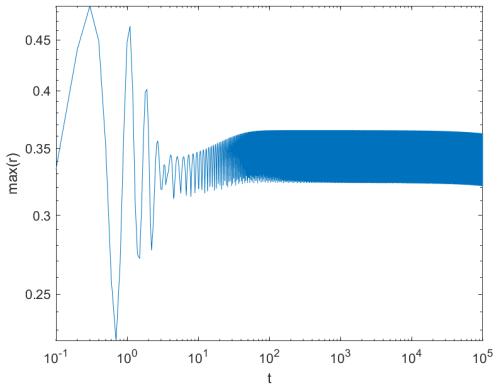

Figure 4.95: Loglog plot of general dimer leading solitary wave amplitude with $\kappa = 20$ for all t up to 10^5.

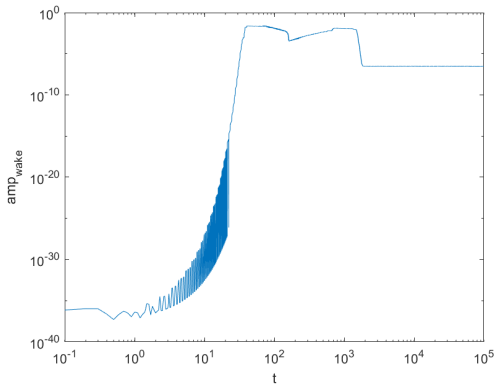

Figure 4.96: Loglog plot of general dimer ripple amplitude with $\kappa = 20$ for all t up to 10^5.

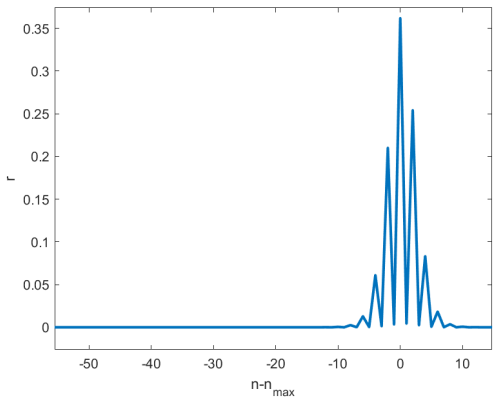

Figure 4.97: General dimer with $\kappa = 100$.

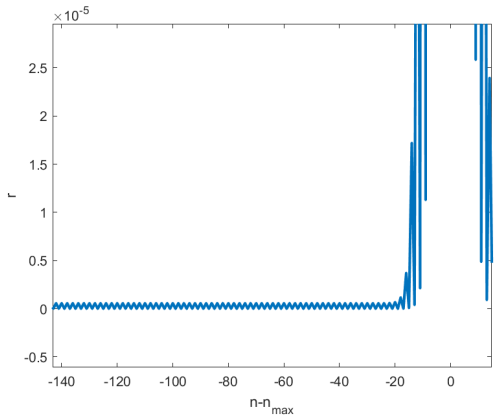

Figure 4.98: General dimer ripples with $\kappa = 100$.

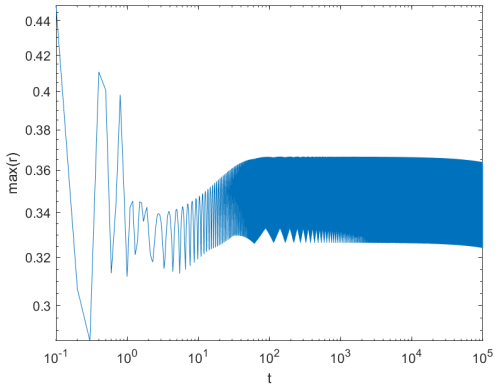

Figure 4.99: Loglog plot of general dimer leading solitary wave amplitude with $\kappa = 5$ for all t up to 10^5.

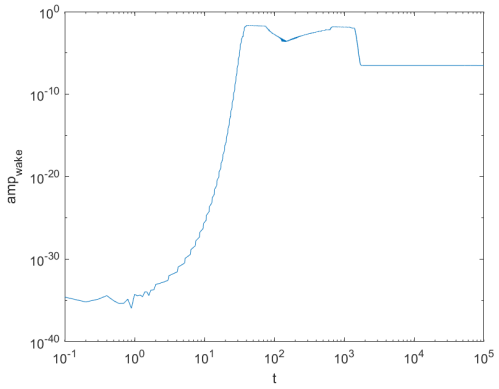

Figure 4.100: Loglog plot of general dimer ripple amplitude with $\kappa = 100$ for all t up to 10^5.

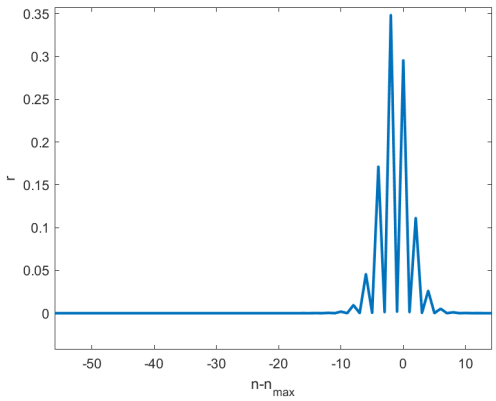

Figure 4.101: General dimer with $\kappa = 250$.

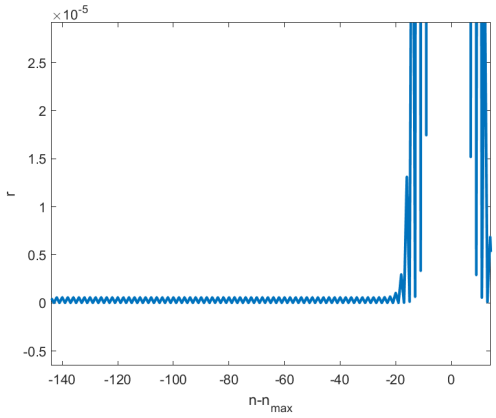

Figure 4.102: General dimer ripples with $\kappa = 250$.

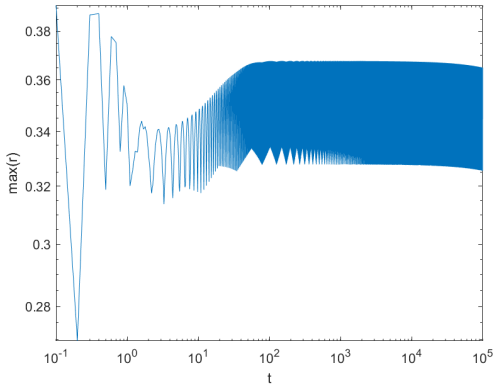

Figure 4.103: Loglog plot of general dimer leading solitary wave amplitude with $\kappa = 250$ for all t up to 10^5.

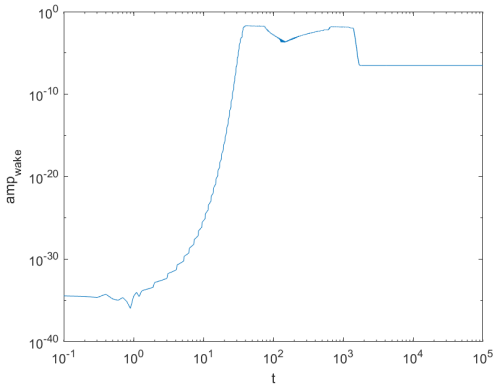

Figure 4.104: Loglog plot of general dimer ripple amplitude with $\kappa = 250$ for all t up to 10^5.

For the stiff spring limit in the general dimer case, we see again the same behavior for the amplitude of the leading solitary wave. The amplitudes starts oscillating around a certain value and decays very slowly from $t = 10^2$ onward, which is similar to the monatomic case, except for the fact that the amplitude is more than doubled. The ripple shows similar behavior as in the spring dimer case. There is no clear behavioral pattern to be seen as κ gets bigger, but eventually the ripple settles into a regular patterned, jagged ripple. For the latter two values of κ the ripple appears to show no difference in size or pattern. Just as in the spring dimer case, we observe again the "stegoton"-type effect in the relative displacement figures.

4.5 Odd and even simulations

We will be looking at the behavior of the even and odd indexed relative displacements of the various limits. For the simulations we take $\epsilon = 1/4$. The results of the simulations are seen in the following subsections. The figures shown are at $t = 10^5$.

4.5.1 Small mass limit

For the small mass limit we have $m_1 = 1$ and $m_2 = \mu$ with $\mu = 2^{-n}$ for $n \in \{2, 3\}$.

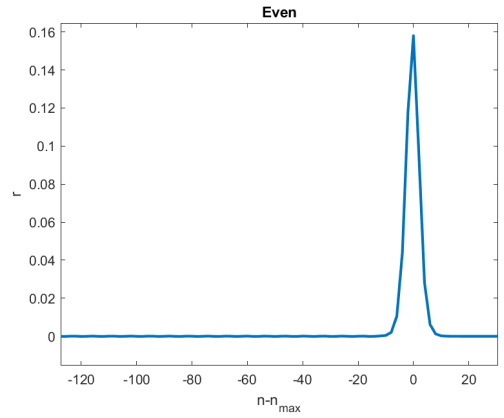

Figure 4.105: Even indexed small mass limit with $\mu = 1/4$.

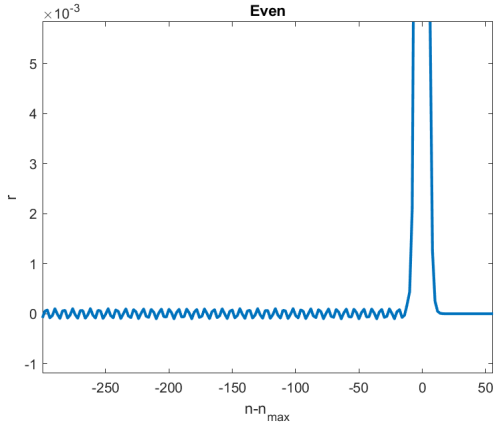

Figure 4.106: Even indexed small mass limit ripples with $\mu = 1/4$.

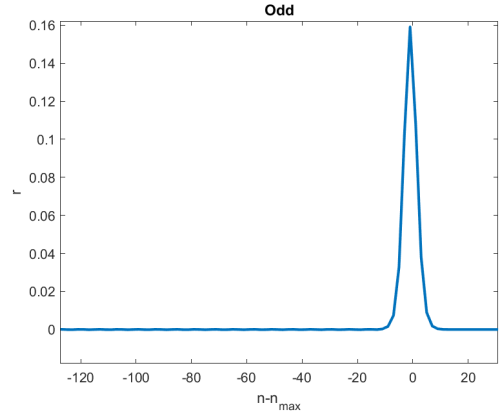

Figure 4.107: Odd indexed small mass limit with $\mu = 1/4$.

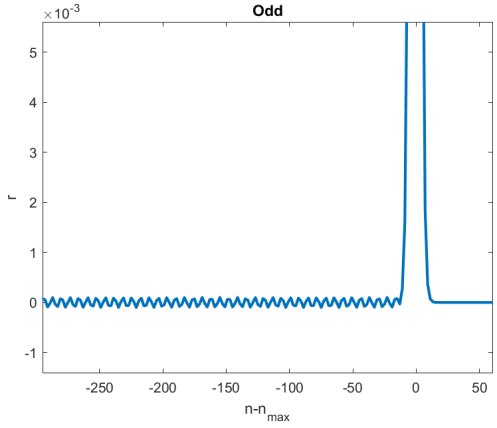

Figure 4.108: Odd indexed small mass limit ripples with $\mu = 1/4$.

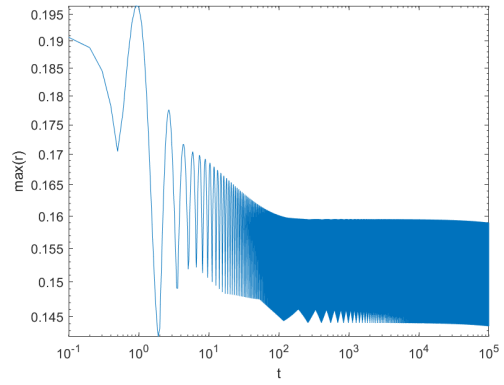

Figure 4.109: Even indexed small mass limit solitary wave amplitude with $\mu = 1/4$.

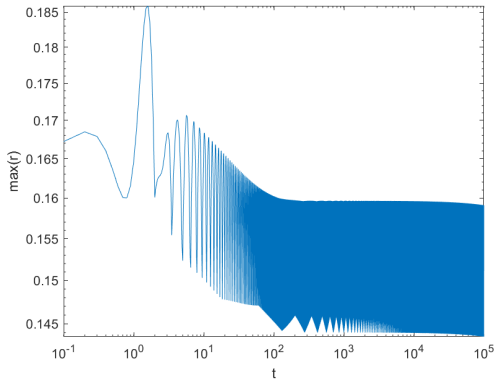

Figure 4.110: Odd indexed small mass limit solitary wave amplitude with $\mu = 1/4$.

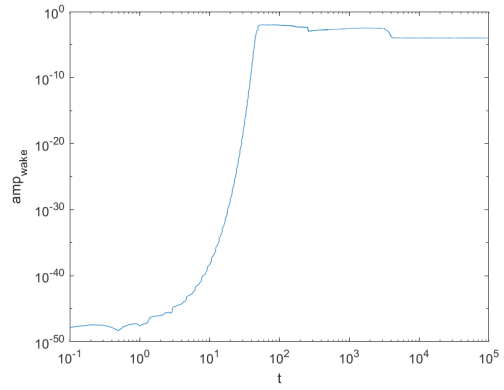

Figure 4.111: Even indexed small mass limit ripple amplitude with $\mu = 1/4$.

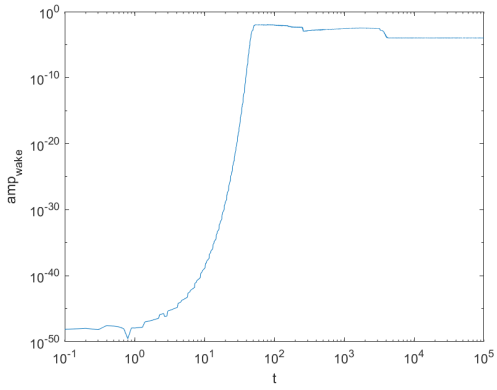

Figure 4.112: Odd indexed small mass limit ripple amplitude with $\mu = 1/4$.

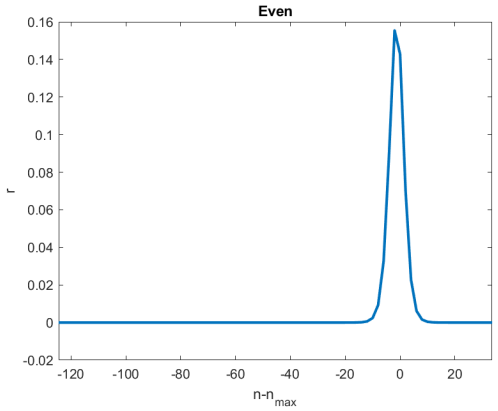

Figure 4.113: Even indexed small mass limit with $\mu = 1/8$.

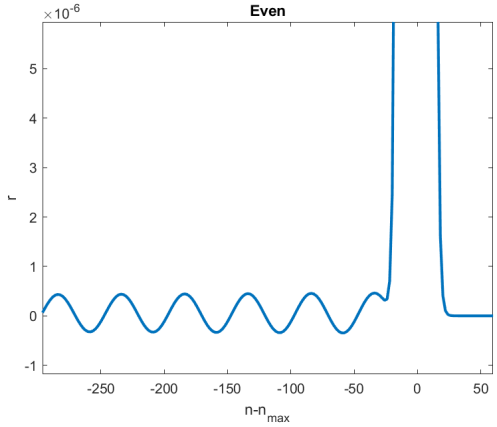

Figure 4.114: Even indexed small mass limit ripples with $\mu = 1/8$.

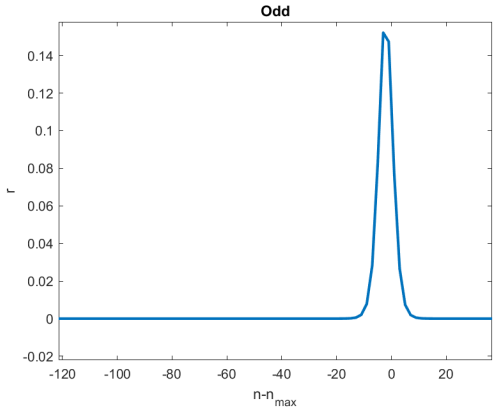

Figure 4.115: Odd indexed small mass limit with $\mu = 1/8$.

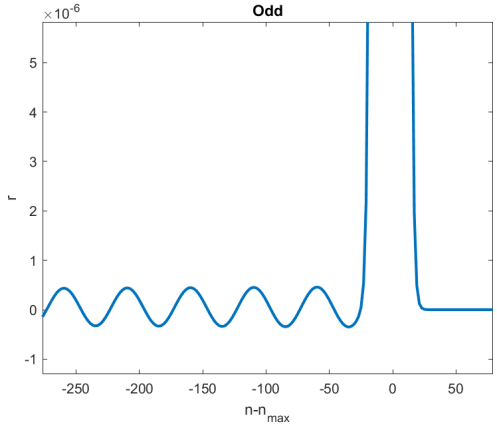

Figure 4.116: Odd indexed small mass limit ripples with $\mu = 1/8$.

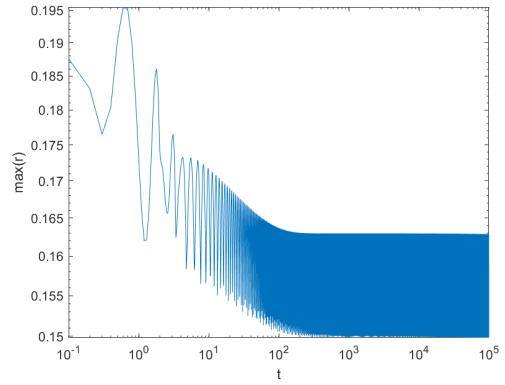

Figure 4.117: Even indexed small mass limit solitary wave amplitude with $\mu = 1/8$.

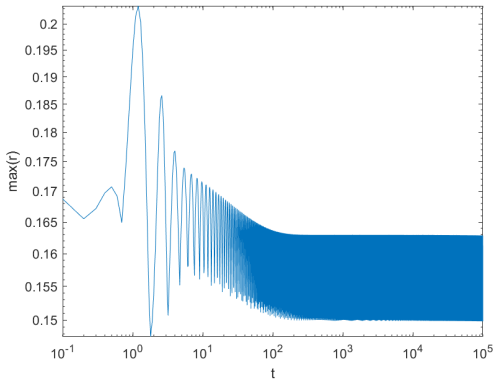

Figure 4.118: Odd indexed small mass limit solitary wave amplitude with $\mu = 1/8$.

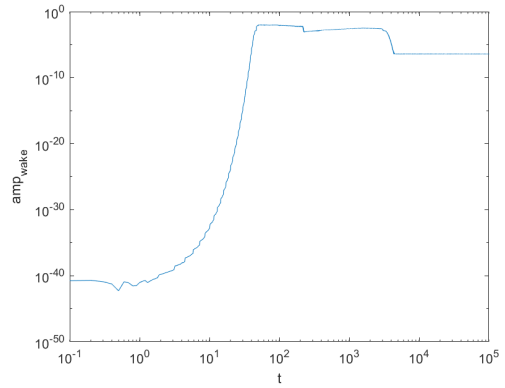

Figure 4.119: Even indexed small mass limit ripple amplitude with $\mu = 1/8$.

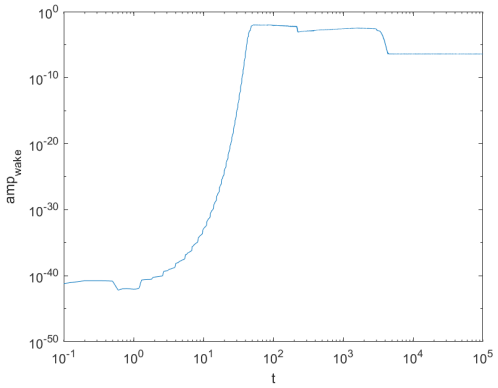

Figure 4.120: Odd indexed small mass limit ripple amplitude with $\mu = 1/8$.

For these values of μ we do not see a lot of differences in the amplitudes of the even and odd solitary waves. The ripples on the other hand are completely different from one another. For $\mu = 1/4$, we observe a certain jaggedness, similar to what we saw in the stegotons in the regular spring dimer and general dimer figures. This is not a real surprise, since if we compare these ripples to the regular small mass limit ripples in Figure 4.6, we observe similar behavior. For $\mu = 1/8$, we observe a calm and wavy ripple. Comparing these to Figure 4.11, we see instead some sort of envelopes taking shape, which would be the result of combining these even and odd graphs, since it appears that there is a peak in the even graph where there is a trough in the odd graph, and vice versa.

4.5.2 Equal mass limit

For the equal mass limit we have $m_1 = 1$ and $m_2 = 1 + \mu$ with $\mu = 2^{-n}$ for $n \in \{2, 3\}$. In these graphs we see how the period of the ripples gets smaller and smaller, which corresponds to the ripples getting more squished together in the regular graphs of the equal mass limit. Here, for $\mu = 1/4$ the ripples show a bigger period than for $\mu = 1/8$, which indicates that as μ gets smaller, the period of the ripples in these odd and even graphs gets smaller.

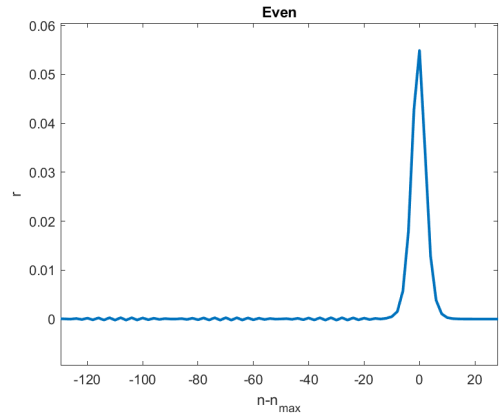

Figure 4.121: Even indexed equal mass limit with $\mu = 1/4$.

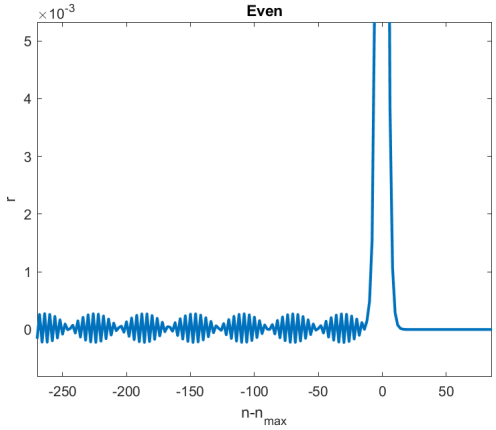

Figure 4.122: Even indexed equal mass limit ripples with $\mu = 1/4$.

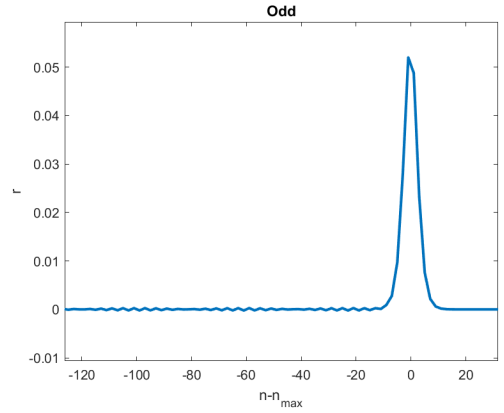

Figure 4.123: Odd indexed equal mass limit with $\mu = 1/4$.

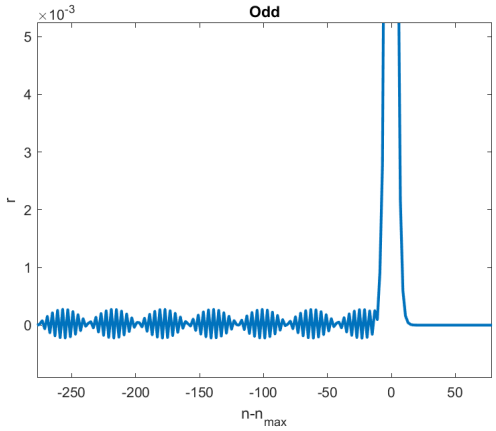

Figure 4.124: Odd indexed equal mass limit ripples with $\mu = 1/4$.

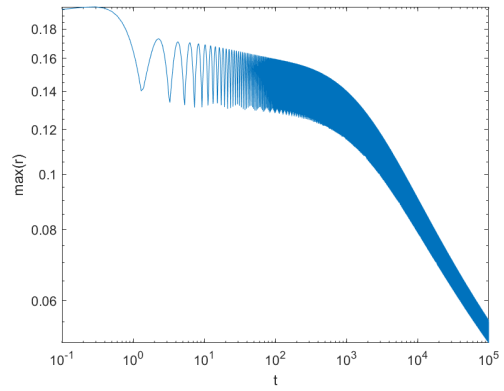

Figure 4.125: Even indexed equal mass limit solitary wave amplitude with $\mu = 1/4$.

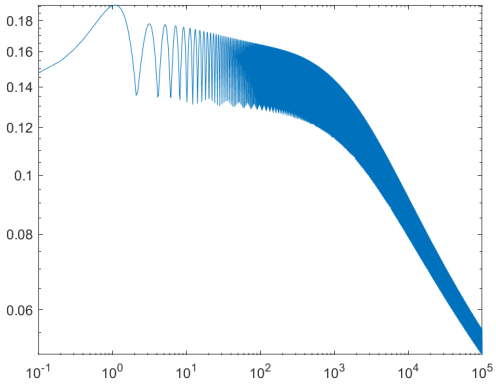

Figure 4.126: Odd indexed equal mass limit solitary wave amplitude with $\mu = 1/4$.

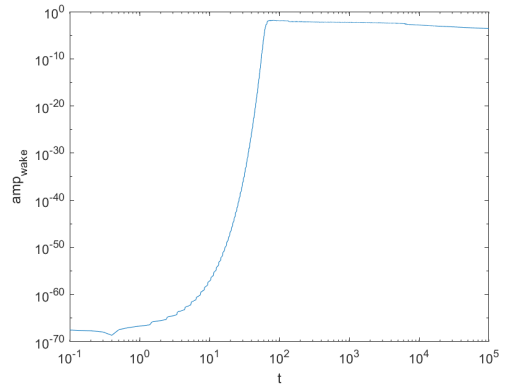

Figure 4.127: Even indexed equal mass limit ripple amplitude with $\mu = 1/4$.

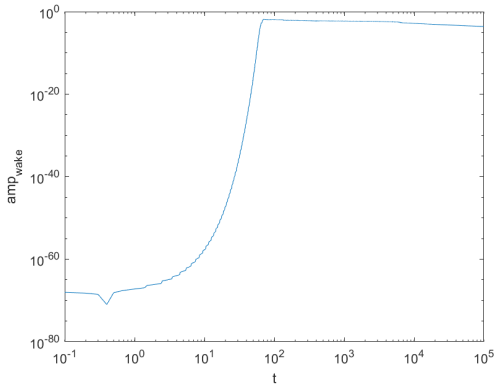

Figure 4.128: Odd indexed equal mass limit ripple amplitude with $\mu = 1/4$.

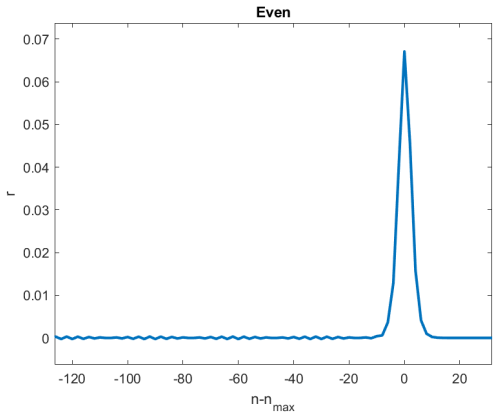

Figure 4.129: Even indexed equal mass limit with $\mu = 1/8$.

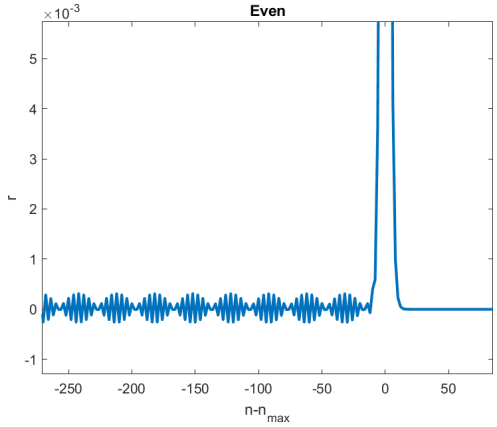

Figure 4.130: Even indexed equal mass limit ripples with $\mu = 1/8$.

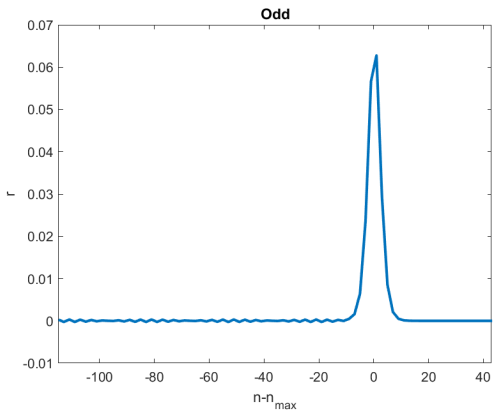

Figure 4.131: Odd indexed equal mass limit with $\mu = 1/8$.

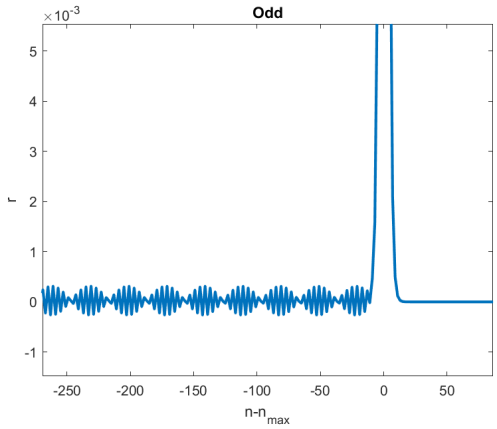

Figure 4.132: Odd indexed equal mass limit ripples with $\mu = 1/8$.

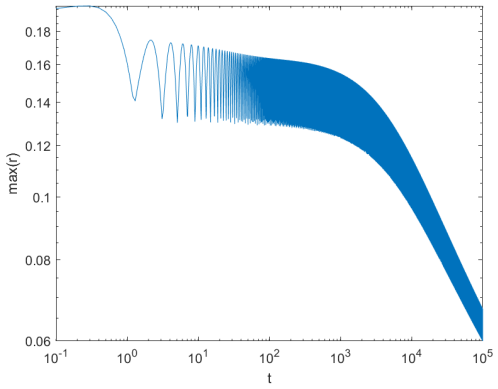

Figure 4.133: Even indexed equal mass limit solitary wave amplitude with $\mu = 1/8$.

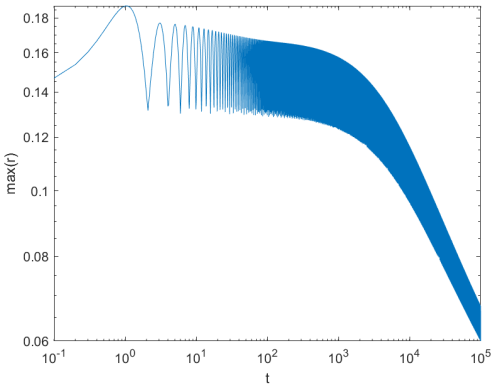

Figure 4.134: Odd indexed equal mass limit solitary wave amplitude with $\mu = 1/8$.

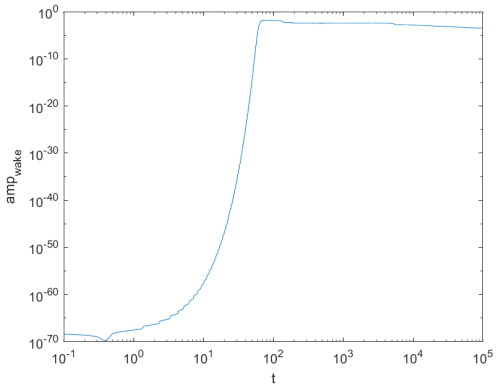

Figure 4.135: Even indexed equal mass limit ripple amplitude with $\mu = 1/8$.

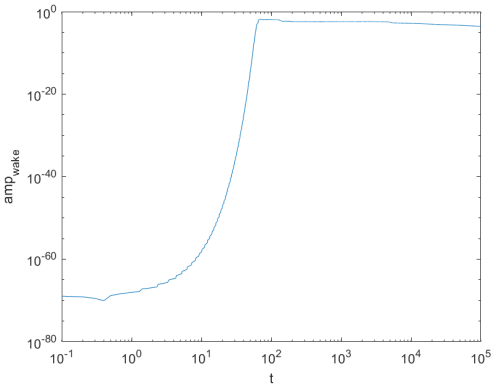

Figure 4.136: Odd indexed equal mass limit ripple amplitude with $\mu = 1/8$.

4.5.3 Stiff spring limit: spring dimer

For the spring dimer case of the stiff spring limit we have $m_1 = m_2 = 1$, $F_1(r) = \kappa r + r^2$ and $F_2(r) = r + r^2$ with $\kappa \in \{5, 10, 15, 20, 25, 100\}$.

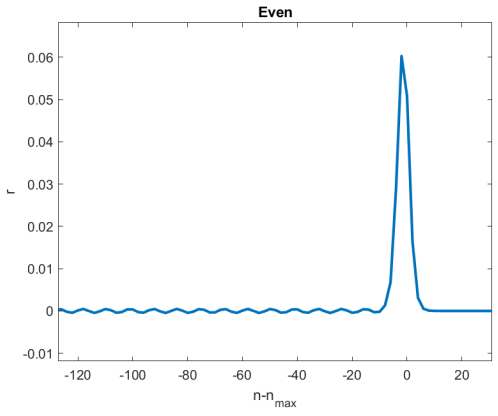

Figure 4.137: Even indexed spring dimer with $\kappa = 5$.

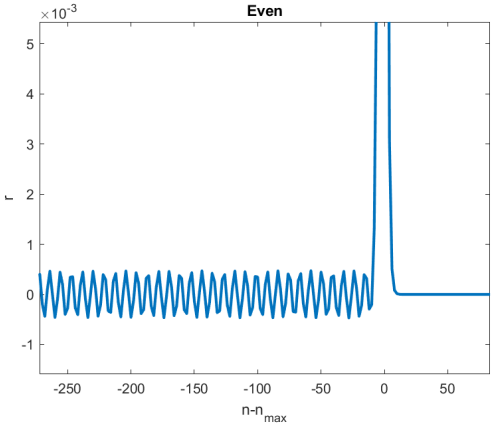

Figure 4.138: Even indexed spring dimer ripples with $\kappa = 5$.

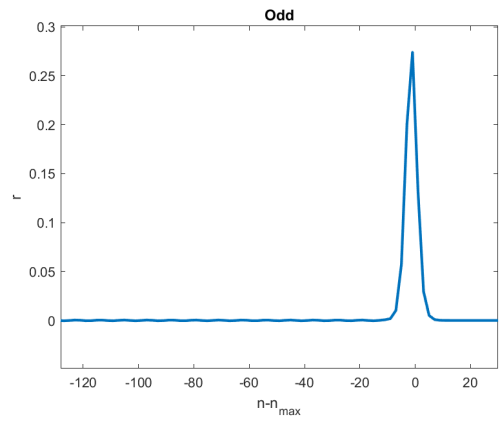

Figure 4.139: Odd indexed spring dimer with $\kappa = 5$.

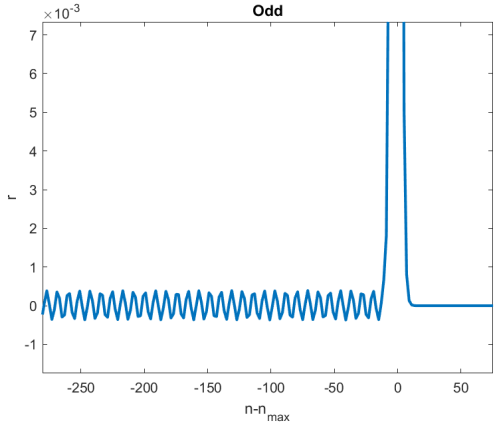

Figure 4.140: Odd indexed spring dimer ripples with $\kappa = 5$.

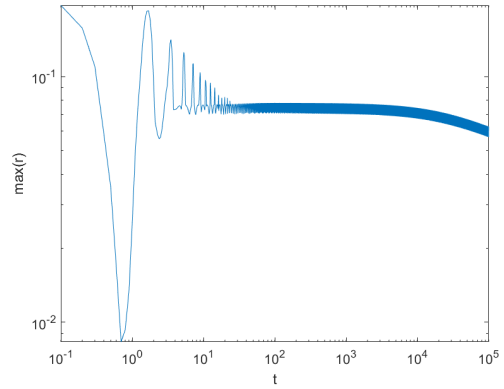

Figure 4.141: Even indexed spring dimer solitary wave amplitude with $\kappa = 5$.

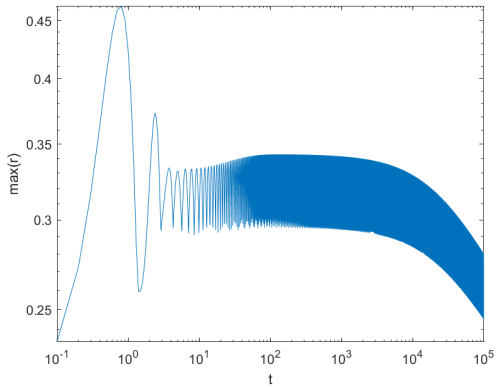

Figure 4.142: Odd indexed spring dimer solitary wave amplitude with $\kappa = 5$.

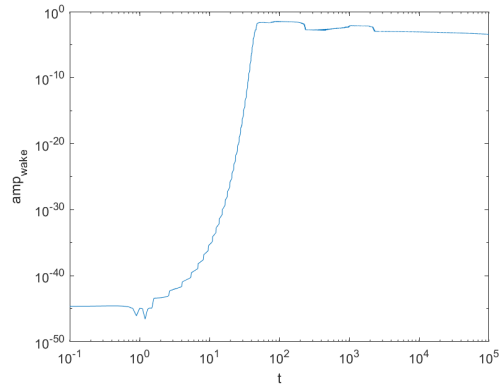

Figure 4.143: Even indexed spring dimer ripple amplitude with $\kappa = 5$.

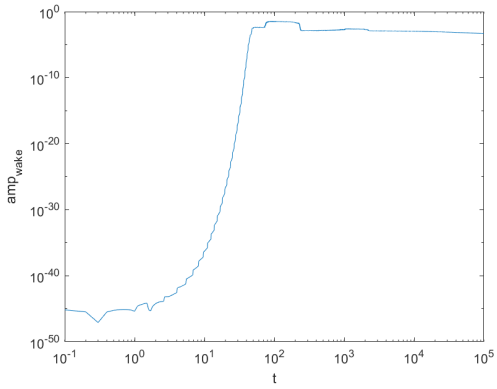

Figure 4.144: Odd indexed spring dimer ripple amplitude with $\kappa = 5$.

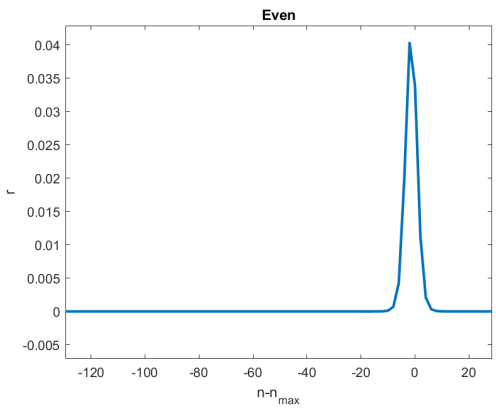

Figure 4.145: Even indexed spring dimer with $\kappa = 10$.

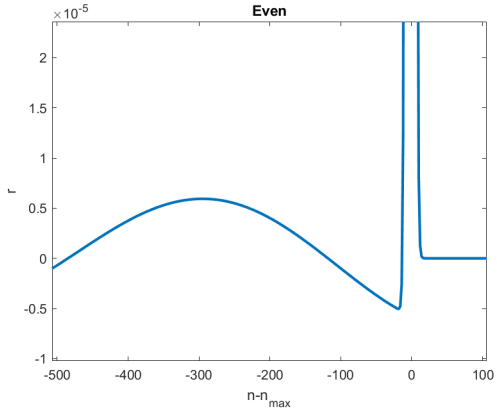

Figure 4.146: Even indexed spring dimer ripples with $\kappa = 10$.

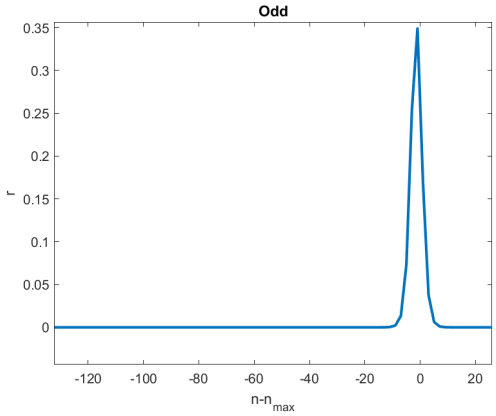

Figure 4.147: Odd indexed spring dimer with $\kappa = 10$.

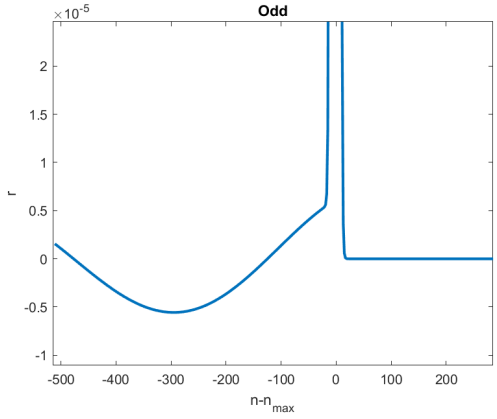

Figure 4.148: Odd indexed spring dimer ripples with $\kappa = 10$.

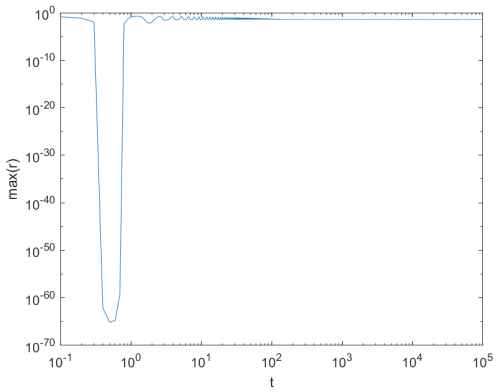

Figure 4.149: Even indexed spring dimer solitary wave amplitude with $\kappa = 10$.

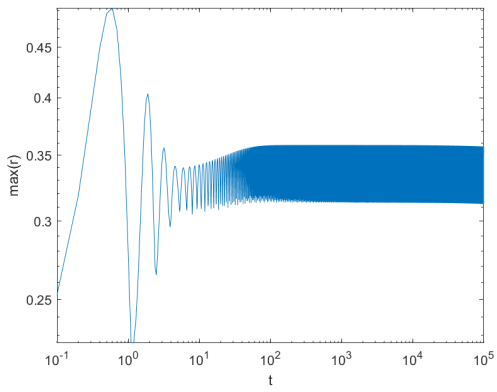

Figure 4.150: Odd indexed spring dimer solitary wave amplitude with $\kappa = 10$.

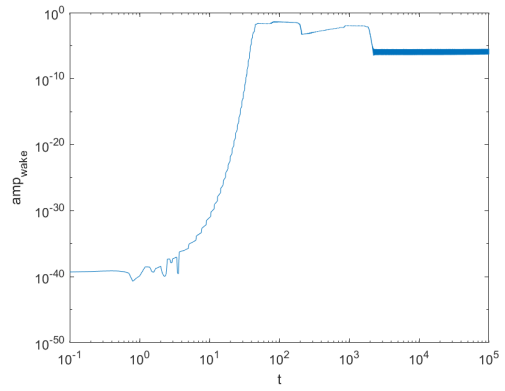

Figure 4.151: Even indexed spring dimer ripple amplitude with $\kappa = 10$.

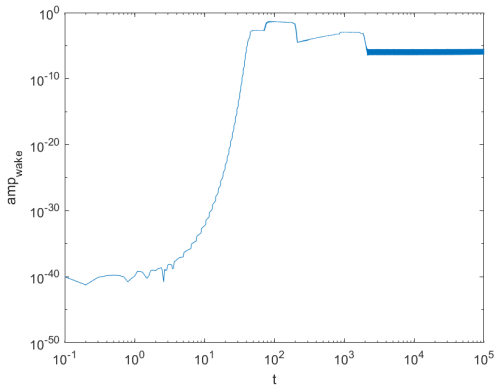

Figure 4.152: Odd indexed spring dimer ripple amplitude with $\kappa = 10$.

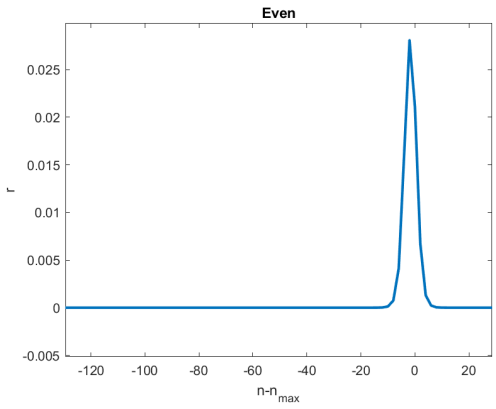

Figure 4.153: Even indexed spring dimer with $\kappa = 15$.

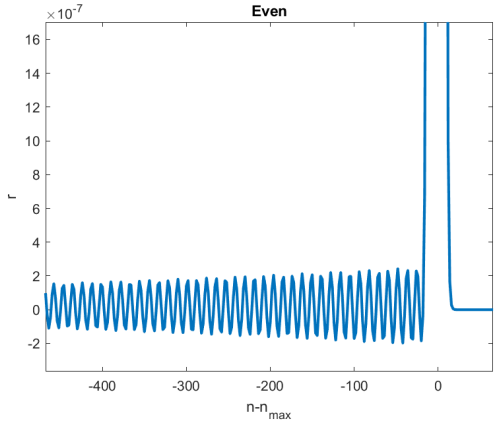

Figure 4.154: Even indexed spring dimer ripples with $\kappa = 15$.

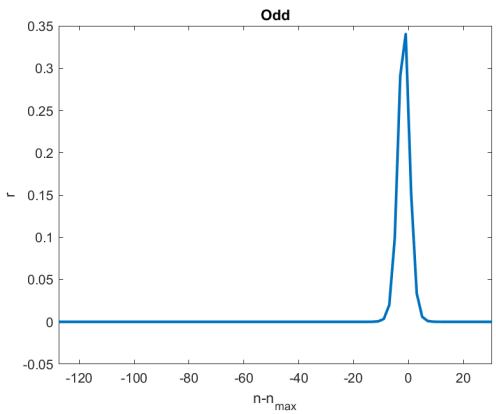

Figure 4.155: Odd indexed spring dimer with $\kappa = 15$.

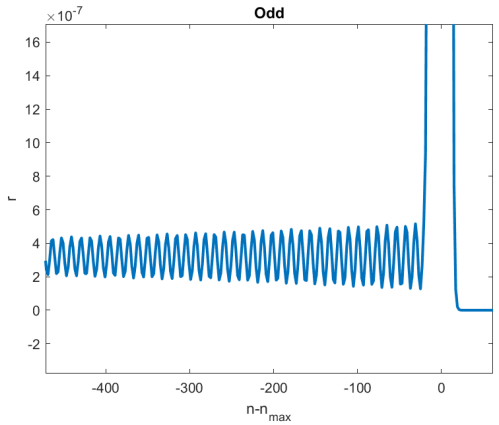

Figure 4.156: Odd indexed spring dimer ripples with $\kappa = 15$.

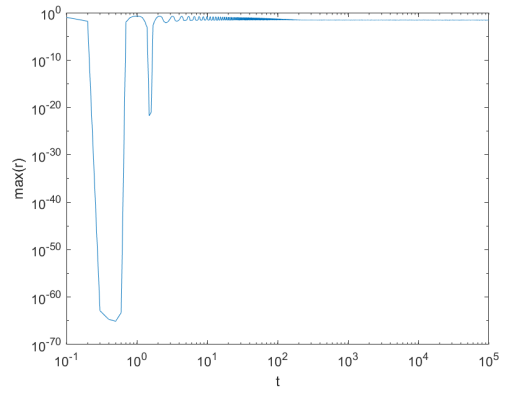

Figure 4.157: Even indexed spring dimer solitary wave amplitude with $\kappa = 15$.

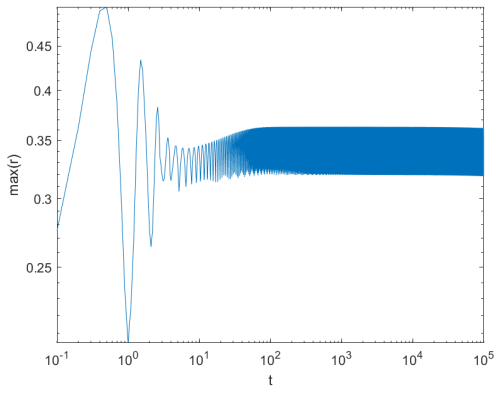

Figure 4.158: Odd indexed spring dimer solitary wave amplitude with $\kappa = 15$.

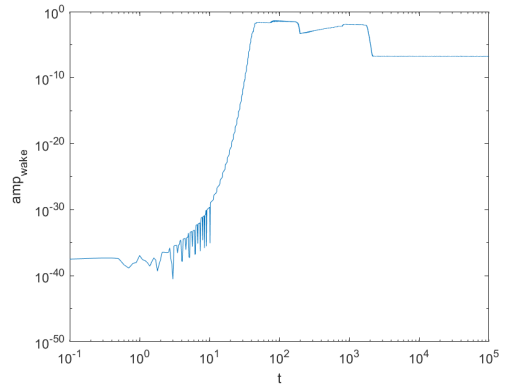

Figure 4.159: Even indexed spring dimer ripple amplitude with $\kappa = 15$.

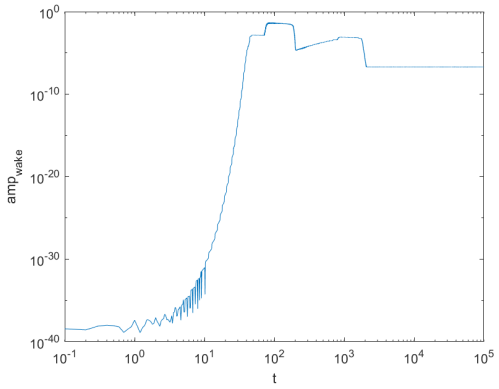

Figure 4.160: Odd indexed spring dimer ripple amplitude with $\kappa = 15$.

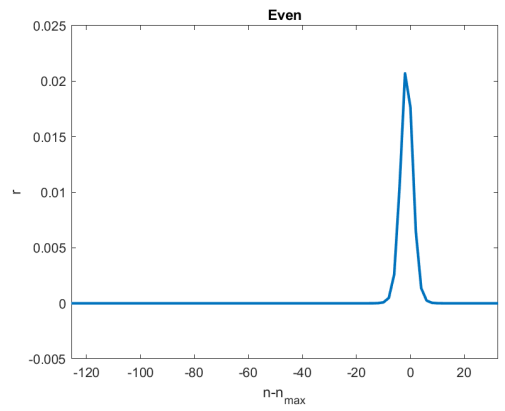

Figure 4.161: Even indexed spring dimer with $\kappa = 20$.

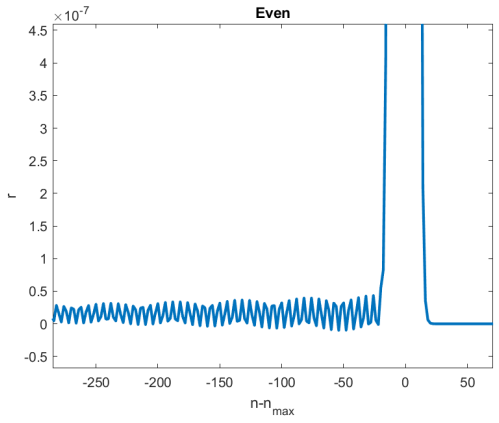

Figure 4.162: Even indexed spring dimer ripples with $\kappa = 20$.

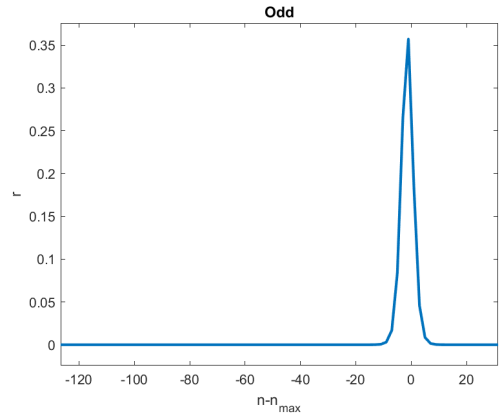

Figure 4.163: Odd indexed spring dimer with $\kappa = 20$.

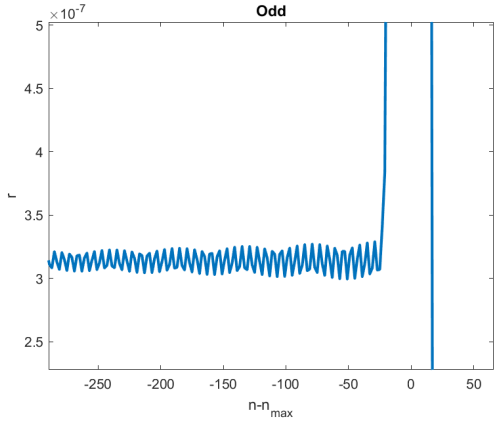

Figure 4.164: Odd indexed spring dimer ripples with $\kappa = 20$.

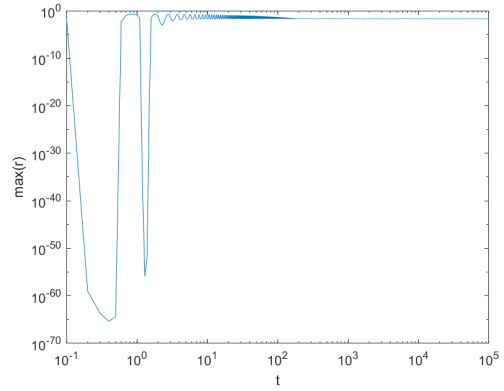

Figure 4.165: Even indexed spring dimer solitary wave amplitude with $\kappa = 20$.

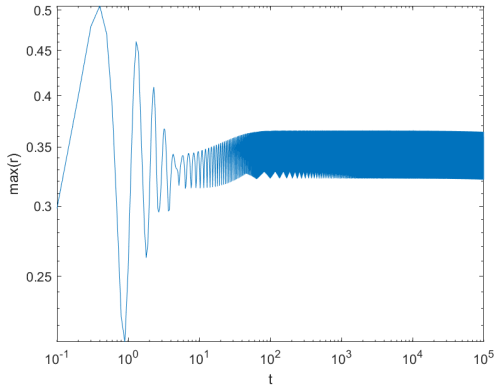

Figure 4.166: Odd indexed spring dimer solitary wave amplitude with $\kappa = 20$.

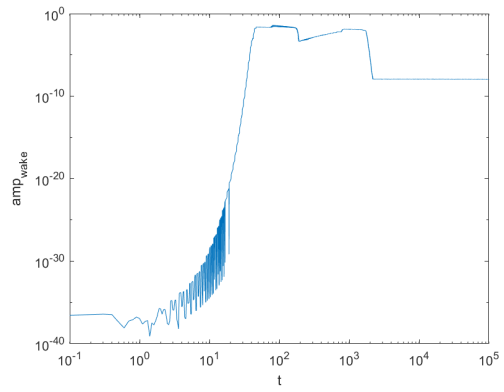

Figure 4.167: Even indexed spring dimer ripple amplitude with $\kappa = 20$.

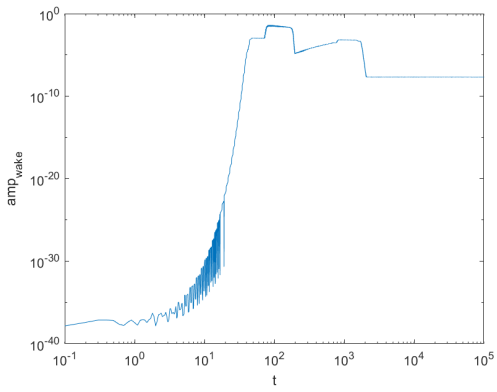

Figure 4.168: Odd indexed spring dimer ripple amplitude with $\kappa = 20$.

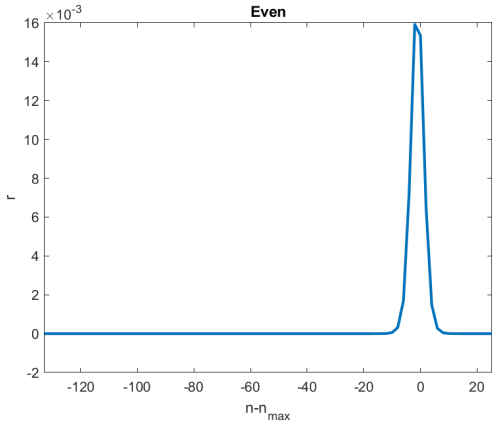

Figure 4.169: Even indexed spring dimer with $\kappa = 25$.

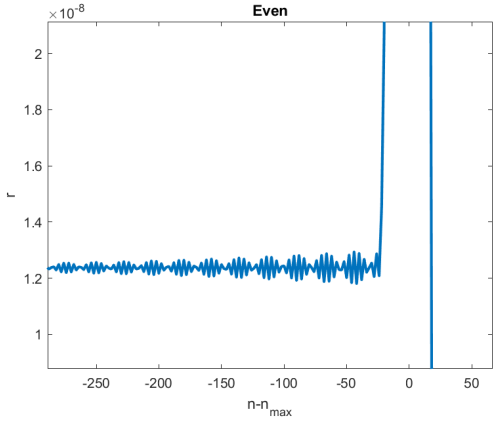

Figure 4.170: Even indexed spring dimer ripples with $\kappa = 25$.

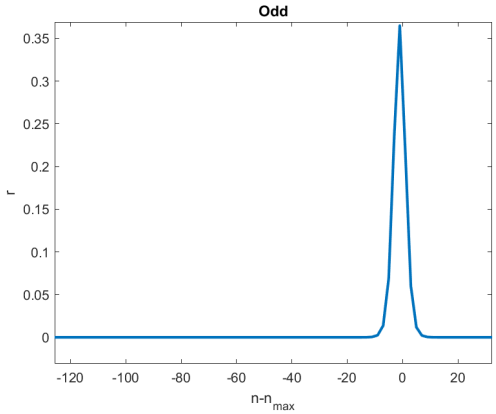

Figure 4.171: Odd indexed spring dimer with $\kappa = 25$.

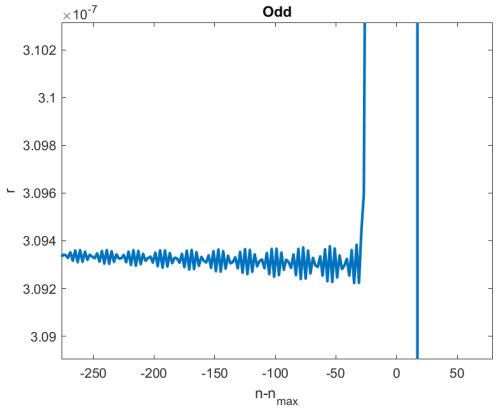

Figure 4.172: Odd indexed spring dimer ripples with $\kappa = 25$.

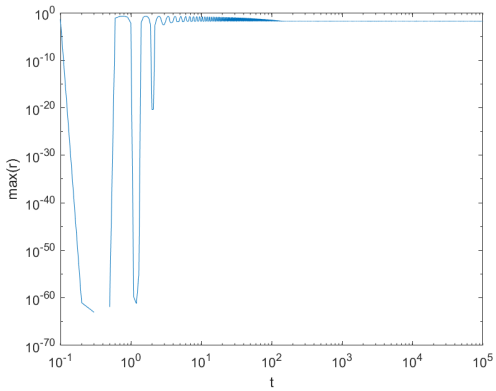

Figure 4.173: Even indexed spring dimer solitary wave amplitude with $\kappa = 25$.

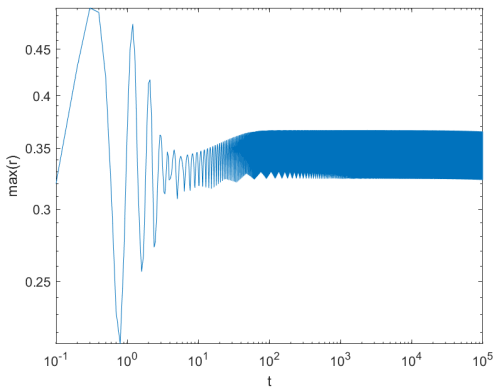

Figure 4.174: Odd indexed spring dimer solitary wave amplitude with $\kappa = 25$.

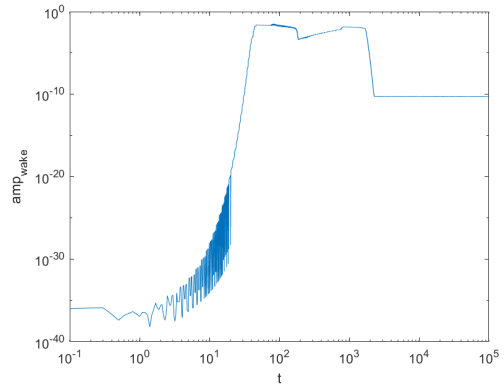

Figure 4.175: Even indexed spring dimer ripple amplitude with $\kappa = 25$.

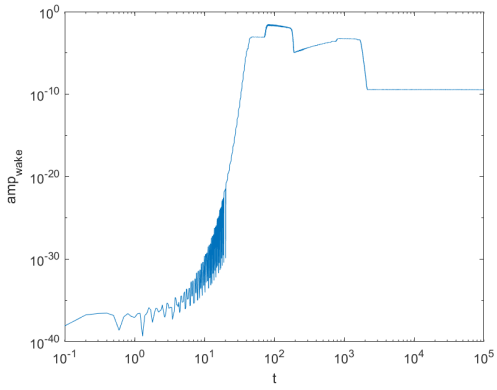

Figure 4.176: Odd indexed spring dimer ripple amplitude with $\kappa = 25$.

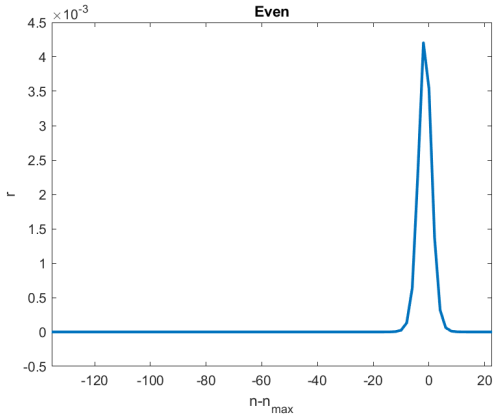

Figure 4.177: Even indexed spring dimer with $\kappa = 100$.

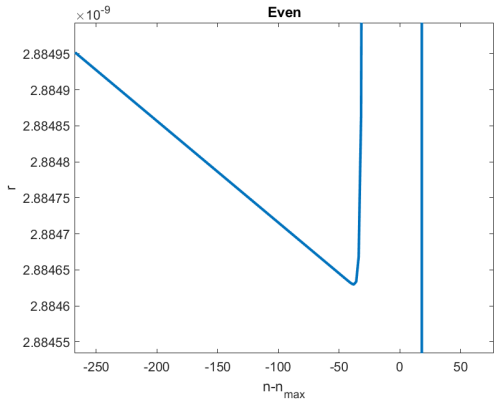

Figure 4.178: Even indexed spring dimer ripples with $\kappa = 100$.

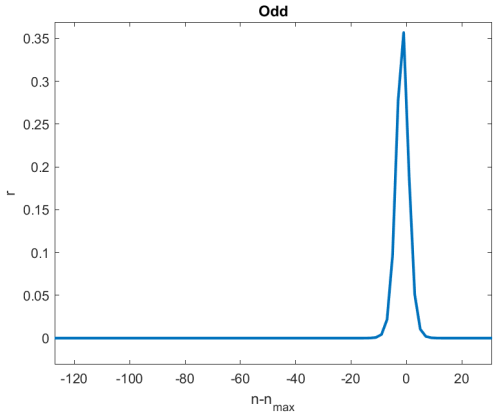

Figure 4.179: Odd indexed spring dimer with $\kappa = 100$.

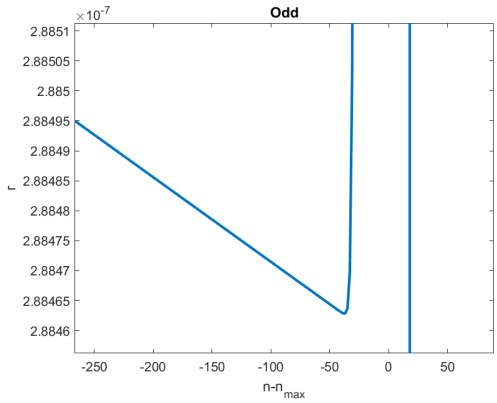

Figure 4.180: Odd indexed spring dimer ripples with $\kappa = 100$.

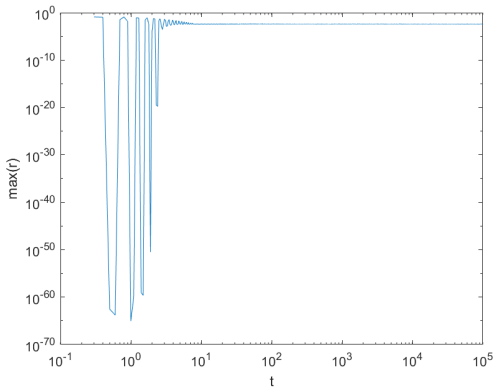

Figure 4.181: Even indexed spring dimer solitary wave amplitude with $\kappa = 100$.

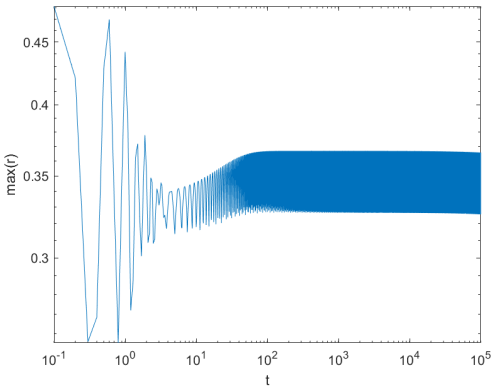

Figure 4.182: Odd indexed spring dimer solitary wave amplitude with $\kappa = 100$.

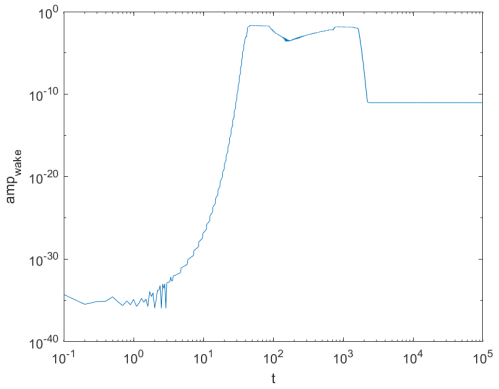

Figure 4.183: Even indexed spring dimer ripple amplitude with $\kappa = 100$.

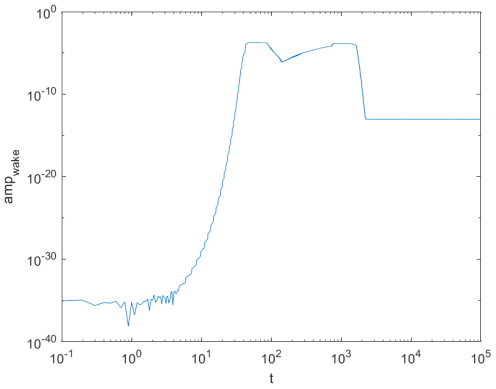

Figure 4.184: Odd indexed spring dimer ripple amplitude with $\kappa = 100$.

We see significant changes in the graphs as κ gets bigger. The amplitude of the even indexed solitary wave gets more and more distorted at the start, while the amplitude of the odd indexed solitary wave only displays the regular, slight distortion. The amplitude of the even indexed solitary waves is smaller than the amplitude of the odd indexed ones. As κ gets bigger, the ripples of the graphs show different behavior. Starting off as a jagged ripple, the ripple suddenly changes to a very large period wave, which does not fit our interval, just to change back again to the jagged ripples. Finally, the ripples seem to have disappeared completely for $\kappa = 100$. This corresponds to the fact that in the regular relative displacement graphs, the ripples show no clear behavioral pattern as κ gets bigger. The odd indexed ripples appear to oscillate around a higher value than the even indexed ones.

4.5.4 Stiff spring limit: general dimer

For the general dimer case of the stiff spring limit we have $m_1 = 1$, $m_2 = 1/2$, $F_1(r) = \kappa r + r^2$ and $F_2(r) = r + r^2$ with $\kappa \in \{5, 10, 15, 17, 20, 100\}$.

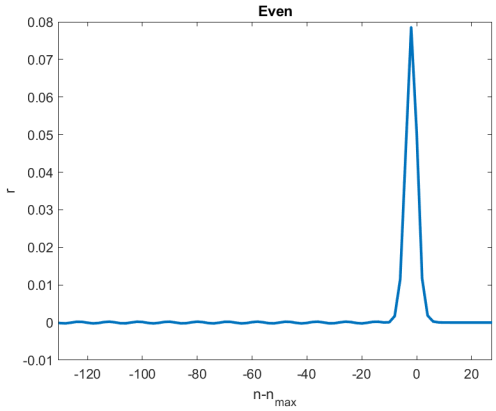

Figure 4.185: Even indexed general dimer with $\kappa = 5$.

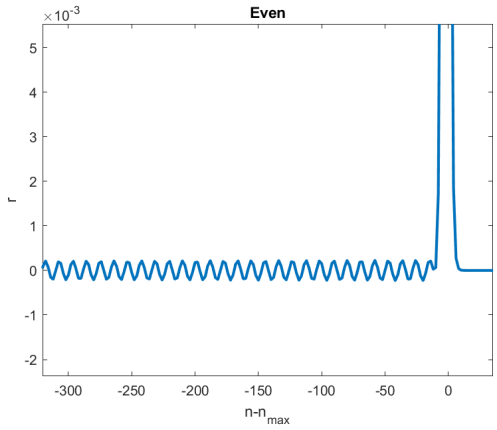

Figure 4.186: Even indexed general dimer ripples with $\kappa = 5$.

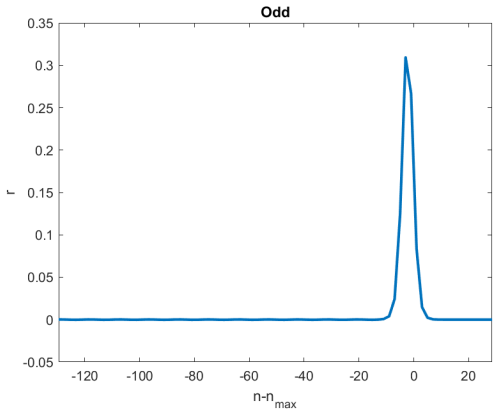

Figure 4.187: Odd indexed general dimer with $\kappa = 5$.

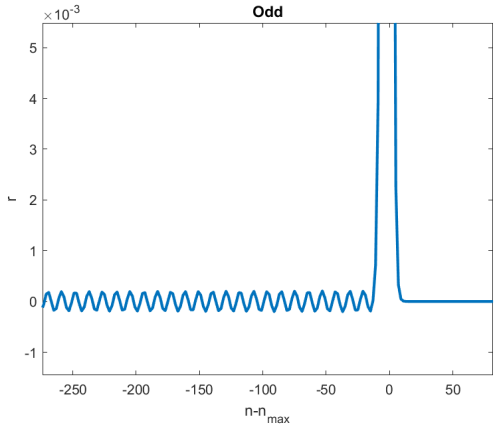

Figure 4.188: Odd indexed general dimer ripples with $\kappa = 5$.

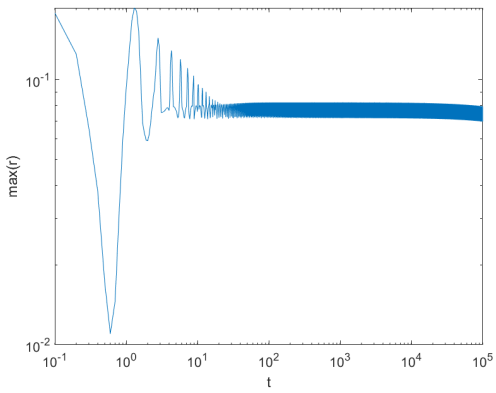

Figure 4.189: Even indexed general dimer solitary wave amplitude with $\kappa = 5$.

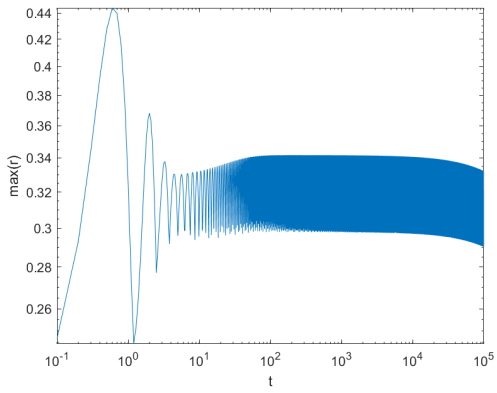

Figure 4.190: Odd indexed general dimer solitary wave amplitude with $\kappa = 5$.

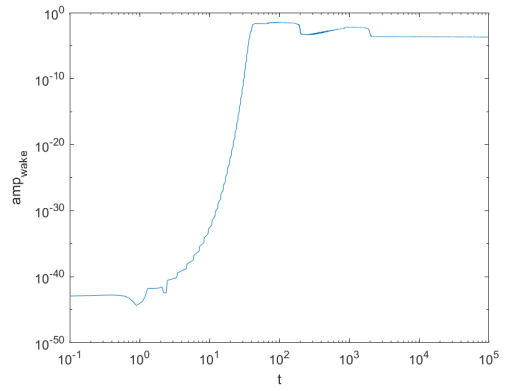

Figure 4.191: Even indexed general dimer ripple amplitude with $\kappa = 5$.

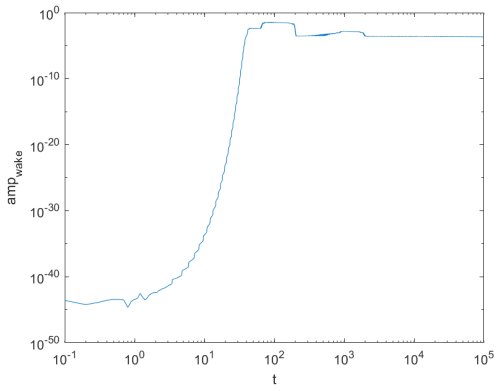

Figure 4.192: Odd indexed general dimer ripple amplitude with $\kappa = 5$.

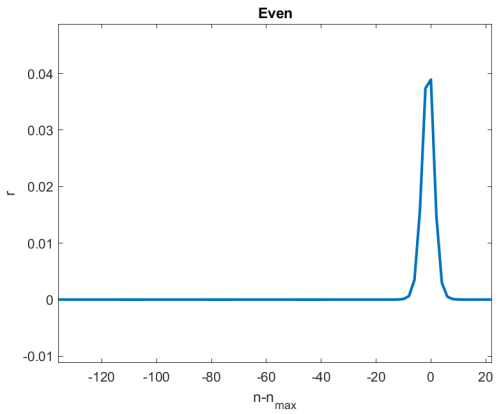

Figure 4.193: Even indexed general dimer with $\kappa = 10$.

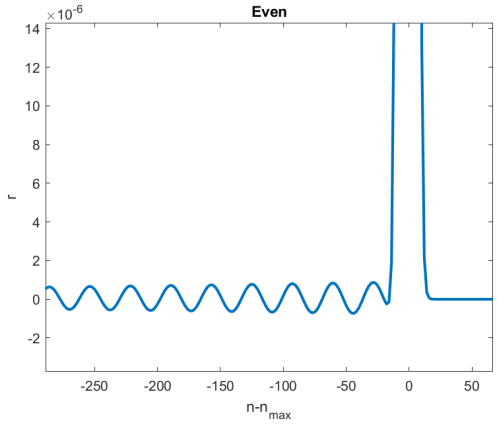

Figure 4.194: Even indexed general dimer ripples with $\kappa = 10$.

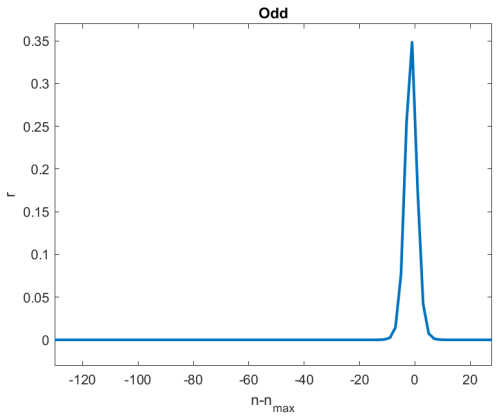

Figure 4.195: Odd indexed general dimer with $\kappa = 10$.

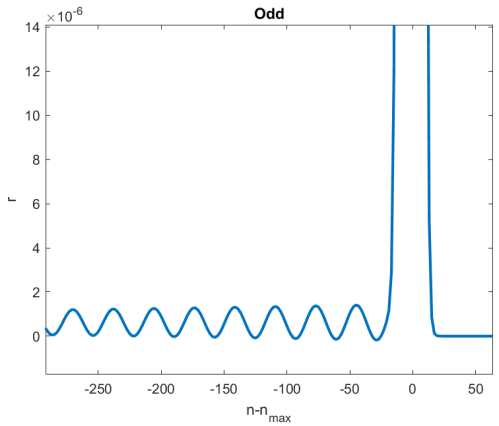

Figure 4.196: Odd indexed general dimer ripples with $\kappa = 10$.

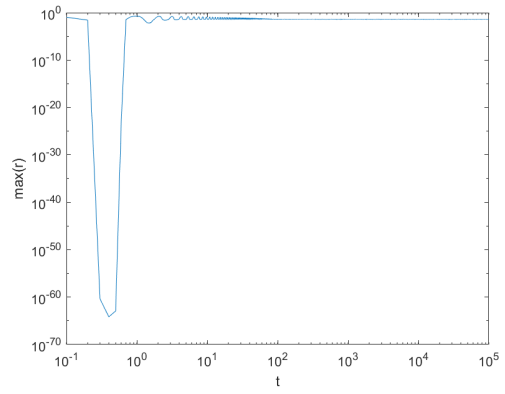

Figure 4.197: Even indexed general dimer solitary wave amplitude with $\kappa = 10$.

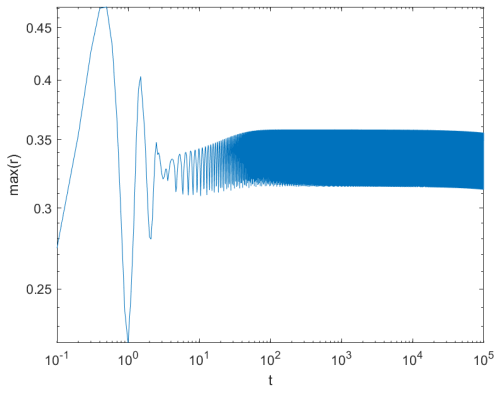

Figure 4.198: Odd indexed general dimer solitary wave amplitude with $\kappa = 10$.

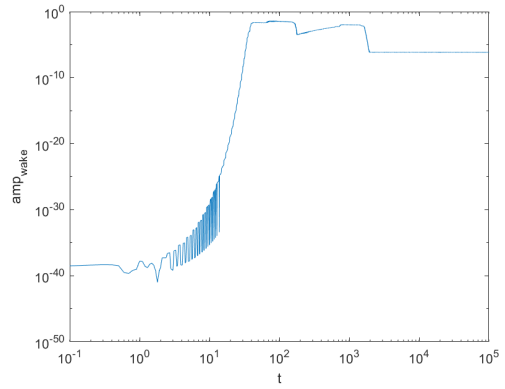

Figure 4.199: Even indexed general dimer ripple amplitude with $\kappa = 10$.

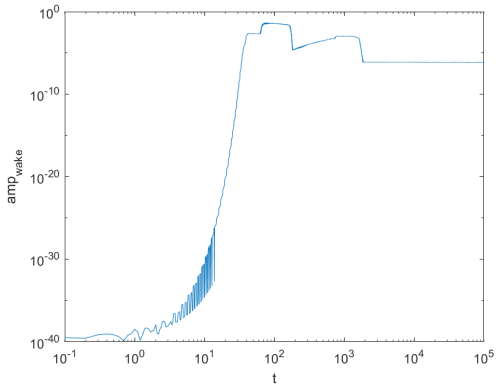

Figure 4.200: Odd indexed general dimer ripple amplitude with $\kappa = 10$.

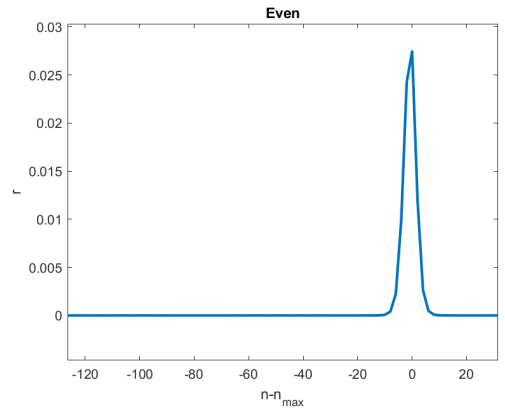

Figure 4.201: Even indexed general dimer with $\kappa = 15$.

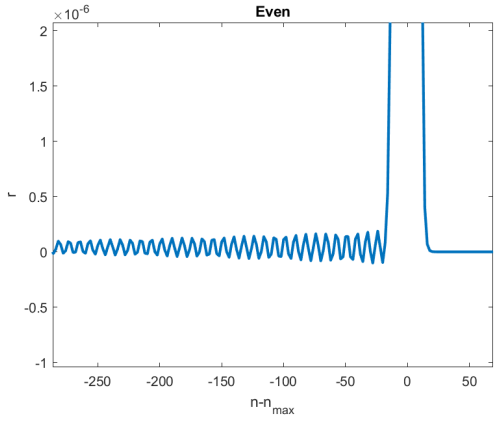

Figure 4.202: Even indexed general dimer ripples with $\kappa = 15$.

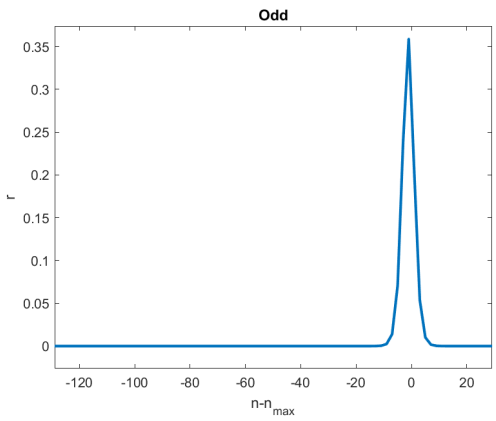

Figure 4.203: Odd indexed general dimer with $\kappa = 15$.

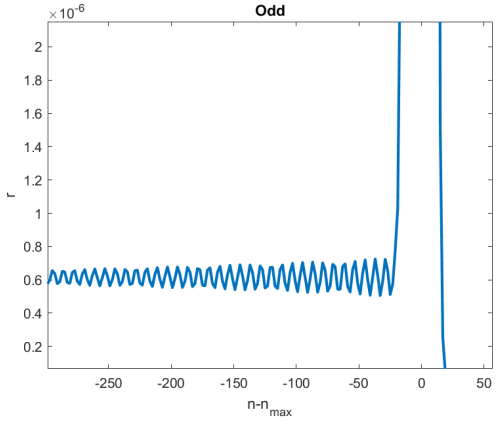

Figure 4.204: Odd indexed general dimer ripples with $\kappa = 15$.

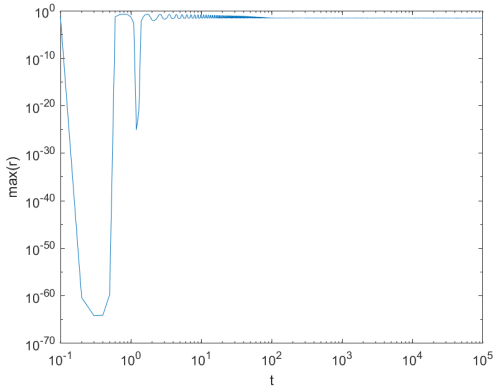

Figure 4.205: Even indexed general dimer solitary wave amplitude with $\kappa = 15$.

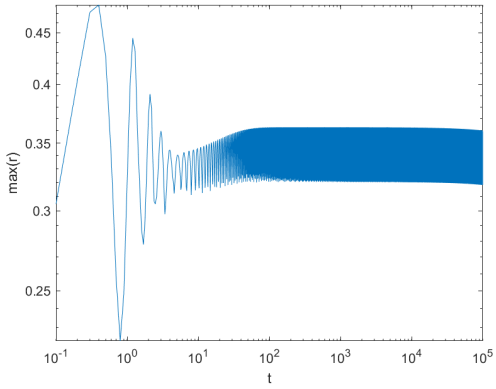

Figure 4.206: Odd indexed general dimer solitary wave amplitude with $\kappa = 15$.

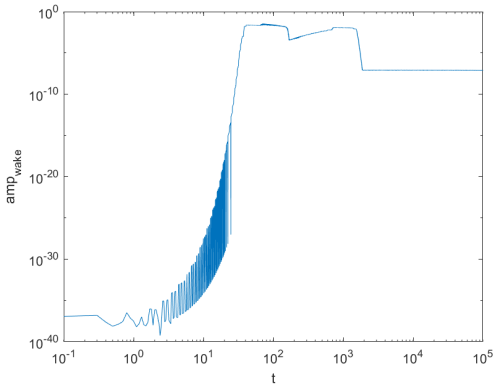

Figure 4.207: Even indexed general dimer ripple amplitude with $\kappa = 15$.

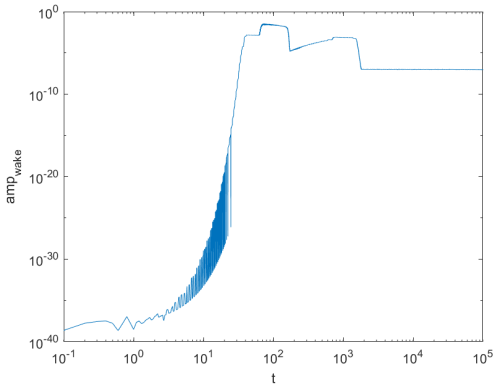

Figure 4.208: Odd indexed general dimer ripple amplitude with $\kappa = 15$.

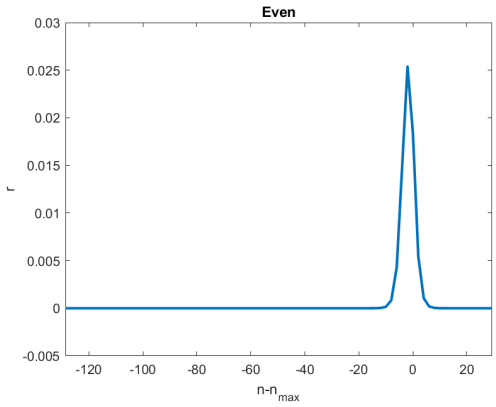

Figure 4.209: Even indexed general dimer with $\kappa = 17$.

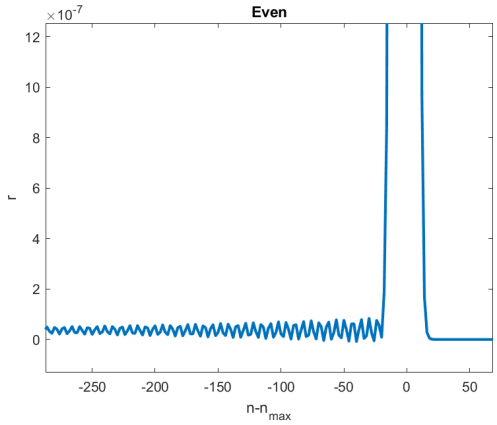

Figure 4.210: Even indexed general dimer ripples with $\kappa = 17$.

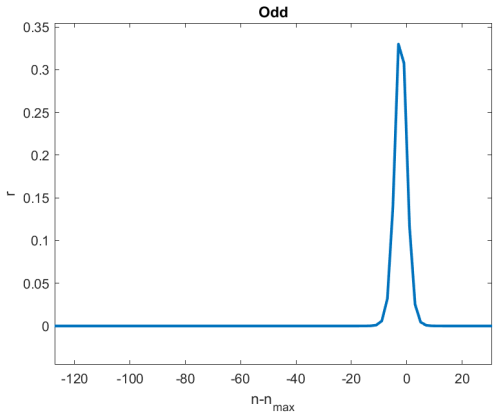

Figure 4.211: Odd indexed general dimer with $\kappa = 17$.

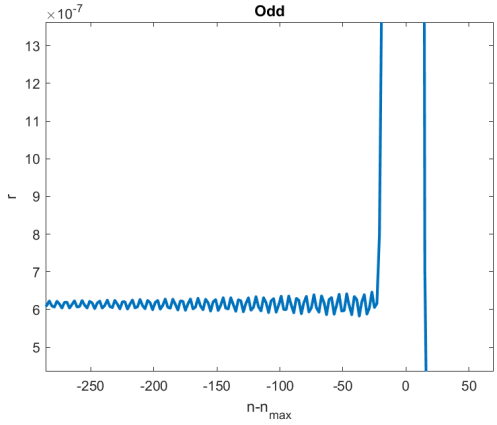

Figure 4.212: Odd indexed general dimer ripples with $\kappa = 17$.

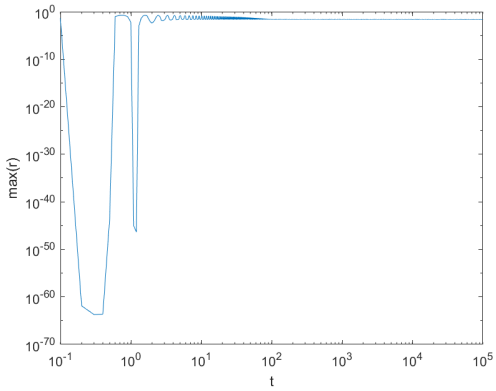

Figure 4.213: Even indexed general dimer solitary wave amplitude with $\kappa = 17$.

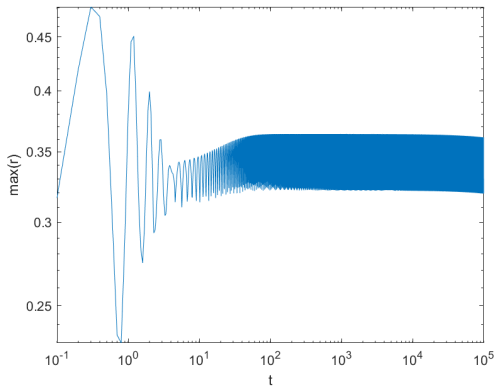

Figure 4.214: Odd indexed general dimer solitary wave amplitude with $\kappa = 17$.

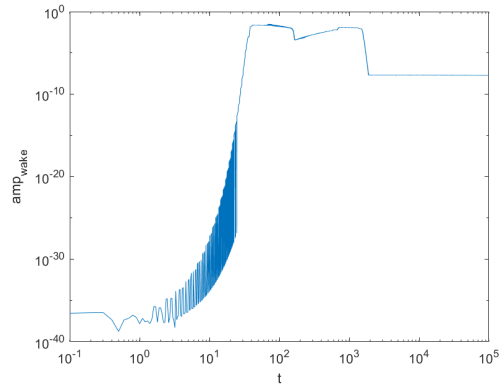

Figure 4.215: Even indexed general dimer ripple amplitude with $\kappa = 17$.

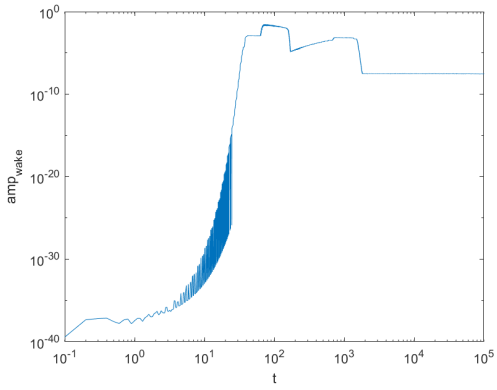

Figure 4.216: Odd indexed general dimer ripple amplitude with $\kappa = 17$.

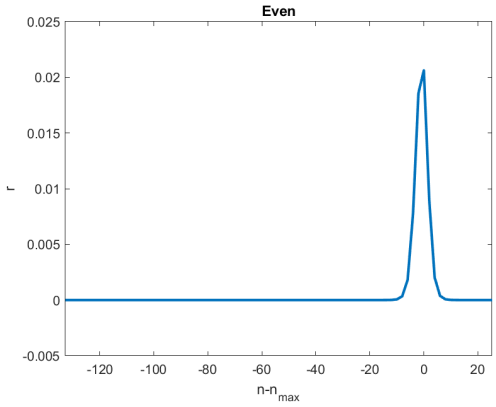

Figure 4.217: Even indexed general dimer with $\kappa = 20$.

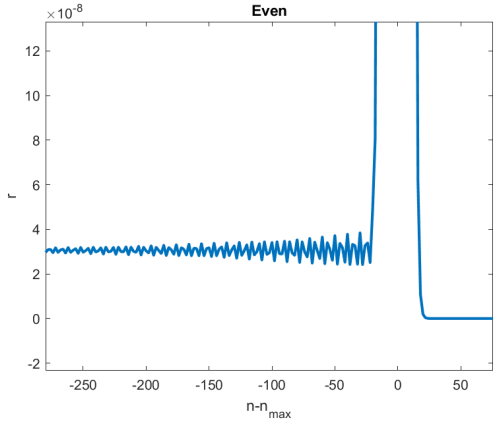

Figure 4.218: Even indexed general dimer ripples with $\kappa = 20$.

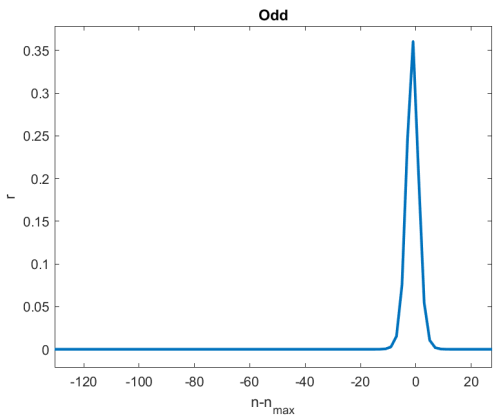

Figure 4.219: Odd indexed general dimer with $\kappa = 20$.

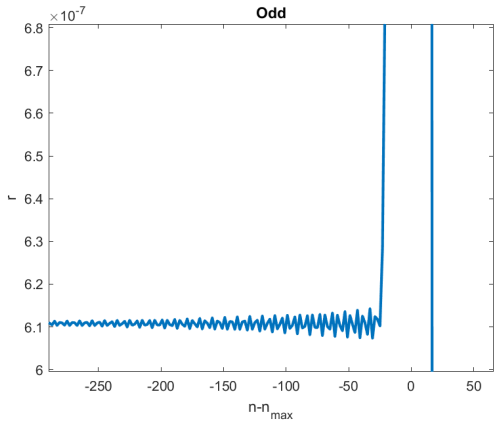

Figure 4.220: Odd indexed general dimer ripples with $\kappa = 20$.

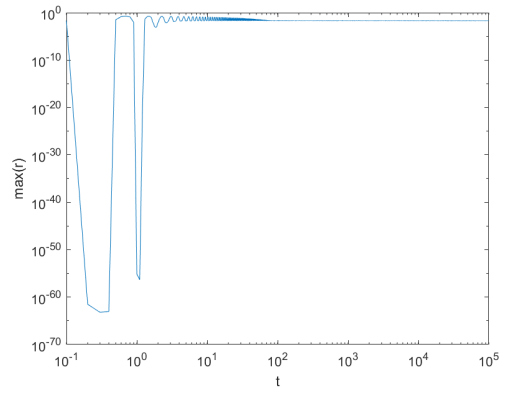

Figure 4.221: Even indexed general dimer solitary wave amplitude with $\kappa = 20$.

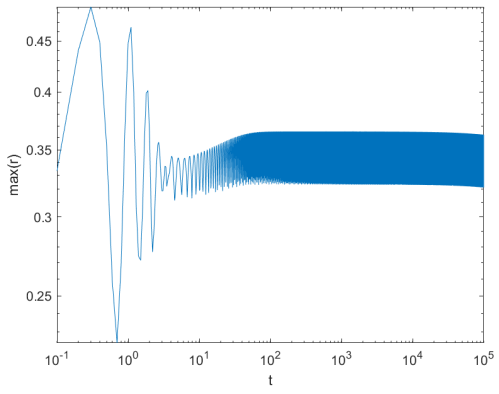

Figure 4.222: Odd indexed general dimer solitary wave amplitude with $\kappa = 20$.

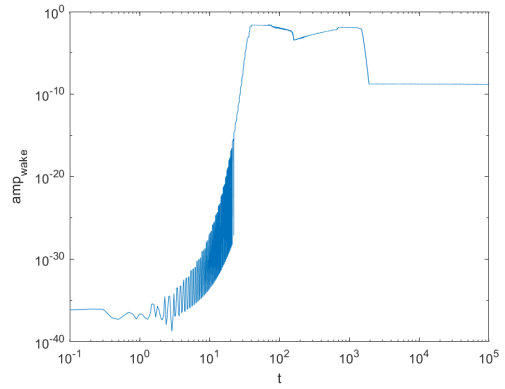

Figure 4.223: Even indexed general dimer ripple amplitude with $\kappa = 20$.

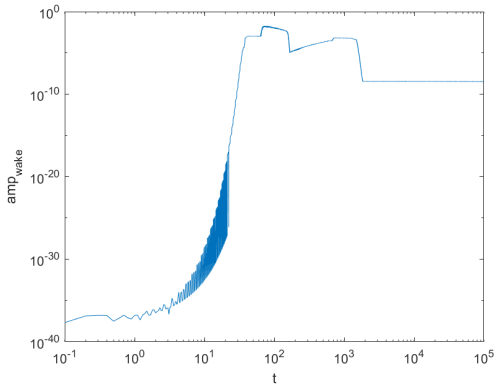

Figure 4.224: Odd indexed general dimer ripple amplitude with $\kappa = 20$.

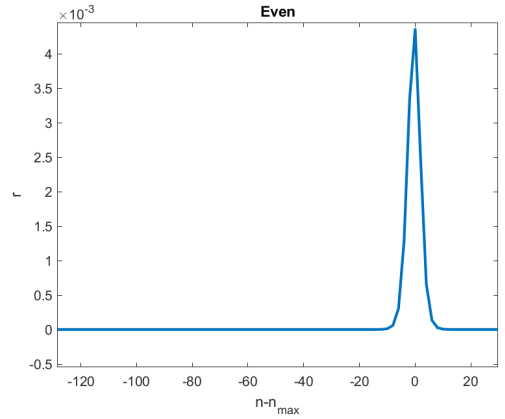

Figure 4.225: Even indexed general dimer with $\kappa = 100$.

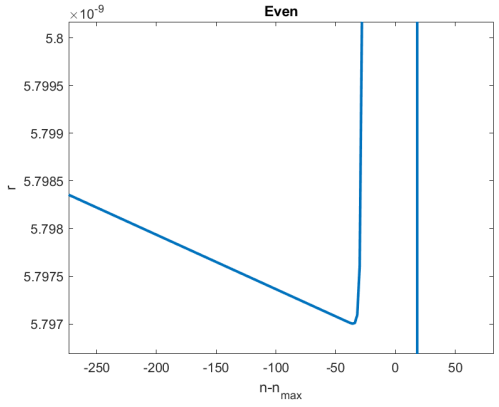

Figure 4.226: Even indexed general dimer ripples with $\kappa = 100$.

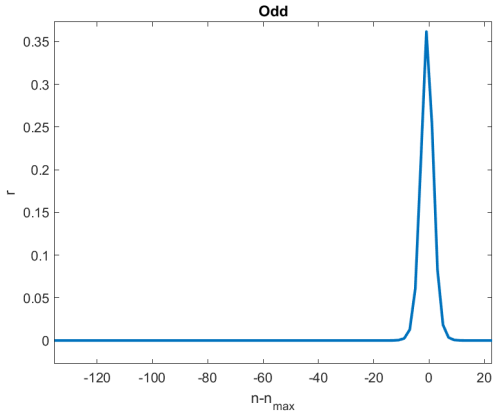

Figure 4.227: Odd indexed general dimer with $\kappa = 100$.

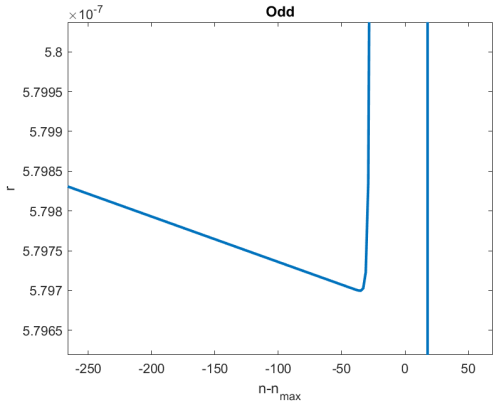

Figure 4.228: Odd indexed general dimer ripples with $\kappa = 100$.

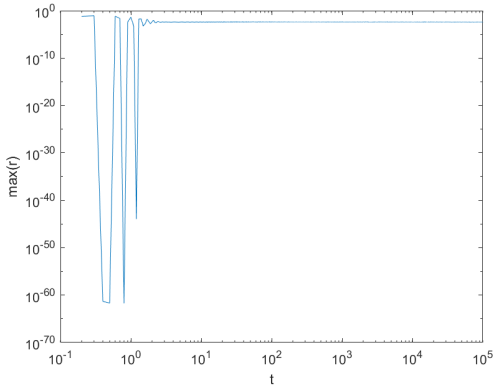

Figure 4.229: Even indexed general dimer solitary wave amplitude with $\kappa = 100$.

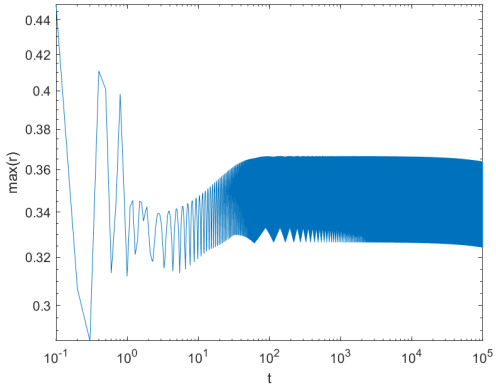

Figure 4.230: Odd indexed general dimer solitary wave amplitude with $\kappa = 100$.

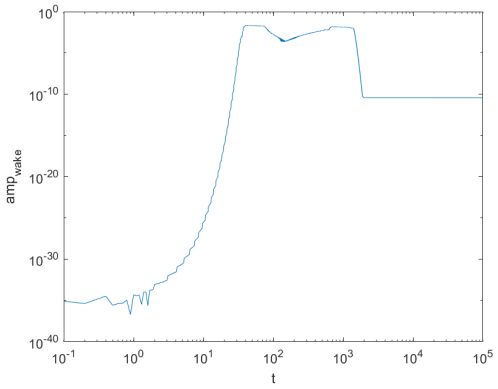

Figure 4.231: Even indexed general dimer ripple amplitude with $\kappa = 100$.

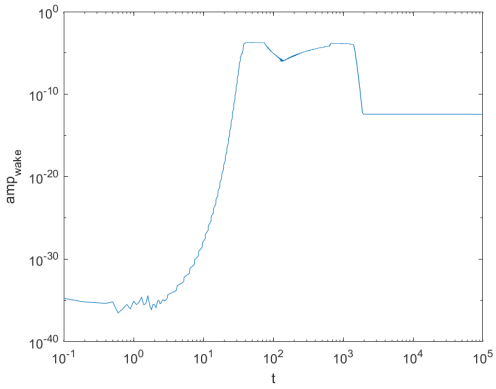

Figure 4.232: Odd indexed general dimer ripple amplitude with $\kappa = 100$.

We see quite similar behavior to the spring dimer case, where the ripples showed no clear behavioral pattern. Here, we see various ripple shapes, from jagged to regular wave shaped ripples. However, after $\kappa = 10$ the ripples show a decay in amplitude as the ripples get further away from the solitary wave. The even amplitudes show a similar distorted behavior at the start to the spring dimer case. The amplitude of the even indexed solitary wave is also smaller than the amplitude of the odd indexed ones.

4.6 Large wave speeds

In this section, we will look at the equal mass limit when we take $\epsilon \geqslant 1$. Since the long wave theory of [15, 17, 19, 13, 3] all presume that ϵ is small, there is no guarantee that the code should produce anything reasonable for larger ϵ. For these ϵ, it turns out that the simulations we run "explode" after a short period of time, in the sense that the solutions take on a "NaN" value in MATLAB, which means somewhere along the way there was done one of the following operations: $0/0$, $0 \cdot \infty$, ∞/∞ or $\infty - \infty$. It is hard to trace back when or why this happens, which is why we decide to look at what happens if we turn the initial condition into

$$\mathbf{r}_n(0) = 3\epsilon_1^2 \operatorname{sech}^2(\beta\epsilon_2 n)\mathbf{v}$$

in which we will be looking at the behavior of the simulations as we take various values of ϵ_1 and ϵ_2 as opposed to the single ϵ in (3.6). Here, as a reminder, $\mathbf{v} = (1, -c_0)$, where c_0 is the speed of sound. If ϵ_1 is large we have a large amplitude wave and if ϵ_2 is large, we have a small wavelength. It turns out that as long as we take $\epsilon_1 \leqslant 1/2$, we can take any arbitrary large number for ϵ_2, meaning we get results for a small amplitude, small wavelength wave. We fix ϵ_1 at $1/4$ and take $\mu = 1/4, 1/8, 1/16$ in the equal mass limit. We simulate for $\epsilon_2 = 100, 1000, 10000$. The results for these values of ϵ_2 appear to be the same and follow below. These are figures at $t = 10^5$.

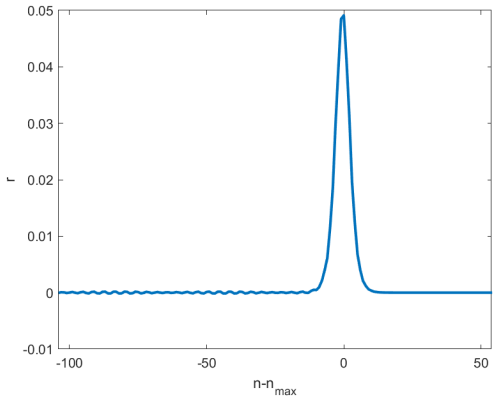

Figure 4.233: Equal mass limit with $\mu = 1/4$, $\epsilon_1 = 1/4$ and $\epsilon_2 = 100, 1000, 10000$.

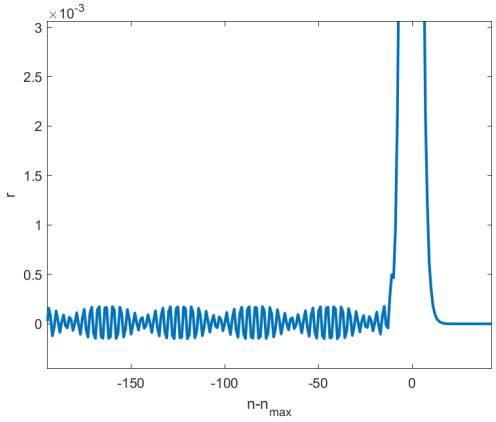

Figure 4.234: Equal mass limit ripples with $\mu = 1/4$, $\epsilon_1 = 1/4$ and $\epsilon_2 = 100, 1000, 10000$.

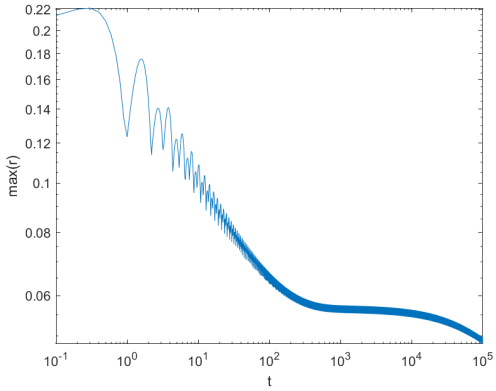

Figure 4.235: Loglog plot of equal mass limit leading solitary wave amplitude with $\mu = 1/4$ and $\epsilon_1 = 1/4$ and $\epsilon_2 = 100, 1000, 10000$.

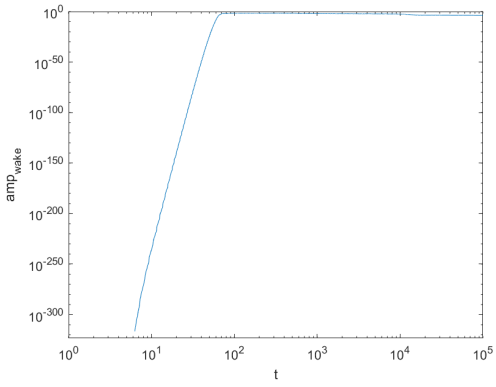

Figure 4.236: Loglog plot of equal mass limit ripple amplitude with $\mu = 1/4$ and $\epsilon_1 = 1/4$ and $\epsilon_2 = 100, 1000, 10000$.

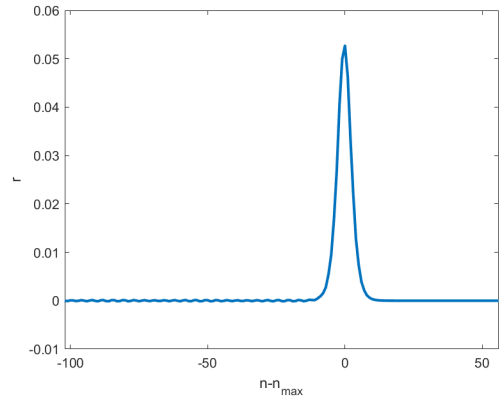

Figure 4.237: Equal mass limit with $\mu = 1/8$, $\epsilon_1 = 1/4$ and $\epsilon_2 = 100, 1000, 10000$.

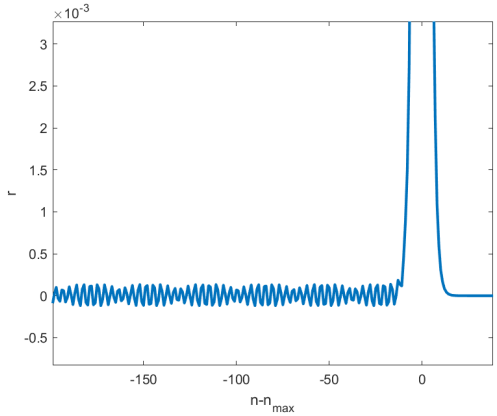

Figure 4.238: Equal mass limit ripples with $\mu = 1/8$, $\epsilon_1 = 1/4$ and $\epsilon_2 = 100, 1000, 10000$.

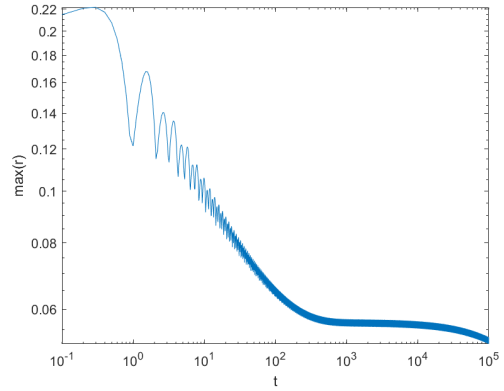

Figure 4.239: Loglog plot of equal mass limit leading solitary wave amplitude with $\mu = 1/8$ and $\epsilon_1 = 1/4$ and $\epsilon_2 = 100, 1000, 10000$.

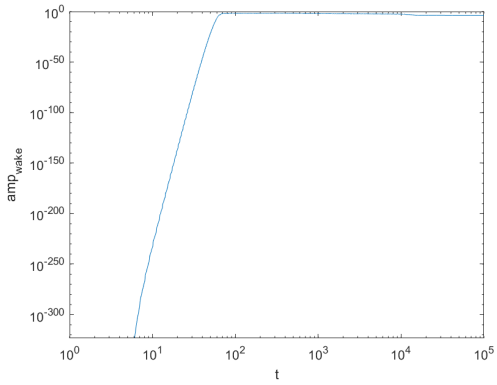

Figure 4.240: Loglog plot of equal mass limit ripple amplitude with $\mu = 1/8$ and $\epsilon_1 = 1/4$ and $\epsilon_2 = 100, 1000, 10000$.

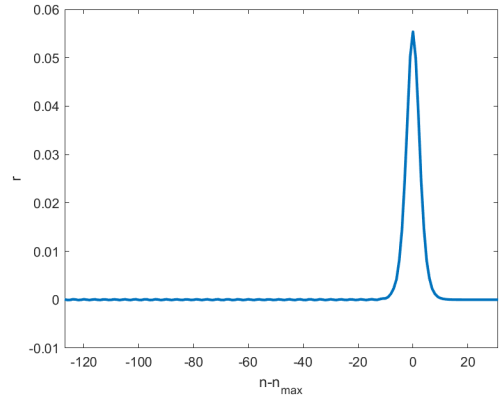

Figure 4.241: Equal mass limit with $\mu = 1/16$, $\epsilon_1 = 1/4$ and $\epsilon_2 = 100, 1000, 10000$.

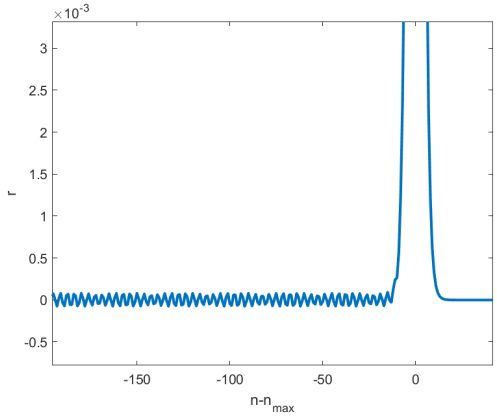

Figure 4.242: Equal mass limit ripples with $\mu = 1/16$, $\epsilon_1 = 1/4$ and $\epsilon_2 = 100, 1000, 10000$.

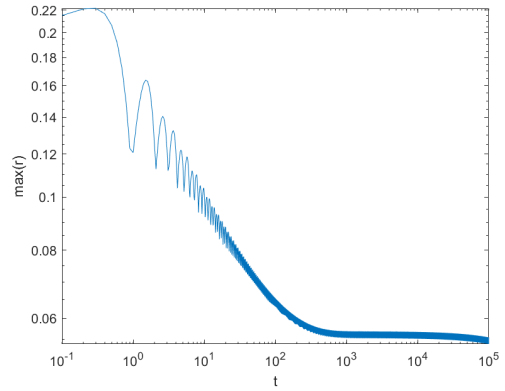

Figure 4.243: Loglog plot of equal mass limit leading solitary wave amplitude with $\mu = 1/16$ and $\epsilon_1 = 1/4$ and $\epsilon_2 = 100, 1000, 10000$.

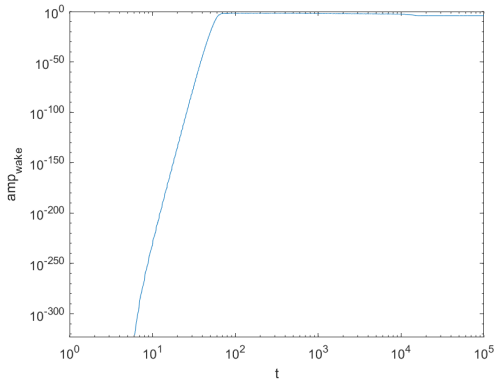

Figure 4.244: Loglog plot of equal mass limit ripple amplitude with $\mu = 1/16$ and $\epsilon_1 = 1/4$ and $\epsilon_2 = 100, 1000, 10000$.

If we compare these figures to the figures in Section 4.3, we see slight differences. We see that the amplitude at $t = 10^5$ is smaller in the small wavelength, small amplitude case. We also see that the amplitude of the leading solitary wave decays faster at the start than in Section 4.3, to reach the almost constant state at around $t = 10^2$, after which it decays, which is comparable to the figures in Section 4.3. The amplitudes of the ripples seem to have gotten somewhat smaller, whereas in Section 4.3, the amplitudes of the ripples for these values of μ only seem to get bigger.

4.7 Conclusions

We see similar behavior in the various limits in the sense that they all converge in to the monatomic behavior in a certain way. Broadly, we see what they saw in [2] in the diatomic long wave problem, namely a "solitary wave plus oscillatory wake".

If we compare all the limits by solitary wave amplitudes over time, we see the same pattern occuring over and over. First, there is an initial disorder in amplitude, which eventually settles into an oscillation around a value which decays very slowly. For the equal mass limit, we see that after an extended amount of time, there is a "rapid" decay, which, since the amplitude plots are loglog plots, translates to algebraic decay in real time vs. real amplitude. For the stiff spring limit in both the spring dimer and general dimer cases, we observe that the amplitude is almost double the amplitude of the monatomic, equal mass and small mass cases. As we look at the even and odd indexed amplitudes, the same pattern of initial disorder and settling is observed, with slight variations. In the even cases of the spring dimer and general dimer for example, there is an extreme drop in amplitude in the initial disorder. Also, for the spring dimer and general dimer cases, the amplitude of the even indexed solitary waves is often much smaller than the amplitude of the odd indexed ones.

Looking at the ripples left behind, we observe different behavior in all the different limits. In the small mass limit we see the ripples' amplitude decaying as it moves away from the leading solitary wave and as μ gets smaller, the amplitudes of the ripples get smaller too. In the equal mass limit we see the ripples getting squished together and not so much decaying in amplitude. In the spring dimer and general dimer cases of the stiff spring limit we see no clear pattern in the behavior of the ripples as κ gets bigger, but in both cases, the ripples converge to a seemingly constant amplitude, jagged shaped ripple. The even and odd indexed figures often show very different behavior in the ripple from their composite counterparts. For example, for some values of κ in the spring dimer and general dimer cases, we see the jaggedness disappear as we graph the odd and even indices separately, which is remarkable behavior which we already hinted at at the start of this chapter. As was mentioned before, in [19] this stegoton-type behavior is covered. The absence of the stegoton-type behavior in the equal mass limit is due to the fact that for alternating lattice indices n, there is no difference in the equal mass limit, as opposed to the stiff spring limit. It is peculiar, however, that the jagged behavior does not arise in the small mass limit, since the difference in masses is pretty significant. This could mean that there is some sort of, not yet seen before, mechanism in the stiff spring limit which induces additional differences based on the parity of the index site n. This is only speculation, however, since there are no proofs yet on nanopterons in the stiff spring limit, which means we are treading on uncharted territory.

4.8 Different ϵ

Since we only used $\epsilon = 1/4$ in our simulations, it could be interesting to see what kind of behavior the limits show for different values of ϵ. Below are a few example figures of the equal mass limit and small mass limit for $\epsilon = 1/8$, which already show quite interesting results in comparison to what we have found for $\epsilon = 1/4$.

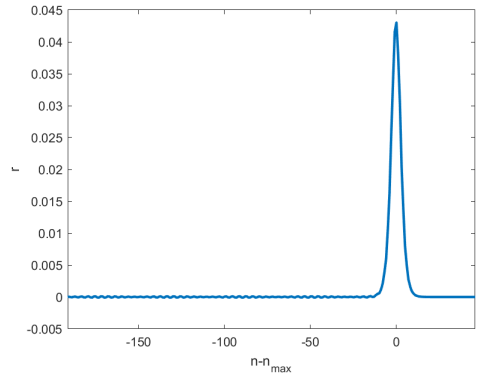

Figure 4.245: Equal mass limit with $\mu = 1/4$ and $\epsilon = 1/8$.

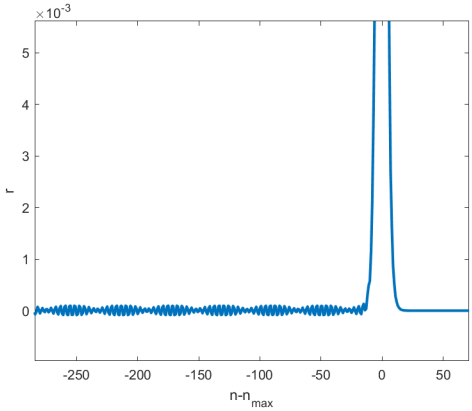

Figure 4.246: Equal mass limit ripples with $\mu = 1/4$ and $\epsilon = 1/8$.

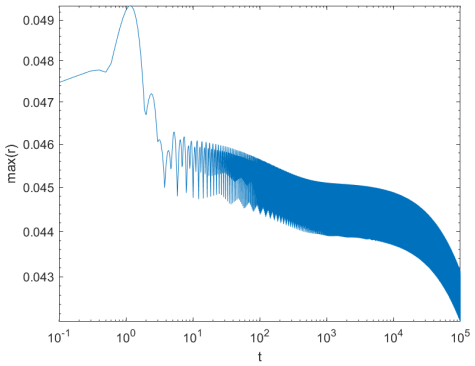

Figure 4.247: Loglog plot of equal mass limit leading solitary wave amplitude with $\mu = 1/4$ and $\epsilon = 1/8$.

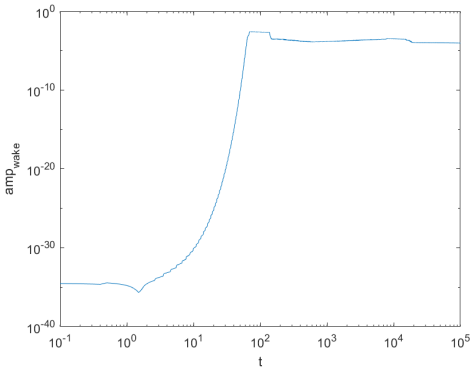

Figure 4.248: Loglog plot of equal mass limit ripple amplitude with $\mu = 1/4$ and $\epsilon = 1/8$.

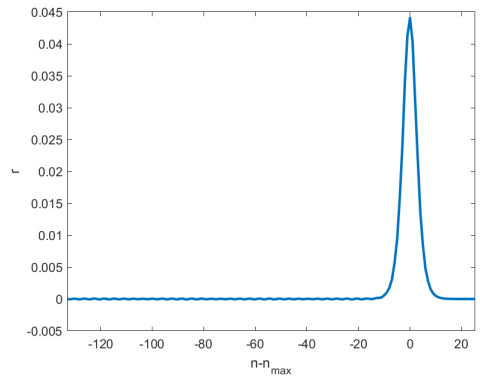

Figure 4.249: Equal mass limit with $\mu = 1/8$ and $\epsilon = 1/8$.

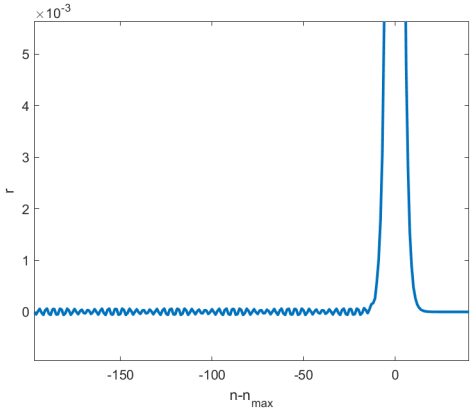

Figure 4.250: Equal mass limit ripples with $\mu = 1/8$ and $\epsilon = 1/8$.

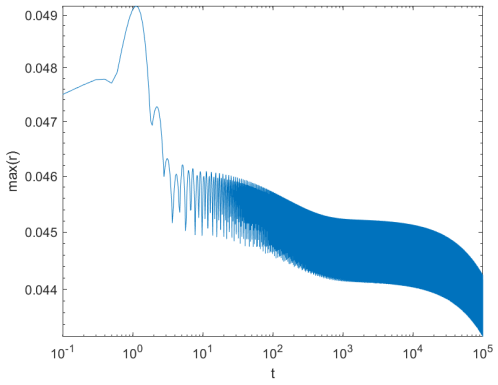

Figure 4.251: Loglog plot of equal mass limit leading solitary wave amplitude with $\mu = 1/8$ and $\epsilon = 1/8$.

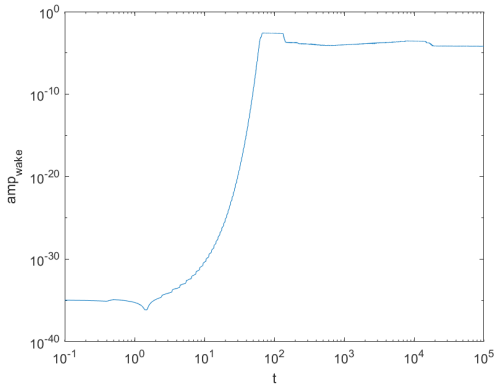

Figure 4.252: Loglog plot of equal mass limit ripple amplitude with $\mu = 1/8$ and $\epsilon = 1/8$.

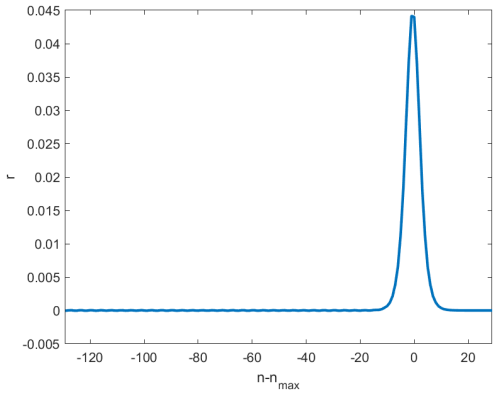

Figure 4.253: Equal mass limit with $\mu = 1/16$ and $\epsilon = 1/8$.

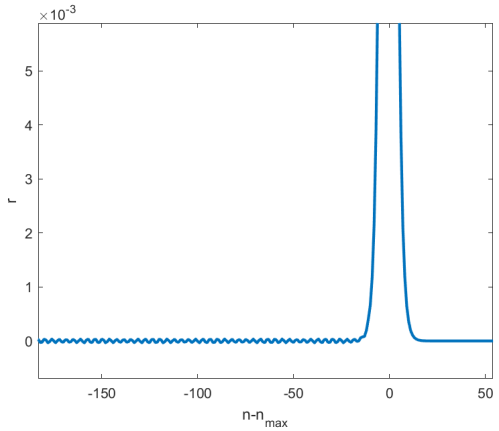

Figure 4.254: Equal mass limit ripples with $\mu = 1/16$ and $\epsilon = 1/8$.

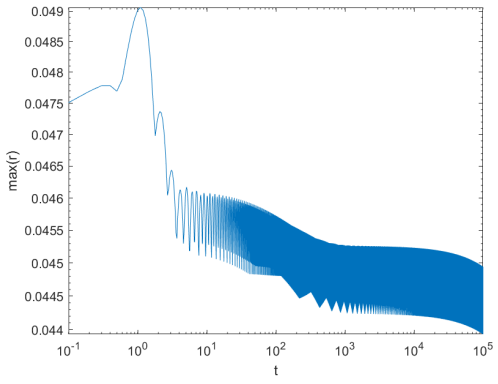

Figure 4.255: Loglog plot of equal mass limit leading solitary wave amplitude with $\mu = 1/16$ and $\epsilon = 1/8$.

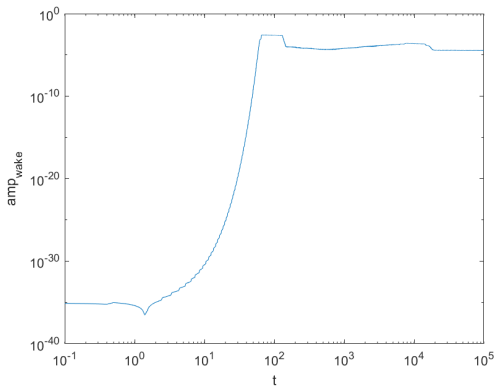

Figure 4.256: Loglog plot of equal mass limit ripple amplitude with $\mu = 1/16$ and $\epsilon = 1/8$.

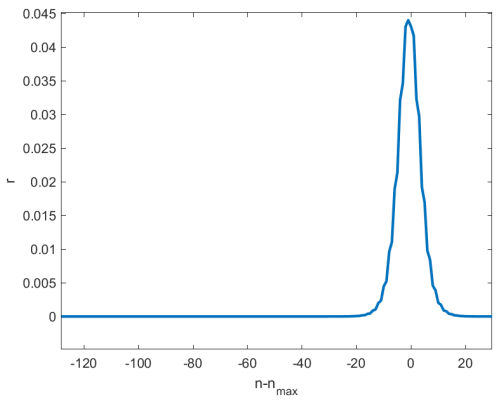

Figure 4.257: Small mass limit with $\mu = 1/4$ and $\epsilon = 1/8$.

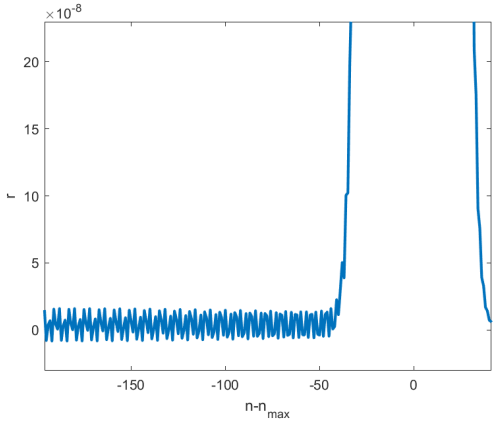

Figure 4.258: Small mass limit ripples with $\mu = 1/4$ and $\epsilon = 1/8$.

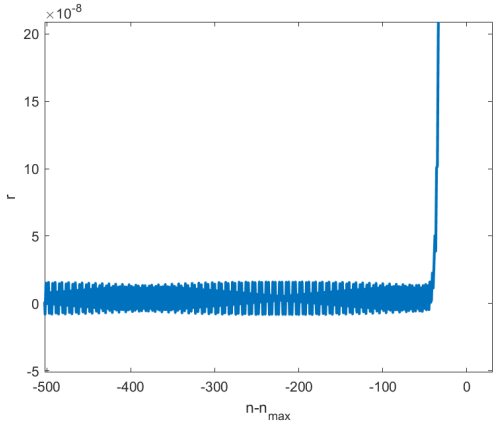

Figure 4.259: Small mass limit ripples with $\mu = 1/4$ and $\epsilon = 1/8$, zoomed out.

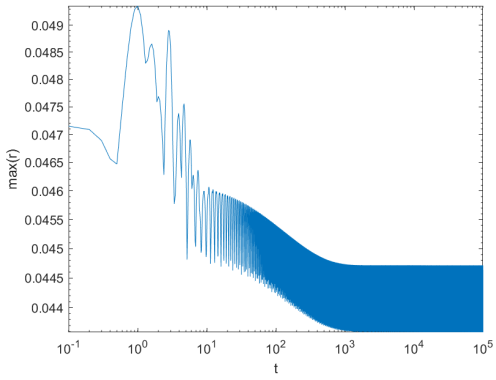

Figure 4.260: Loglog plot of small mass limit leading solitary wave amplitude with $\mu = 1/4$ and $\epsilon = 1/8$.

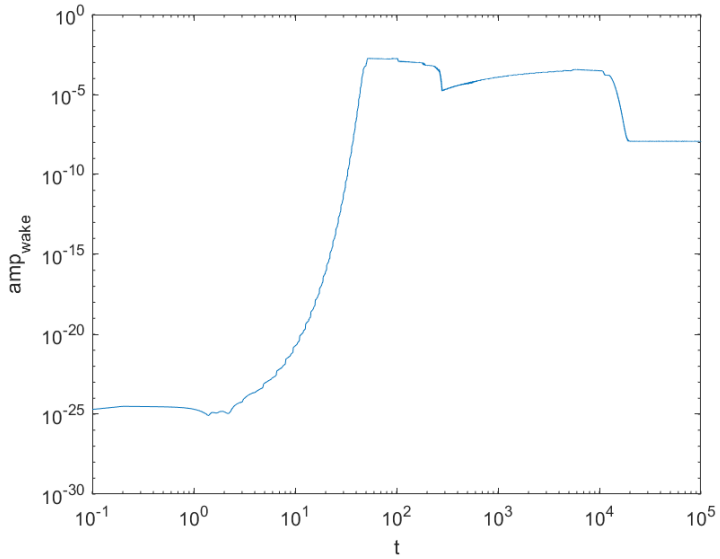

Figure 4.261: Loglog plot of small mass limit ripple amplitude with $\mu = 1/4$ and $\epsilon = 1/8$.

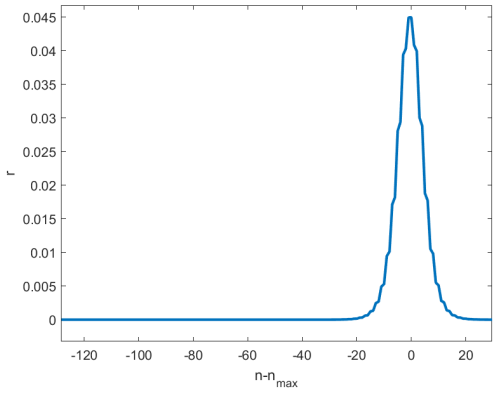

Figure 4.262: Small mass limit with $\mu = 1/8$ and $\epsilon = 1/8$.

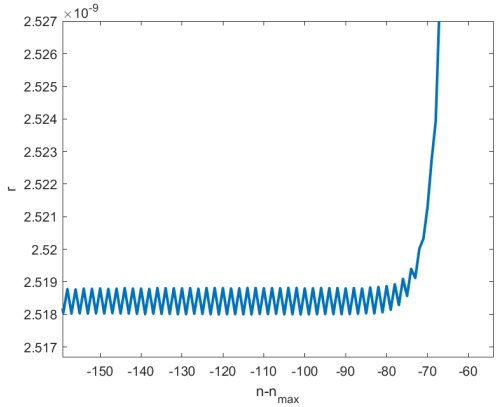

Figure 4.263: Small mass limit ripples with $\mu = 1/8$ and $\epsilon = 1/8$.

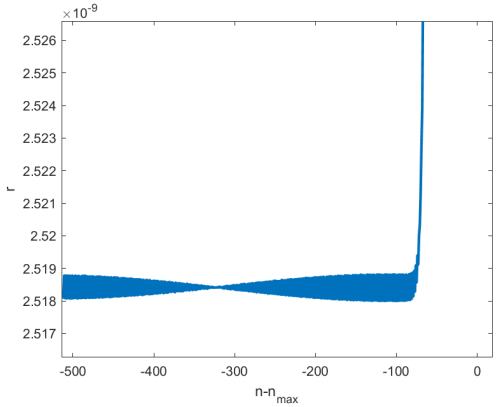

Figure 4.264: Small mass limit ripples with $\mu = 1/8$ and $\epsilon = 1/8$, zoomed out.

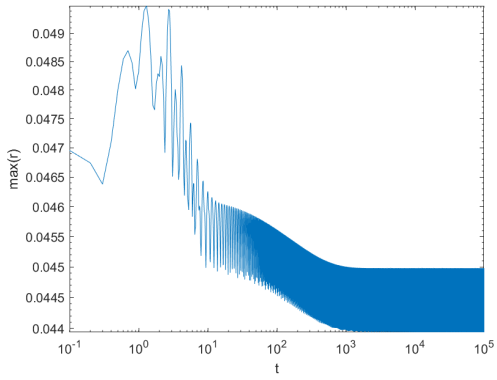

Figure 4.265: Loglog plot of small mass limit leading solitary wave amplitude with $\mu = 1/8$ and $\epsilon = 1/8$.

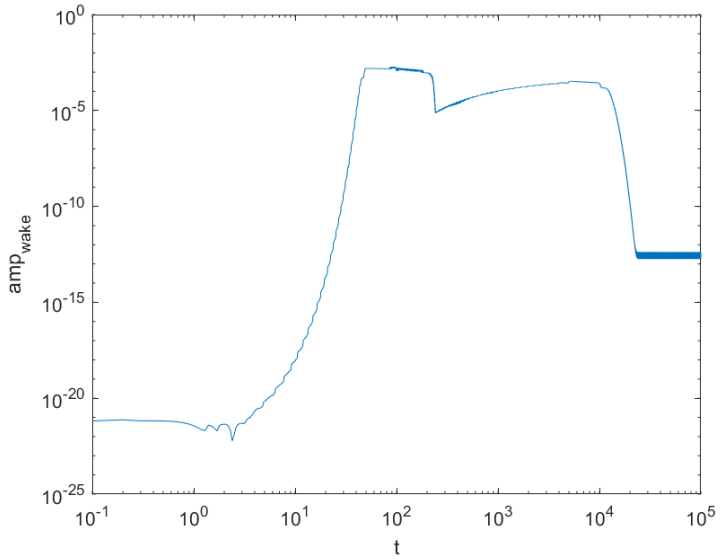

Figure 4.266: Loglog plot of small mass limit ripple amplitude with $\mu = 1/8$ and $\epsilon = 1/8$.

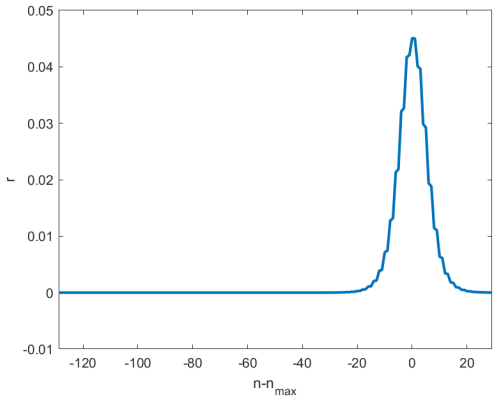

Figure 4.267: Small mass limit with $\mu = 1/16$ and $\epsilon = 1/8$.

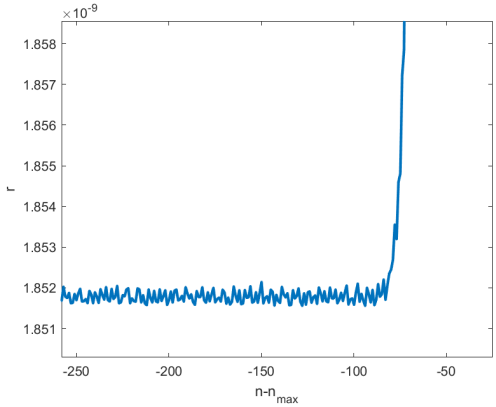

Figure 4.268: Small mass limit ripples with $\mu = 1/16$ and $\epsilon = 1/8$.

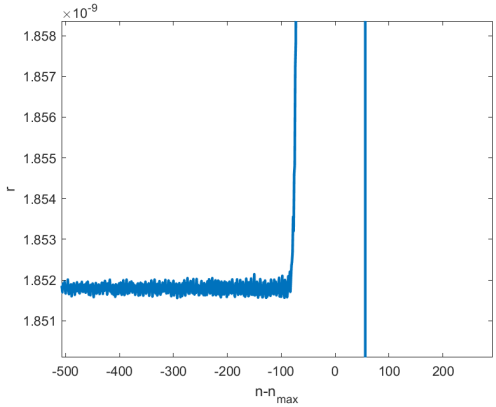

Figure 4.269: Small mass limit ripples with $\mu = 1/16$ and $\epsilon = 1/8$, zoomed out.

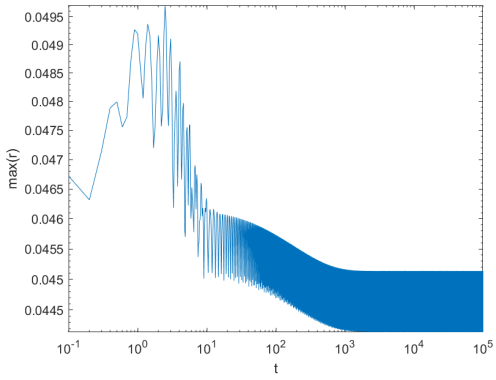

Figure 4.270: Loglog plot of small mass limit leading solitary wave amplitude with $\mu = 1/16$ and $\epsilon = 1/8$.

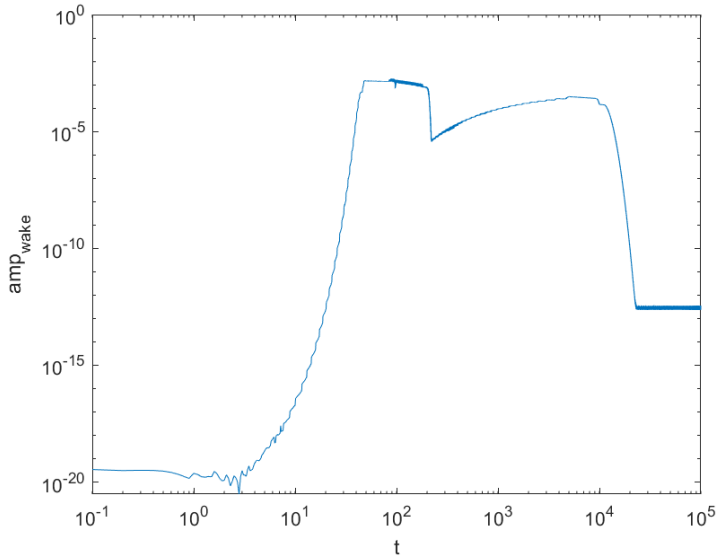

Figure 4.271: Loglog plot of small mass limit ripple amplitude with $\mu = 1/16$ and $\epsilon = 1/8$.

Chapter 5

Further Research

5.1 Improved initial conditions

In our simulations we took the initial conditions as in [2]. While these initial conditions work well, they may not be optimal for the small mass, equal mass and stiff spring limits. Recall that in Chapter 3 we brought up the forms of the traveling waves for the small mass and equal mass limits. We mentioned that the leading order terms of the small mass and equal mass solutions are not sech^2-type functions, but rather monatomic traveling waves. Ofcourse, by (3.4), a sech^2-type function definitely approximates a monatomic wave, but there is some room for improvement. For the sake of convenience, we assumed the sech^2-type initial conditions in this thesis. The suggestion for improvement on the initial condition could be satisfied by using the Fourier multiplier theory. For this, we use the Fourier transform. If $f : \mathbb{R} \to \mathbb{C}$ is absolutely integrable, meaning the improper integral $\int_{-\infty}^{\infty} |f(x)|dx$ converges, then the Fourier transform of f is

$$\mathfrak{F}[f](k) = \widehat{f}(k) := \frac{1}{\sqrt{2\pi}} \int_{-\infty}^{\infty} f(x)e^{-ikx}dx$$

and the inverse Fourier transform is

$$\mathfrak{F}^{-1}[f](x) = \check{f}(x) := \frac{1}{\sqrt{2\pi}} \int_{-\infty}^{\infty} f(k)e^{-ikx}dk.$$

Some important properties of the Fourier transform for us are the following. If f is differentiable and if $\widehat{f}'(k)$ is defined, then

$$\widehat{f}'(k) = ik\widehat{f}(k). \tag{5.1}$$

Next, let $d \in \mathbb{R}$ and $(S^d f)(x) = f(x + d)$. Then, following from the definition of the Fourier transform, we get

$$\widehat{S^d f}(k) = e^{ikd}\widehat{f}(k). \tag{5.2}$$

If we make a traveling wave ansatz for (1.2) and (1.3) on the monatomic version of the system, that is, with $m_j = 1$ for all j:

$$r_j(t) = \rho(j - ct) \quad \text{and} \quad p_j(t) = \phi(j - ct),$$

we obtain the following first-order system

$$\begin{cases} \rho' = -\dfrac{1}{c}(S^1 - 1)\phi \\ \phi' = -\dfrac{1}{c}(F(\rho) - F(S^{-1}\rho)) = -\dfrac{1}{c}(1 - S^{-1})F(\rho), \end{cases}$$

where $(S^{\pm 1} f)(X) = f(X \pm 1)$ for any function f. Combining the Fourier transform, (5.1) and (5.2) yields

$$\widehat{\rho}'(k) = \frac{\widehat{S^1\phi}(k) - \widehat{\phi}(k)}{-c} = \frac{e^{ik} - 1}{-c}\widehat{\phi}(k) = ik\widehat{\rho}(k)$$

and

$$\widehat{\phi}'(k) = \frac{\widehat{F(\rho)}(k) - \widehat{S^{-1}F(\rho)}}{-c} = \frac{1 - e^{-ik}}{-c}\widehat{F(\rho)}(k) = ik\widehat{\phi}(k)$$

which give the identities

$$\widehat{\rho}(k) = \frac{1-e^{ik}}{ick}\widehat{\phi}(k) \quad \text{and} \quad \widehat{\phi}(k) = \frac{e^{-ik}-1}{ick}\widehat{F(\rho)}(k). \tag{5.3}$$

Combining these latter two equations gives us

$$\widehat{\rho}(k) = \frac{e^{ik}+e^{-ik}-2}{-(ck)^2}\widehat{F(\rho)}(k) = \frac{2\cos(k)-2}{-(ck)^2}\widehat{F(\rho)}(k) = \frac{4\sin^2(\frac{k}{2})}{(ck)^2}\widehat{F(\rho)}(k) = \frac{\operatorname{sinc}^2(\frac{k}{2})}{c^2}\widehat{F(\rho)}(k),$$

where $\operatorname{sinc}(K) := \sin(K)/K$. Next, assume $F(r) = r + \mathcal{Q}(r)$, where $\mathcal{Q}(r)$ is roughly quadratic in r. We get

$$\widehat{\rho}(k) = \frac{\operatorname{sinc}^2(\frac{k}{2})}{c^2}(\widehat{\rho}(k) + \widehat{\mathcal{Q}(\rho)}(k)) = \frac{\operatorname{sinc}^2(\frac{k}{2})}{c^2}\widehat{\rho}(k) + \frac{\operatorname{sinc}^2(\frac{k}{2})}{c^2}\widehat{\mathcal{Q}(\rho)}(k).$$

Bringing all $\widehat{\rho}(k)$ factors to one side and writing out $\operatorname{sinc}(\frac{k}{2})$ again gives us

$$\frac{c^2(\frac{k}{2})^2 - \sin^2(\frac{k}{2})}{c^2(\frac{k}{2})^2}\widehat{\rho}(k) = \frac{\sin^2(\frac{k}{2})}{c^2(\frac{k}{2})^2}\widehat{\mathcal{Q}(\rho)}(k)$$

which in turn gives us

$$\widehat{\rho}(k) = \mathcal{M}_c(k)\widehat{\mathcal{Q}(\rho)}(k) \quad \text{where} \quad \mathcal{M}_c(k) := \frac{\sin^2(\frac{k}{2})}{c^2(\frac{k}{2})^2 - \sin^2(\frac{k}{2})}.$$

Finally, using the inverse Fourier transform yields

$$\rho = \mathfrak{F}^{-1}[\mathcal{M}_c\widehat{\mathcal{Q}(\rho)}] =: \mathcal{N}_c(\rho).$$

It has been proved by Friesecke and Pego [3] that there exists a unique solution to this equation when $|c|$ is close to 1 by using Banach's fixed point theorem. We call this solution σ_c. Banach's fixed point theorem makes sure that we can create this solution iteratively, namely for appropriate $\alpha_c, \beta_c \in \mathbb{R}$, set

$$\rho_{0,c}(x) := \alpha_c \operatorname{sech}^2(\beta_c x) \quad \text{and} \quad \rho_{k+1,c} := \mathcal{N}_c(\rho_{k,c}), k \geqslant 0.$$

Then $(\rho_{k,c})$ converges to σ_c. Once σ_c has been found, ϕ can also be found by taking the inverse Fourier transform of the representation for $\widehat{\phi}$ in (5.3). Friesecke and Pego [3] look for long wave traveling wave solutions, so they rescale

$$\rho(x) = \epsilon^2\varrho(\epsilon x),$$

where now ϱ is the unknown function. They take $c = c_\epsilon = \sqrt{1+\epsilon^2}$, which turns the fixed point problem into

$$\varrho = \mathfrak{F}^{-1}[\mathcal{M}^\epsilon_{c_\epsilon}\widehat{\mathcal{Q}(\varrho)}] =: \mathcal{G}_\epsilon(\varrho) \quad \text{where} \quad \mathcal{M}^\epsilon_{c_\epsilon} = \epsilon^2\mathcal{M}_{c_\epsilon}(\epsilon k).$$

Friesecke and Pego's findings indicate we should look for ϱ close to

$$\varrho_{0,\epsilon}(x) = \frac{\epsilon^2}{4}\operatorname{sech}^2(\frac{\epsilon x}{4}).$$

We have attempted coding a solver to this fixed point problem in MATLAB, the code of which can be found in Appendix B. The numerics and code from [27] could point the way to a better monatomic FPUT solitary wave solver, but such work is beyond the scope of this thesis.

We did not explore the long wave problem for the springs dimers or the general dimers, which is still a project that is worthwhile to explore independently of this thesis, even though we expect the simulations for that to closely resemble the diatomic work done in [2].

5.2 Stability of the material limits

If we compare our findings to what they had found in [2], we can make some conjectures about the stability of the solutions to the various material limits we presented here. If we allow for stegoton-type variations in the stiff spring limit, the behaviors of the small mass and stiff spring limits closely resemble the long wave limit in [2]. That is, solutions that start close to a nanopteron ultimately turn

into a solitary wave and an oscillatory part, where the solitary wave amplitude and the frequency and amplitude of the oscillatory part behave like the long wave limit in [2]. If we look at the observations done listed on page 424, 427 and 428, we see several similarities to what we have observed.

Firstly, we see that the decay in amplitude of the solitary wave is so slow that it is indeed barely visible. Secondly, although the shape of the oscillatory wake is different for each value of μ or κ, we see that the frequency of the ripples is near constant as time goes on. We see also, as we zoom in more on the oscillatory wake, that in some cases the ripples oscillate around a value not equal to zero. Thirdly, if we compare our amplitude plots to the ones in [2], we find that we also see the initial disorder in both solitary wake and oscillatory wake amplitudes, which is followed by a settling into a more regular behavior. We see also the kind of linear decay in the loglog plots which corresponds to algebraic decay in real time vs. real amplitude. After the initial disorder, all the amplitudes seem to settle around a constant value, but they actually decay very slowly. All these observations lead us to making the conjecture that in the small mass limit and the stiff spring limit, the solutions are metastable, which was first conjectured for the long wave problem in Section 7 of [17].

As a reminder, the definition of metastability as quoted from [17] reads: "metastable solutions which look for very long times like localized solitary waves but eventually converge to zero." On the other hand, if we observe what we have found for the equal mass limit, the results differ very much from the other limits. If we look at the differences in theory, this might not come so much as a surprise. The equal mass limit traveling wave problem is not singularly perturbed, and the solutions ripples are not small beyond all orders of ϵ, which is to say the solutions are micropterons. These differences apparently lead to a much more fast decay of the amplitude of the solitary wave. We conjecture instability, solutions that start near the equal mass solution do not necessarily stay close for very long times, but erode much faster. Any proofs or refutals of these conjectures will most likely involve the periodic term in the nanopteron/micropteron and the singular perturbation of the stiff spring, small mass and long wave problems, neither of which appears in the stability analyses of Mizumachi [23] and Friesecke and Pego [28, 29, 30].

Appendix A

Sequence and Sobolev spaces

In this appendix, we use [31] for all definitions and conventions.

Definition 1. The $\ell^2 = \ell^2(\mathbb{Z})$ space is the space of square-summable bi-infinite sequences of complex numbers. That is to say, it is the set of infinite sequences (z_n) such that

$$||(z_n)||_{\ell^2} = \left(\sum_{n=-\infty}^{\infty} |z_n|^2 \right)^{1/2} < \infty.$$

In the case of $\ell^2 \times \ell^2$ and a sequence $\mathbf{z}_n := (z_{n,1}, z_{n,2})$ the norm is

$$||\mathbf{z}_n||_{\ell^2 \times \ell^2} = ||(z_{n,1})||_{\ell^2} + ||(z_{n,2})_{\ell^2}.$$

Definition 2. Let $p \in \mathbb{R}$ such that $1 < p < \infty$. We set

$$L^p(\Omega) = \left\{ f : \Omega \to \mathbb{R} : f \text{ is measurable and } |f|^p \in L^1(\Omega) \right\}$$

where $L^1(\Omega)$ is the space of integrable functions from Ω into $\mathbb{R}$. The L^p space has the following norm:

$$||f||_{L^p} = ||f||_p = \left(\int_\Omega |f(x)|^p d\mu \right)^{1/p}.$$

Definition 3. We set

$$L^\infty(\Omega) = \{ f : \Omega \to \mathbb{R} : f \text{ measurable and } \exists C : |f(x)| \leqslant C \text{ a.e. on } \Omega \}$$

with the norm

$$||f||_{L^\infty} = ||f||_\infty = \inf \{ C : |f(x)| \leqslant C \text{ a.e. on } \Omega \}.$$

Definition 4. The space $C_c^1(I)$ is the space of once continuously differentiable functions on I with compact support, that is,

$$C_c^1(I) = \{ f \in C^1(I) : f(x) = 0 \quad \forall x \in I \backslash K, \text{ where } K \text{ is compact} \}.$$

Definition 5. Let $I = (a, b)$ be an open interval, possibly unbounded. Let $p \in \mathbb{R}$ such that $1 \leqslant p \leqslant \infty$. The defintion of the Sobolev space $W^{1,p}$ is given by

$$W^{1,p}(I) = \left\{ u \in L^p(I) : \exists g \in L^p(I) \text{ such that } \int_I u\phi' = -\int_I g\phi \quad \forall \phi \in C_c^1(I) \right\}.$$

We set

$$H^1(I) = W^{1,2}(I).$$

If there is no confusion we write $W^{1,p}$ instead of $W^{1,p}(I)$ and H^1 instead of $H^1(I)$. The space $W^{1,p}$ has the following equivalent norms,

$$||u||_{W^{1,p}} = ||u||_{L^p} + ||u'||_{L_p},$$

and if $1 < p < \infty$,

$$||u||_{W^{1,p}} = (||u||_{L^p}^p + ||u'||_{L^p}^p)^{1/p}.$$

The norm for H^1 follows from this norm.

Definition 6. Given an integer $s \geqslant 2$ and a real number $1 \leqslant p \leqslant \infty$ we can define by induction the space

$$W^{s,p}(I) = \left\{u \in W^{s-1,p}(I) : u' \in W^{s-1,p}(I)\right\}$$

and we set

$$H^s(I) = W^{s,2}(I).$$

The space $W^{s,p}$ is equipped with the norm

$$||u||_{W^{s,p}} = ||u||_{L^p} + \sum_{k=1}^{s} ||u^{(k)}||_{L^p},$$

where $u^{(k)}$ is the kth derivative of u. Again, for $1 < p < \infty$, sometimes the equivalent norm $(||u||_{L^p}^p + \sum_{k=1}^{s} ||u'||_{L^p}^p)^{1/p}$ is used. The norm for H^s follows from this norm.

Appendix B

Monatomic FPUT fixed point solver coding attempt

```
a = -10000*pi;
b = 10000*pi;
eps = 1/4;
N = 2^10;
n = 0:N-1;
L = b-a;
X = a + (L/N)*n;
rho0 = eps^2/4*sech(eps*X/4).^2;
k = 2*pi/L*[0:N/2-1, 0, -N/2+1:-1];
M = sin(X/2).^2/((1+eps^2)*(X/2).^2-sin(X/2).^2).*k;
rho1 = 1;

while(rho0 ~= rho1)
    rho1 = rho0;
    Qhat = fft(rho0.^2);
    rho0 = ifft(M.*Qhat);
end
plot(X, rho0);
```

Bibliography

[1] P. G. Kevrekidis. Non-linear waves in lattices: past, present, future. *IMA Journal of Applied Mathematics*, 76(3):389–423, April 2011.

[2] Nickolas Giardetti, , Amy Shapiro, Stephen Windle, and J. Douglas Wright. Metastability of solitary waves in diatomic FPUT lattices. *Mathematics in Engineering*, 1(3):419–433, 2019.

[3] G. Friesecke and R. L. Pego. Solitary waves on FPU lattices: I. qualitative properties, renormalization and continuum limit. *Nonlinearity*, 12(6):1601–1627, October 1999.

[4] Gero Friesecke and Jonathan A. D. Wattis. Existence theorem for solitary waves on lattices. *Communications in Mathematical Physics*, 161(2):391–418, March 1994.

[5] Michael Herrmann and Karsten Matthies. Asymptotic formulas for solitary waves in the high-energy limit of FPU-type chains. *Nonlinearity*, 28(8):2767–2789, July 2015.

[6] Michael Herrmann and Karsten Matthies. Uniqueness of solitary waves in the high-energy limit of FPU-type chains. In *Patterns of Dynamics*, pages 3–15. Springer International Publishing, 2017.

[7] Michael Herrmann and Karsten Matthies. Stability of high-energy solitary waves in Fermi-Pasta-Ulam-Tsingou chains. *Transactions of the American Mathematical Society*, 372(5):3425–3486, June 2019.

[8] Carmen Chicone. *Ordinary Differential Equations with Applications*. Springer New York, 2006.

[9] Thierry Dauxois. Fermi, Pasta, Ulam, and a mysterious lady. *Physics Today*, 61(1):55–57, January 2008.

[10] E. Fermi, P. Pasta, S. Ulam, and M. Tsingou. Studies of the nonlinear problems. Technical report, May 1955.

[11] Mason Porter, Norman Zabusky, Bambi Hu, and David Campbell. Fermi, Pasta, Ulam and the birth of experimental mathematics. *American Scientist*, 97(3):214, 2009.

[12] Mark J. Ablowitz. *Nonlinear Dispersive Waves*. Cambridge University Press, 2009.

[13] Guido Schneider and C. Eugene Wayne. Counter-propagating waves on fluid surfaces and the continuum limit of the Fermi-Pasta-Ulam model. In *Equadiff 99*, pages 390–404. World Scientific Publishing Company, September 2000.

[14] A. Hoffman and C. E. Wayne. Counter-propagating two-soliton solutions in the Fermi–Pasta–Ulam lattice. *Nonlinearity*, 21(12):2911–2947, November 2008.

[15] Jeremy Gaison, Shari Moskow, J. Douglas Wright, and Qimin Zhang. Approximation of polyatomic FPU lattices by KdV equations. *Multiscale Modeling & Simulation*, 12(3):953–995, January 2014.

[16] Alexander Pankov. *Travelling Waves and Periodic Oscillations in Fermi-Pasta-Ulam Lattices*. Published by Imperial College Press and distributed by World Scientific Publishing Co., March 2005.

[17] Timothy E. Faver and J. Douglas Wright. Exact diatomic Fermi–Pasta–Ulam–Tsingou solitary waves with optical band ripples at infinity. *SIAM Journal on Mathematical Analysis*, 50(1):182–250, January 2018.

[18] John P. Boyd. *Weakly Nonlocal Solitary Waves and Beyond-All-Orders Asymptotics*. Springer US, 1998.

[19] Timothy E. Faver. Nanopteron-stegoton traveling waves in spring dimer Fermi-Pasta-Ulam-Tsingou lattices. *Quarterly of Applied Mathematics*, 78(3):363–429, August 2019.

[20] J. Thomas Beale. Exact solitary water waves with capillary ripples at infinity. *Communications on Pure and Applied Mathematics*, 44(2):211–257, March 1991.

[21] S.M. Sun. Existence of a generalized solitary wave solution for water with positive bond number less than 1/3. *Journal of Mathematical Analysis and Applications*, 156(2):471–504, April 1991.

[22] Eric Lombardi. *Oscillatory Integrals and Phenomena Beyond all Algebriac Orders*. Springer Berlin Heidelberg, 2000.

[23] Tetsu Mizumachi. Asymptotic stability of lattice solitons in the energy space. *Communications in Mathematical Physics*, 288(1):125–144, March 2009.

[24] Aaron Hoffman and J. Douglas Wright. Nanopteron solutions of diatomic Fermi–Pasta–Ulam–Tsingou lattices with small mass-ratio. *Physica D: Nonlinear Phenomena*, 358:33–59, November 2017.

[25] Timothy E. Faver and Hermen Jan Hupkes. Micropteron traveling waves in diatomic Fermi–Pasta–Ulam–Tsingou lattices under the equal mass limit. *Physica D: Nonlinear Phenomena*, 410:132538, September 2020.

[26] Timothy E. Faver. *Nanopteron-stegoton traveling waves in mass and spring dimer Fermi-Pasta-Ulam-Tsingou lattices*. PhD thesis, Drexel University, Philadelphia, PA, May 2018.

[27] Timothy E. Faver, Roy H. Goodman, and J. Douglas Wright. Solitary waves in mass-in-mass lattices. arXiv:2002.05573, accepted to *ZAMP* in 2020.

[28] G. Friesecke and R. L. Pego. Solitary waves on FPU lattices: II. linear implies nonlinear stability. *Nonlinearity*, 15(4):1343–1359, June 2002.

[29] G. Friesecke and R. L. Pego. Solitary waves on Fermi–Pasta–Ulam lattices: III. Howland-type Floquet theory. *Nonlinearity*, 17(1):207–227, October 2003.

[30] G. Friesecke and R. L. Pego. Solitary waves on Fermi–Pasta–Ulam lattices: IV. proof of stability at low energy. *Nonlinearity*, 17(1):229–251, October 2003.

[31] Haim Brezis. *Functional Analysis, Sobolev Spaces and Partial Differential Equations*. Springer New York, 2010.